AFRL-RZ-ED-TR-2012-0034

Nanostructured Materials

Joseph M. Mabry

Air Force Research Laboratory (AFMC)
AFRL/RQRP
10 E. Saturn Blvd
Edwards AFB CA 93524-7680

August 2012

In-House Final Report

AIR FORCE RESEARCH LABORATORY
AEROSPACE SYSTEMS DIRECTORATE

■ **Air Force Materiel Command** ■ **United States Air Force** ■ **Edwards Air Force Base, CA 93524**

REPORT DOCUMENTATION PAGE

Form Approved
OMB No. 0704-0188

1. REPORT DATE *(DD-MM-YYYY)*	**2. REPORT TYPE**	**3. DATES COVERED** *(From - To)*
30 Aug 2012	In-House Final Report	18 Aug 2004 – 1 Jun 2012

4. TITLE AND SUBTITLE
Nanostructured Materials

5a. CONTRACT NUMBER

5b. GRANT NUMBER

5c. PROGRAM ELEMENT NUMBER
61102F

6. AUTHOR(S)
Mabry, Joseph M.

5d. PROJECT NUMBER

5e. TASK NUMBER

5f. WORK UNIT NUMBER
23030521 / Q0AD

7. PERFORMING ORGANIZATION NAME(S) AND ADDRESS(ES)

Air Force Research Laboratory (AFMC)
AFRL/RQRP
10 E. Saturn Blvd
Edwards AFB CA 93524-7680

8. PERFORMING ORGANIZATION REPORT NO.

9. SPONSORING / MONITORING AGENCY NAME(S) AND ADDRESS(ES)

Air Force Research Laboratory (AFMC)
AFRL/RQR
5 Pollux Drive
Edwards AFB CA 93524-7048

10. SPONSOR/MONITOR'S ACRONYM(S)

11. SPONSOR/MONITOR'S REPORT NUMBER(S)
AFRL-RZ-ED-TR-2012-0034

12. DISTRIBUTION / AVAILABILITY STATEMENT
Approved for public release; distribution unlimited. PA No. 12843.

13. SUPPLEMENTARY NOTES

14. ABSTRACT

The objective of this work is the synthesis of new thermoplastic and thermosetting nanocomposite materials for the study of fundamental properties and phenomena. When the program began, only limited physical, mechanical, and surface property characterization data was available in polymer and composite technologies. This is important because, by controlling polymer composites at the nano-level, ideal property improvements were envisioned. During the program, new materials were produced and new methods for nanoparticle incorporation were developed. These advancements led to numerous property enhancements, particularly in the area of surface properties. This report summarizes only a portion of the results obtained during this program with a particular focus on the non-wetting materials research.

15. SUBJECT TERMS
Fluorinated Polyhedral Oligomeric SilSesquioxanes (FluoroPOSS) compounds, Polyhedral Oligomeric SilSesquioxane (POSS) compounds, Fluoropolymers, Incorporation into Polymers, Synthesis of FluoroPOSS, surface properties, dynamic water and hexadecane contact angles, nanoparticle incorporation, polymer and composite technologies.

16. SECURITY CLASSIFICATION OF:			**17. LIMITATION OF ABSTRACT**	**18. NUMBER OF PAGES**	**19a. NAME OF RESPONSIBLE PERSON**
					Joseph Mabry
a. REPORT	**b. ABSTRACT**	**c. THIS PAGE**			**19b. TELEPHONE NO** *(include area code)*
Unclassified	**Unclassified**	**Unclassified**	SAR	63	661 275-5857

Standard Form 298 (Rev. 8-98)
Prescribed by ANSI Std. 239.18

- STINFO COPY -
NOTICE AND SIGNATURE PAGE

Using Government drawings, specifications, or other data included in this document for any purpose other than Government procurement does not in any way obligate the U.S. Government. The fact that the Government formulated or supplied the drawings, specifications, or other data does not license the holder or any other person or corporation; or convey any rights or permission to manufacture, use, or sell any patented invention that may relate to them.

Qualified requestors may obtain copies of this report from the Defense Technical Information Center (DTIC) (http://www.dtic.mil).

AFRL-RZ-ED-TR-2012-0034 HAS BEEN REVIEWED AND IS APPROVED FOR PUBLICATION IN ACCORDANCE WITH ASSIGNED DISTRIBUTION STATEMENT.

FOR THE DIRECTOR:

// SIGNED//
JOSEPH M. MABRY, Ph.D.
Project Manager

//SIGNED//
HOPE M. KLUKOVICH, CAPT, USAF
Chief, Propellants Branch

// SIGNED//
STEVEN A. SVEJDA, Ph.D.
Science Technical Advisor
Rocket Propulsion Division

This report is published in the interest of scientific and technical information exchange, and its publication does not constitute the Government's approval or disapproval of its ideas or findings.

This Page Intentionally Left Blank

TABLE OF CONTENTS

LIST OF FIGURES

GLOSSARY

AFB	Air Force Base
AFM	Atomic Force Microscopy
AFOSR	Air Force Office of Scientific Research
AFRL	Air Force Research Laboratory
EAFB	Edwards Air Force Base
FD	Fluorodecyl
FH	Fluorohexyl
FluoroPOSS	Fluorinated Polyhedral Oligomeric Silsesquioxanes
FO	Fluorooctyl
PFCB	Perfluorocyclobutyl
POSS	Polyhedral Oligomeric Silsesquioxanes
RMS	Root-Mean-Square
TGA	Thermogravimetric Analysis
γSL	Surface tension of the liquid drop
γSV	Surface energy
θa	Angle of advancing
θr	Angle of receding

1.0 INTRODUCTION

The objective of the recently completed research program at the Air Force Research Laboratory, Edwards AFB (AFRL EAFB) site was to synthesize new thermoplastic and thermosetting nanocomposite materials in order to study fundamental properties and phenomena. When the program began, polymer and composite technology had only limited physical, mechanical, and surface property characterization data available. By controlling polymer composites at the nano-level, ideal property improvements were envisioned. During this program, new materials were produced and new methods for nanoparticle incorporation were developed. These advancements have led to numerous property enhancements, particularly in the area of surface properties. The following paragraphs summarize the results obtained during this program with a particular focus on the non-wetting materials research. Appendices A and B contain copies of recently awarded U.S. patents for the incorporation of Fluorinated Polyhedral Oligomeric Silsesquioxanes (FluoroPOSS) into polymers to produce polymer nanocomposites of varying functionality. Appendices C and D contain copies of two recent refereed journal articles on the synthesis of FluoroPOSS and the incorporation of FluoroPOSS into non-fluorinated polymers to produce the first superoleophobic surfaces, respectively. All published work was done under Air Force Office of Scientific Research (AFOSR) sponsorship.

2.0 POLYHEDRAL OLIGOMERIC SILSESQUIOXANES (POSS)

Polyhedral Oligomeric SilSesquioxane (POSS) compounds are thermally robust cages possessing a silicon-oxygen core framework surrounded by organic functionality on the periphery. Because these materials possess the functionality of both inorganic ceramic materials and organic polymers, they have been described “hybrid” organic/inorganic materials. POSS molecules can be functionally tuned and are easily synthesized with inherent functionality. Certain POSS compounds may possess high degrees of compatibility in blended polymers. Others can easily be covalently linked into a polymer backbone. The incorporation of POSS into polymers produces composites with improved properties, such as glass transition temperature, mechanical strength, thermal and chemical resistance, and ease of processing. Applications include space-survivable coatings, and ablative and fire-resistant materials. POSS can be produced as either completely condensed cages or incompletely condensed cages with silanol groups, which allow further modification. Due to their physical size, POSS incorporation in

polymers generally serves to reduce chain mobility, often improving both thermal and mechanical properties. The generalized structure of octameric POSS compounds (Figure 1) illustrates many of the important features of these molecules. These molecular cages may possess reactive and/or non-reactive functionality, which allows them to be incorporated into polymer systems either covalently or without any covalent attachment (Figure 2). This versatility has allowed POSS to become popular as nanometer-scale building blocks in a wide range of polymer composite materials.

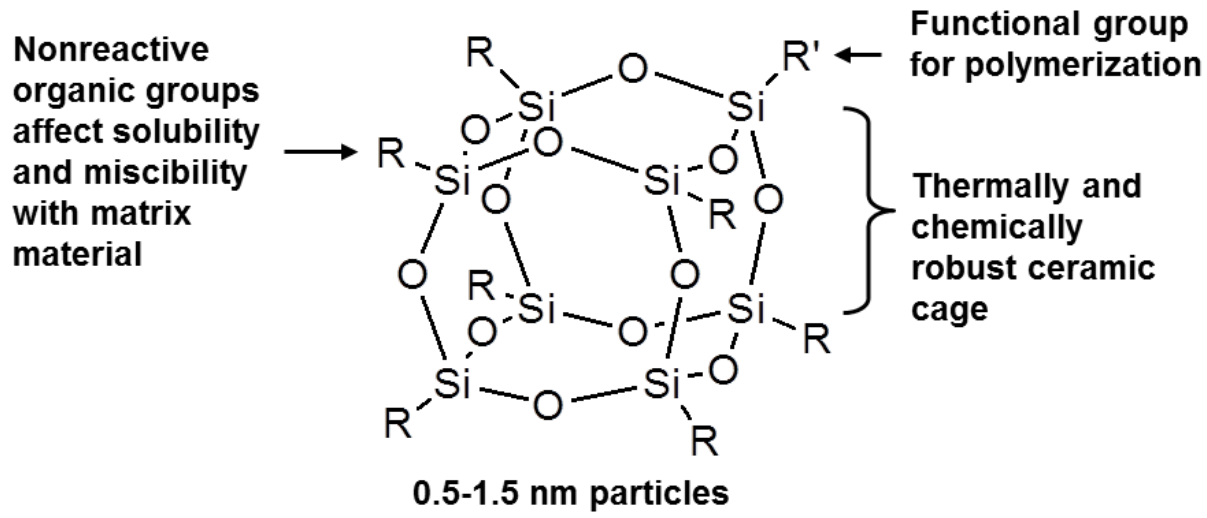

Figure 1. Generalized POSS Structure

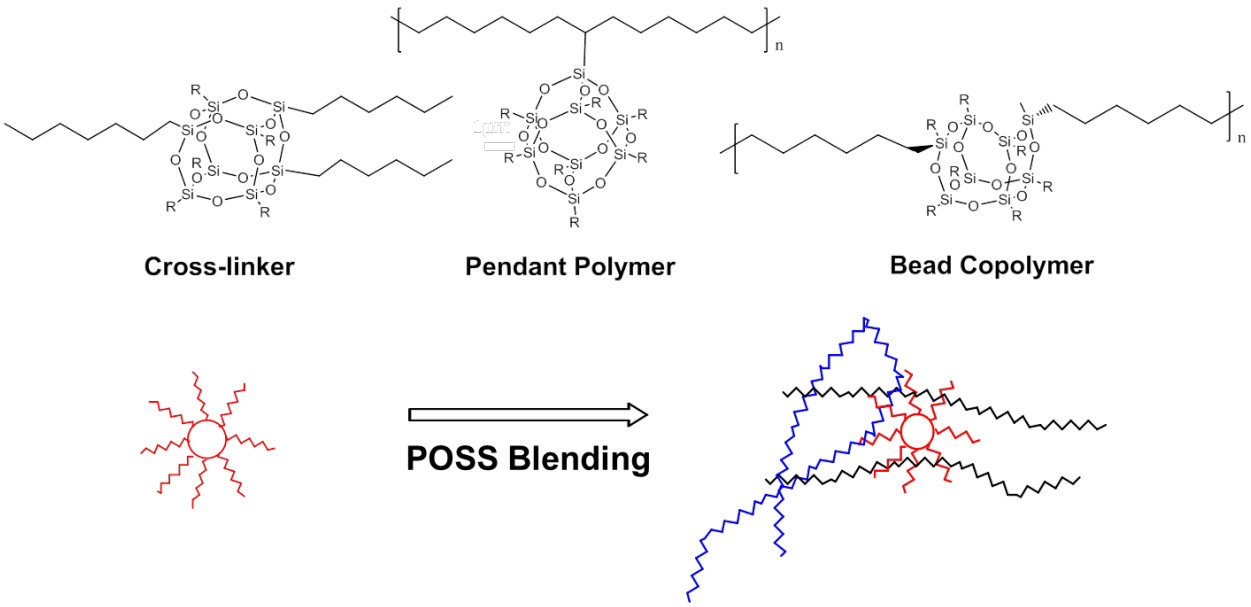

Figure 2. Methods of POSS Incorporation into Polymers

POSS are thermally robust cages consisting of a silicon-oxygen core framework possessing alkyl functionality on the periphery. They are used for the development of high performance materials in several aerospace applications. POSS molecules can be functionally tuned, are easily synthesized with inherent functionality, and are often commercially available.

3.0 FLUORINATED POSS

A number of reports have detailed that POSS materials can act as reinforcing fillers (or reinforcing comonomers) in a number of composite systems with nanometer-sized domains. Our results are somewhat different in that the POSS building blocks are designed to be rather non-interacting. Specifically, the organic "corona" surrounding the silsesquioxane core is composed of fluoroalkyl moieties. Fluoroalkyl compounds are known to be basically inert. This is largely because they are non-polarizable and have low surface free energy values. Fluoroalkyl chains are often rigid, due to steric and electronic repulsion. Similarly, the large corona of the FluoroPOSS compounds should retard the van der Waals attraction between POSS cores. These POSS materials are monodisperse and crystalline.

FluoroPOSS compounds fluorodecyl (**FD**), fluorooctyl (**FO**), and fluorohexyl (**FH**) were produced by the base-catalyzed hydrolysis of trialkoxy silanes (Figure 3). These compounds tend to condense into T8 cages, similar to that observed in acid-catalyzed synthetic methods, rather than cage mixtures, as has been previously observed in the base-catalyzed synthesis. The

yields for these reactions are often nearly quantitative. This is significant because the usual method to produce T8 cages is the acid-catalyzed hydrolysis of trichlorosilanes, which produces an undesirable acidic by-product.

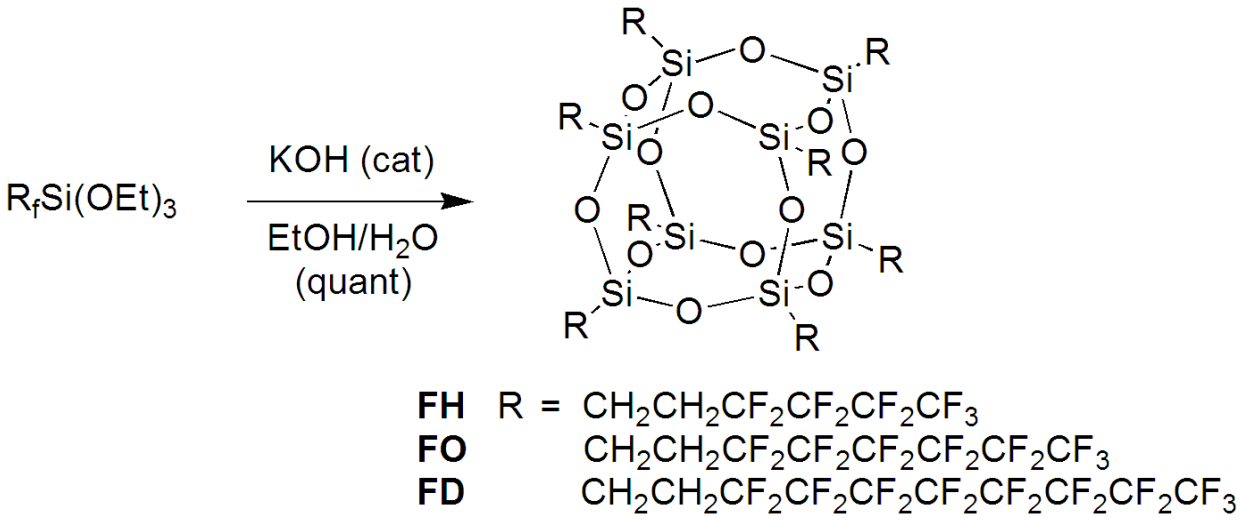

Figure 3. Synthesis of Octahedral FluoroPOSS Compounds

These FluoroPOSS compounds are soluble in fluorinated solvents, such as AK-225G and hexafluorobenzene. Unlike most non-fluorinated POSS compounds, TGA indicates FluoroPOSS volatilize rather than decompose. No residue remains after heating under either nitrogen or dry air. **FD** POSS is the most stable compound, subliming at over 300 °C. FluoroPOSS are also very dense, high molecular weight materials. For example, **FD** POSS has a molecular weight of 3993.54 g/mol and a density of 2.067 g/cm3. As a general trend, melting points become depressed as fluoroalkyl chain lengths increase due to weaker intermolecular wan der Waal attractions. All FluoroPOSS compounds were observed to possess narrow melting points as high molecular weight compounds indicative of high purity. In all cases, no decomposition was observed for these compounds at the melting point.

The ability to crystallize FluoroPOSS compounds from fluorinated solvents, using solvent evaporation/vapor diffusion techniques, enabled the growth of single crystals for high resolution (0.75 Å) X-ray diffraction studies (Figure 4). Both **FH** and **FD** are triclinic (P1) showing the presence of one and two crystallographically independent “half” molecules in the asymmetric unit, respectively. In both cases, there is an inversion center in the middle of the POSS core, which results in four pairs of fluoroalkyl chains with similar conformations. The

molecular structure of FluoroPOSS contains rigid, rod-like fluoroalkyl chains, which are attached to the silicon atoms of the POSS cage via flexible methylene groups. The relative arrangement of these components and resulting molecular interactions determine their thermal properties and may also contribute to surface properties, including hydrophobicity. The crystal structures of **FH** and **FD** showed a near-parallel arrangement of the fluoroalkyl chains. These result from the formation of strong intramolecular interactions between electropositive silicon and electron-rich fluorine atoms. These intramolecular contacts of ~3.0 Å are significantly shorter than the sum of van der Waal radii for silicon and fluorine at 2.10 and 1.47 Å, respectively. The packing of **FD** results in the POSS cores resting at an angle, with respect to the linear fluoroalkyl groups (mean least square angle = ~104°). This results in a rougher packing surface than **FH**, as seen in the electrostatic potential surfaces (Figure 5).

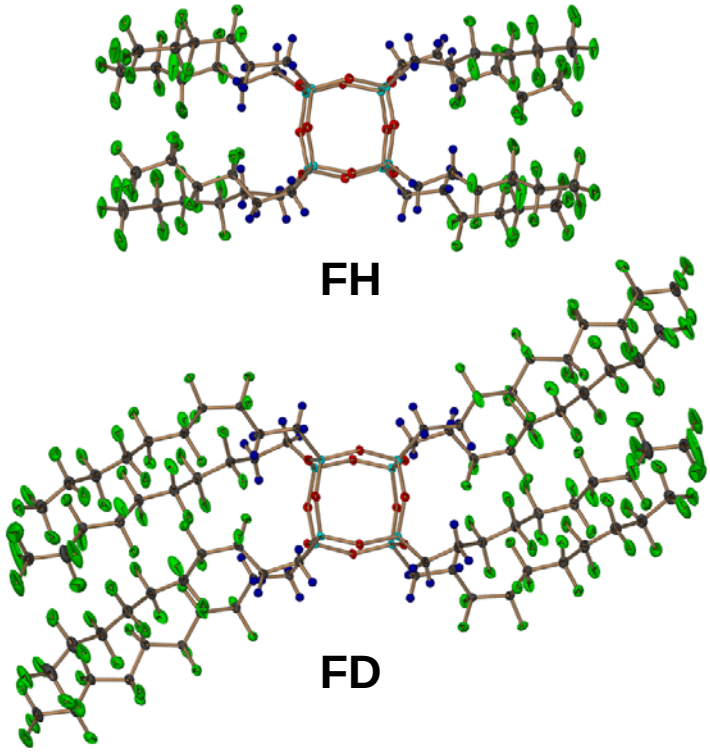

Figure 4. ORTEP representation of FH and FD POSS at 103 K

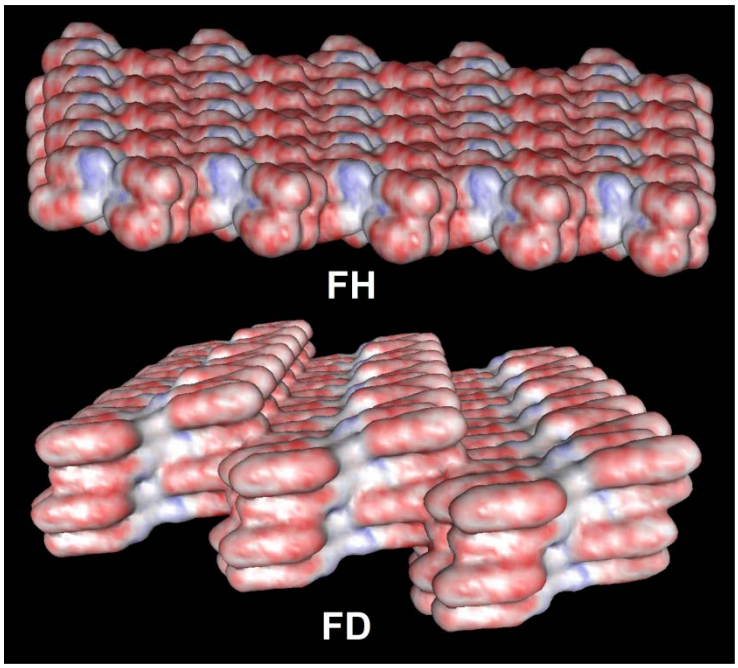

Figure 5. Electrostatic potential surfaces of FH and FD POSS

The fluorinated POSS compounds were spin cast from hexafluorobenzene onto a glass substrate. The spin casting produces well-adhered, white power-like films and did not visually expose any of the glass substrate. Their static (or advancing) contact angles were measured using deionized water and hexadecane as test fluids. Hexadecane is a standard test fluid for determining the oil repellency (or oleophobicity) of a material. The fluorinated POSS series measured water contact angles are on average 50° higher than for hexadecane contact angles. As a consequence of the highest wt % F content, **FD** produced the highest water and hexadecane static contact angle of 154°, and 87°, respectively. Because its water contact angle was greater than 150°, the surface of **FD** as a spin cast powder is classified as being formally superhydrophobic.

It should be noted the water contact angles for the observed trend were analyzed from spin cast, semicrystalline powder films. AFM analysis revealed the spin cast ***FD** POSS surface produced a root-mean-square (RMS) roughness of approximately 4 μm (Figure 6). For the fluorinated POSS octamer series of **FP**, **FH**, **FO**, and **FD**, there is a near linear progression of water and hexadecane contact angle in relation to the increasing fluorine content of the Fluorinated POSS compounds. This is clearly shown by a 13% increase in water contact angle from **FP** (38.2% fluorine content) to the **FH** (57.2% fluorine content) compound. It would

appear a leveling-off effect is anticipated past the series fluoroalkyl substitution beyond the **FO**, since a negligible increase of 5% was observed from **FH** (57.2% fluorine content) to **FO** (61.9% fluorine content). However, the **FD** (64.7% fluorine content) has an abrupt increase of 12% from **FO** POSS. A similar trend was observed for hexadecane contact angles, but the standard deviation would indicate oleophobicities of **FH**, **FO**, and **FD** are the same.

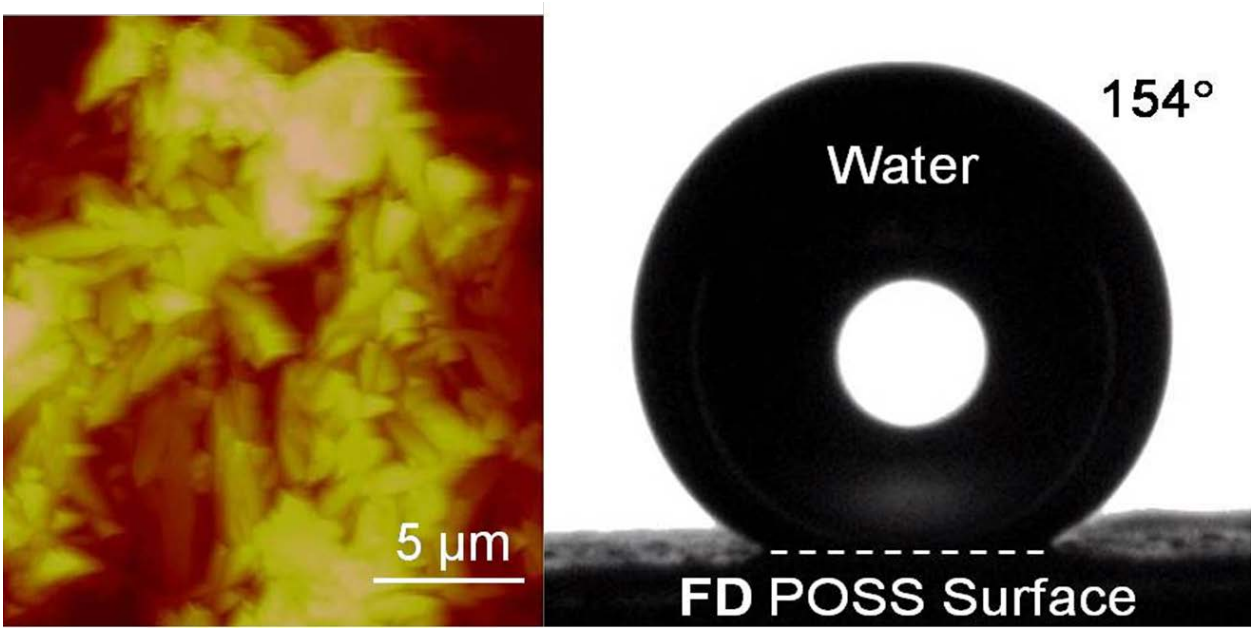

Figure 6. FD POSS water contact angle of 154° on 4 µm rms rough surface

Hepta (3,3,3-trifluoropropyl) tricycloheptasiloxane trisodium silanolate (**1**) was used as an intermediate for the preparation FluoroPOSS compounds **2–7** by "corner-capping" with fluoro-alkyltrichlorosilanes (Figure 7). The intermediate salt (**1**) is stable in air, but decomposes to silsesquioxane resin upon exposure to moisture. The intermediate adduct is the result of a pathway to fully condensed cage structures by simply controlling feedstock stoichiometry.

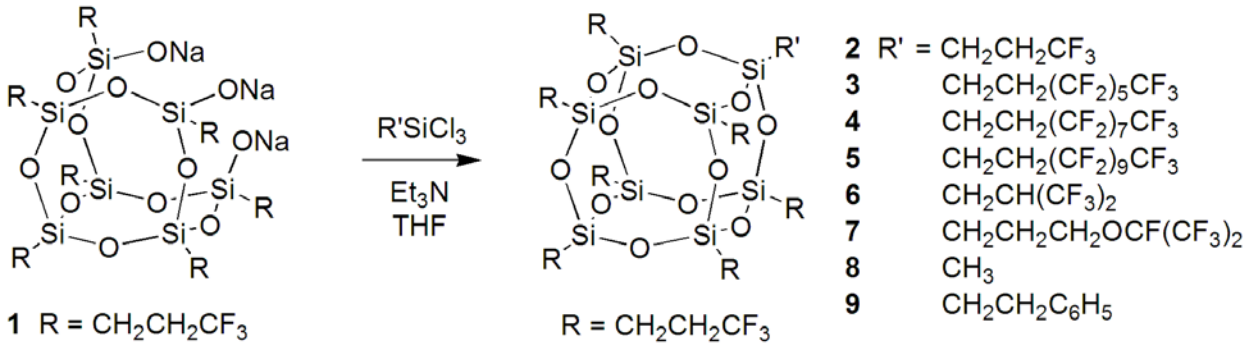

Figure 7. Synthesis of corner-capped FluoroPOSS compounds

4.0 POSS POLYMER COMPOSITES

Selected fluorinated POSS compounds possessing the highest hydrophobicity and oleophobicity were blended into several fluoropolymers in order to develop a preliminary study of fluorinated POSS compatibility in polymer matrices. For the purposes of this paper**, FD** POSS **6F-BP** perfluorocyclobutyl (PFCB) aryl ether (Figure 8) polymer blends will be used to describe fluorinated POSS dispersion and its effect on surface wettability.

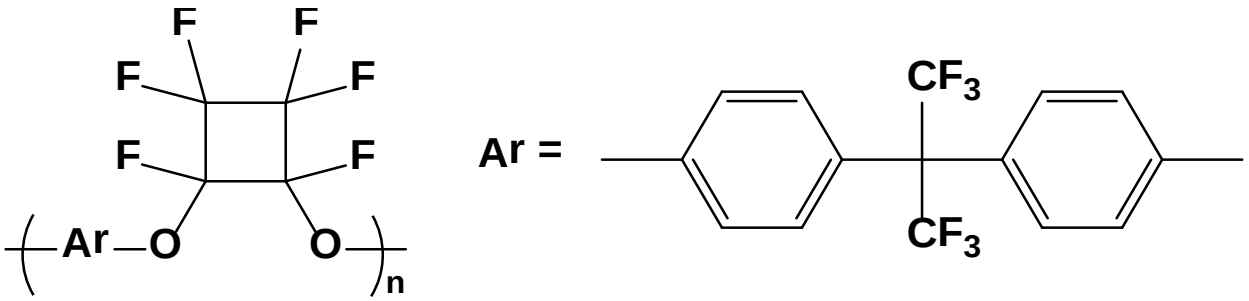

Figure 8. 6F-Biphenyl (6F-BP) perfluorocyclobutyl (PFCB) aryl ether polymer

The level of dispersion of fluorinated POSS compounds into polymer systems is largely dependent on surface chemistry. PFCB aryl ether polymers are of interest in a multitude of materials applications, specifically their ability to produce optically transparent, processable films. Increasing **FD** POSS wt % loadings blended with **6F-BP** PFCB aryl ether polymer showed a gradual increase in water, but profound increase in hexadecane contact angle (Figure 9). The **6F-BP** PFCB aryl ether polymer is intrinsically hydrophobic and produced water, and hexadecane contact angles of 95° and 27°, respectively. **FD** POSS loadings up to 15 wt % developed a plateau from static water contact angle; the blend showed an overall 32% increase in

water contact angle (124°) at this loading compared with unblended **6F-BP**. At optimized **FD** POSS loadings of 10 wt %, a maximum hexadecane contact angle of 80° was observed, increasing hexadecane repellency by 158%. While films prepared from 15 wt % **FD** POSS loading still appeared transparent and homogenous, 20 wt % FD POSS produced slight phase separation. At 30 wt % **FD** POSS, significant incompatibility was observed producing brittle, opaque films with crystalline aggregates on the film surface.

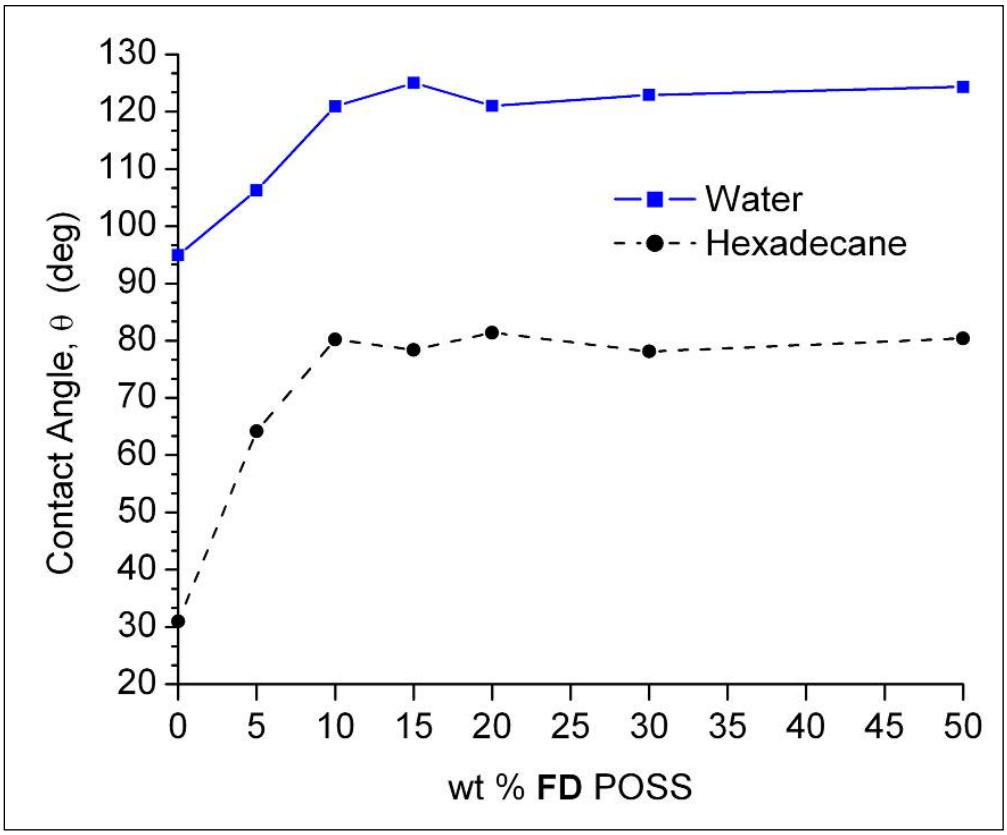

Figure 9. Water and hexadecane contact angles of various wt % of FD POSS blended into 6F-BP PFCB aryl ether polymer

Dynamic water and hexadecane contact angles were evaluated to determine the degree of hysteresis of **FD** POSS blended into **6F-BP** PFCB aryl ether polymer. The angles of advancing (θa) and receding (θr) of water and hexadecane were obtained by placing a liquid drop on the surface and tilting the stage of the goniometer. The results of the measurements for water and hexadecane are shown in Figure 10. At all wt % of **FD** POSS blended into the polymer, the water and hexadecane drops remained pinned on the surface, even when the stage was tilted 90°.

Initially, the advancing and receding angles were taken at the onset of liquid drop perturbation on the uphill and downhill side during as the stage was tilted. However, these measurements were difficult to assess "by eye" and produced a high deviation in recorded values. Therefore, the dynamic angles were recorded at a 90° tilt in order to ensure consistency. These results indicate a condition of high surface hysteresis where the surface energy (γSV) exceeds the surface tension (γSL) of the liquid drop.

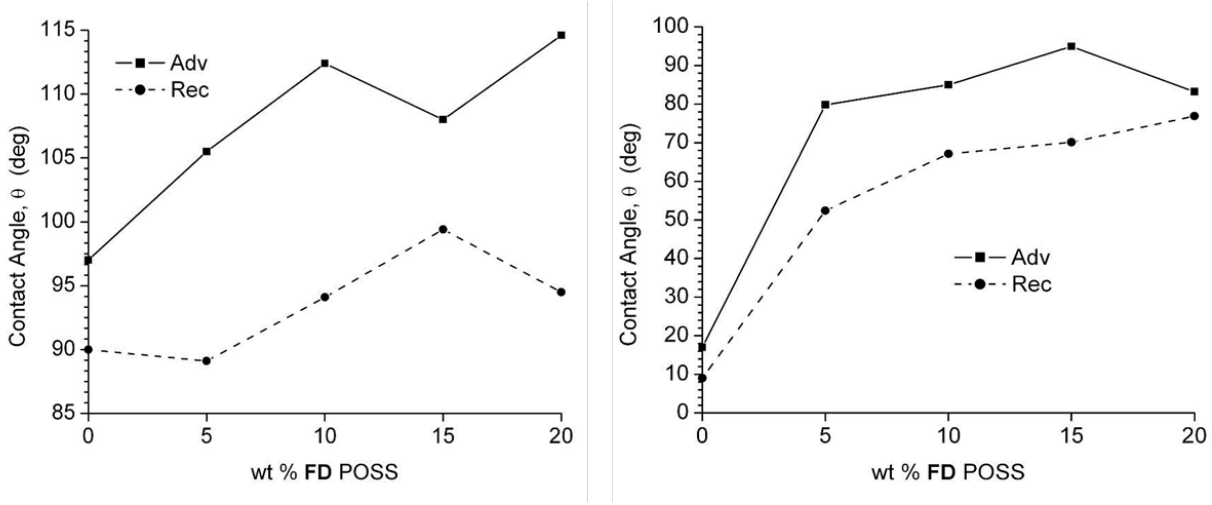

Figure 10. Dynamic water (left) and hexadecane (right) contact angles of various wt % of FD POSS blended into 6F-BP PFCB aryl ether polymer

Blending **FD** POSS into the **BP-6F** PFCB aryl ether polymer introduced additional fluorine content and increased surface roughness. As demonstrated in the beginning of this chapter, the relationship of contact angle and surface energy is governed by Young's equation which relates interfacial tensions among the surface to the liquid and gas phases of water. Furthermore, surface roughness imparts increased hydrophobicity to material as demonstrated by Cassie and Baxter, as well as Wenzel.

Atomic force microscopy (AFM) analysis of 15 wt % **FD** blend compared with the virgin **6F-BP** PFCB aryl ether polymer (Figure 11) showed a marked increase in surface roughness. From AFM analysis, unblended **6F-BP** polymer and 15 wt % **FD** POSS composite blend gave a measured surface roughness (RMS) of 0.527 nm and 1.478 nm, respectively. The incorporation of the fluorinated **FD** POSS structures produced this three-fold increase in surface roughness possibly due to blooming and aggregation of these structures on the surface during the spin

casting process. The increase in surface roughness was nearly 1 nm (the difference of 1.278 nm and 0.527) due to the inclusion of **FD** POSS. Therefore, it is presumed the low surface energy fluorine content contributed by fluorinated POSS has the most influence on the surface contact angle, whereas the surface roughness is an important, but minor contributing parameter. Surface characterization is being investigated in order to determine the concentration gradient of the fluorinated POSS structures on the surface compared to those entrained in the bulk material.

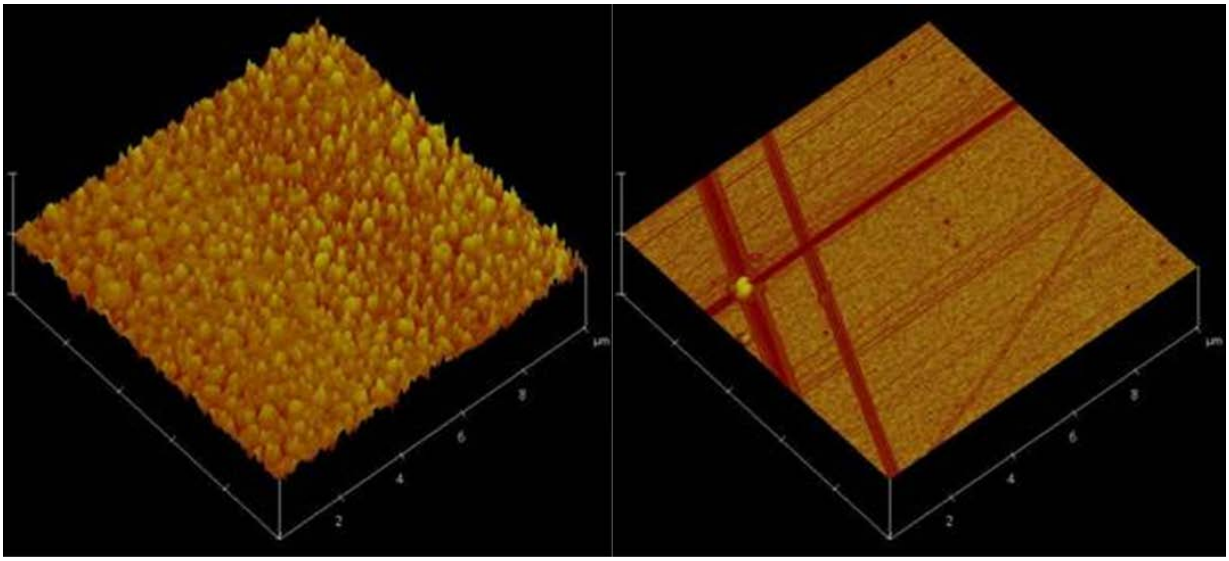

Figure 11. AFM height images of 15 wt % FD POSS (left) and unfilled (right) 6F-BP PFCB aryl ether polymer

5.0 CONCLUSIONS

Various fluorinated polyhedral oligomeric silsesquioxanes (FluoroPOSS) have been solvent or melt blended into a variety of fluoropolymers. These fluoropolymers include perfluorocyclobutyl (PFCB) aryl ether polymers. The composite blends produce well-dispersed FluoroPOSS based on microscopy analysis. The fluoroalkyl groups on the FluoroPOSS cages demonstrate good miscibility in selected fluoropolymer matrices. These FluoroPOSS fluoropolymer composites may be useful as low friction surfaces either as bulk components or coatings. Contact angle measurements of the POSS fluoropolymers show an improvement of water and hexadecane contact angles over the unfilled materials. The low surface energy POSS compounds also appear to act as a processing aid during fluoropolymer processing, significantly reducing both the torque and load measurements in the extruder. Thermal and mechanical

properties of the blended fluoropolymers do not compromise the integrity of the unfilled polymers. Work continues to encompass the other FluoroPOSS as simple drop-in modifiers for other fluoropolymers.

APPENDIX A: U.S. PATENT 7,193,015 B1

US007193015B1

(12) **United States Patent**
Mabry et al.

(10) **Patent No.: US 7,193,015 B1**
(45) **Date of Patent: Mar. 20, 2007**

(54) **NANOSTRUCTURED CHEMICALS AS ALLOYING AGENTS IN FLUORINATED POLYMERS**

(76) Inventors: **Joseph M. Mabry**, 42229 - 57th St. West, Lancaster, CA (US) 93536; **Rene I. Gonzalez**, 28 Paseo del Parque Urb. Los Paseos, San Juan, PR (US) 00926; **Rusty L. Blanski**, 44448 Overland Ave., Lancaster, CA (US) 93536; **Patrick N. Ruth**, 810 S. Mill St., Tehachapi, CA (US) 93561; **Brent D. Viers**, 2542 Stillwater Dr., Lancaster, CA (US) 93536; **Joseph J. Schwab**, 16352 Bradbury, Huntington Beach, CA (US) 92647; **Joseph D. Lichtenhan**, 2 Chestnut Point, Petal, MS (US) 39465

(*) Notice: Subject to any disclaimer, the term of this patent is extended or adjusted under 35 U.S.C. 154(b) by 152 days.

(21) Appl. No.: **10/815,544**

(22) Filed: **Mar. 31, 2004**

Related U.S. Application Data

(63) Continuation-in-part of application No. 09/818,265, filed on Mar. 26, 2001, now Pat. No. 6,716,919.

(60) Provisional application No. 60/459,357, filed on Mar. 31, 2003, provisional application No. 60/192,083, filed on Mar. 24, 2000.

(51) **Int. Cl.**
C08F 8/00 (2006.01)

(52) **U.S. Cl.** **525/101**; 525/104

(58) **Field of Classification Search** 525/101, 525/104
See application file for complete search history.

(56) **References Cited**

U.S. PATENT DOCUMENTS

5,047,492 A * 9/1991 Weidner et al. 528/15
5,412,053 A * 5/1995 Lichtenhan et al. 528/9
5,484,867 A * 1/1996 Lichtenhan et al. 528/9
5,589,562 A * 12/1996 Lichtenhan et al. 528/9
5,726,247 A * 3/1998 Michalczyk et al. 525/102
5,876,686 A * 3/1999 Michalczyk et al. 423/592.1
5,939,576 A * 8/1999 Lichtenhan et al. 556/460
5,942,638 A * 8/1999 Lichtenhan et al. 556/460
6,075,068 A * 6/2000 Bissinger 523/116
6,100,417 A * 8/2000 Lichtenhan et al. 556/460
6,228,904 B1 * 5/2001 Yadav et al. 523/210
6,245,849 B1 * 6/2001 Morales et al. 524/442

* cited by examiner

Primary Examiner—Bernard Lipman
(74) *Attorney, Agent, or Firm*—David H. Jaffer; Pillsbury Winthrop Shaw Pittman LLP

(57) **ABSTRACT**

A method of using nanostructured chemicals as alloying agents for the reinforcement of flouropolymer microstructures, including polymer coils, domains, chains, and segments, at the molecular level. Because of their tailorable compatibility with fluorinated polymers, nanostructured chemicals can be readily and selectively incorporated into polymers by direct blending processes. Properties most favorably improved are time dependent mechanical and thermal properties such as heat distortion, creep, compression set, shrinkage, modulus, hardness and abrasion resistance. ln addition to mechanical properties, other physical properties are favorably improved, including lower thermal conductivity, fire resistance, and improved oxygen permeability. These improved properties may be useful in a number of applications, including space-survivable materials and creep resistant seals and gaskets. lmproved surface properties may be useful for applications such as anti-icing or non-wetting surfaces or as low friction surfaces.

19 Claims, 6 Drawing Sheets

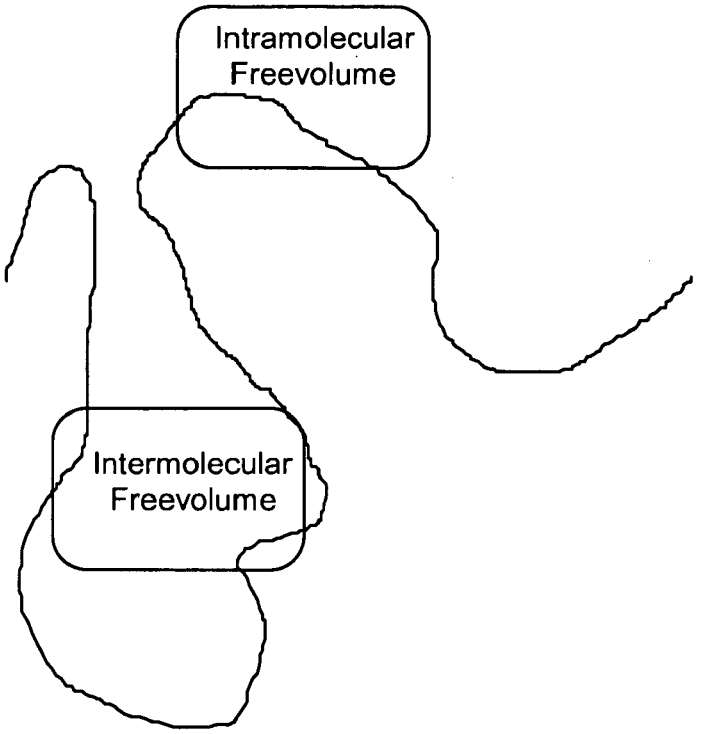
Intramolecular
Freevolume
Intermolecular
Freevolume

FIG. 1

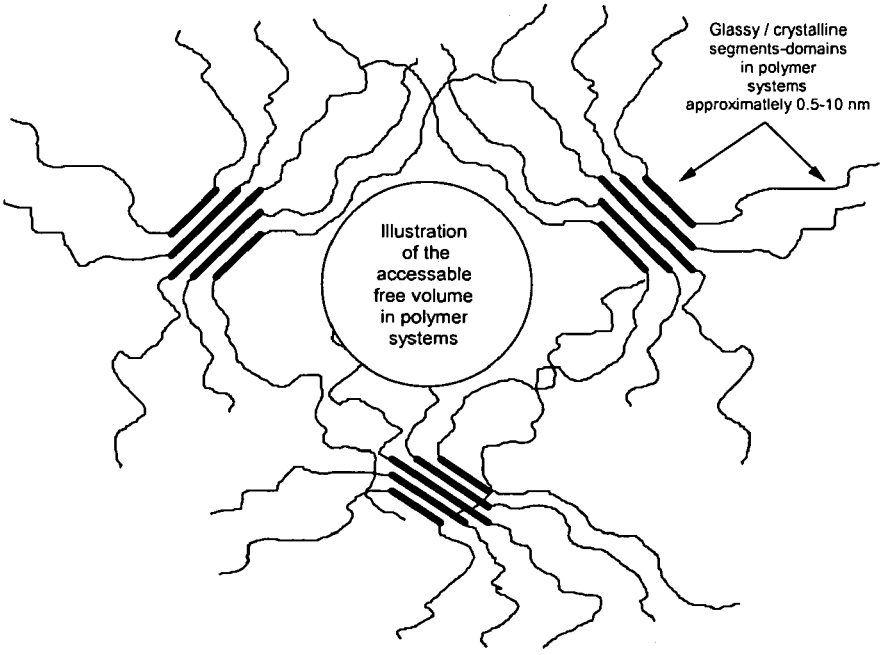
Glassy / crystalline
segments-domains
in polymer
systems
approximatlely 0.5-10 nm
Illustration
of the
accessable
free volume
in polymer
systems

FIG. 2

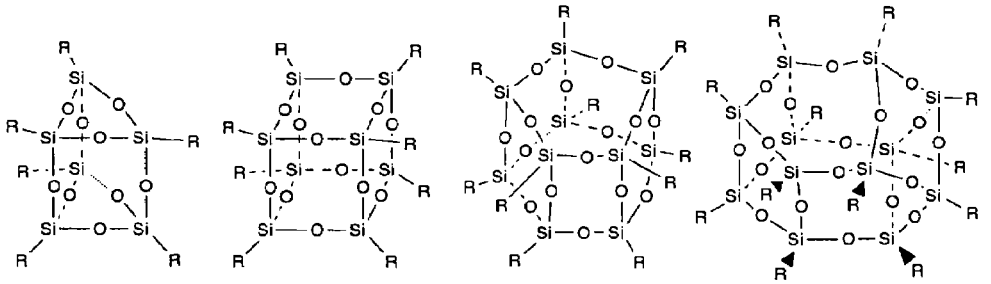

$[(RSiO_{1.5})_6]\Sigma_6$ $[(RSiO_{1.5})_8]\Sigma_8$ $[(RSiO_{1.5})_{10}]\Sigma_{10}$ $[(RSiO_{1.5})_{12}]\Sigma_{12}$

FIG. 3

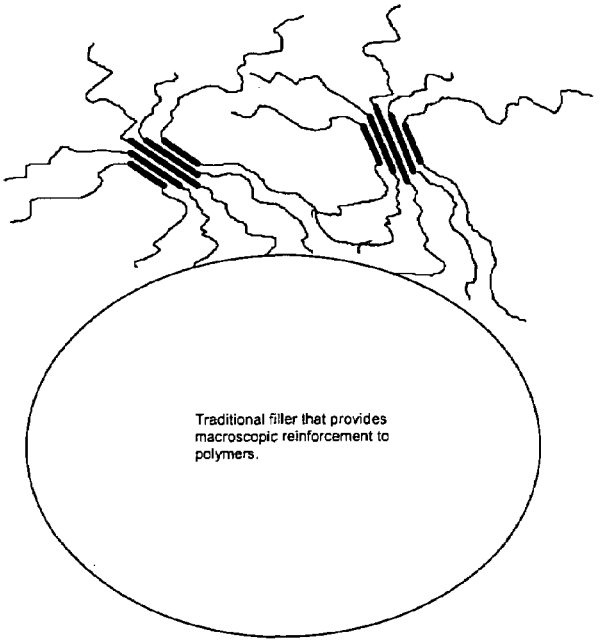

FIG. 4

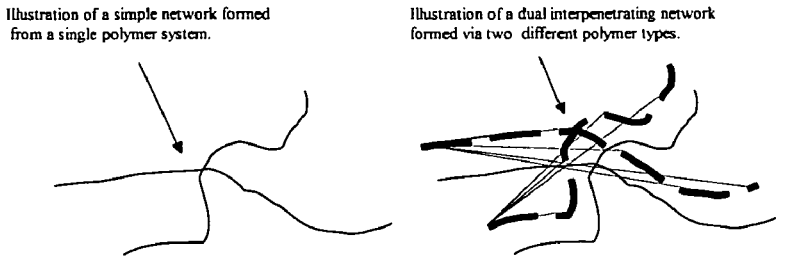
Illustration of a simple network formed from a single polymer system.
Illustration of a dual interpenetrating network formed via two different polymer types.

FIG. 5

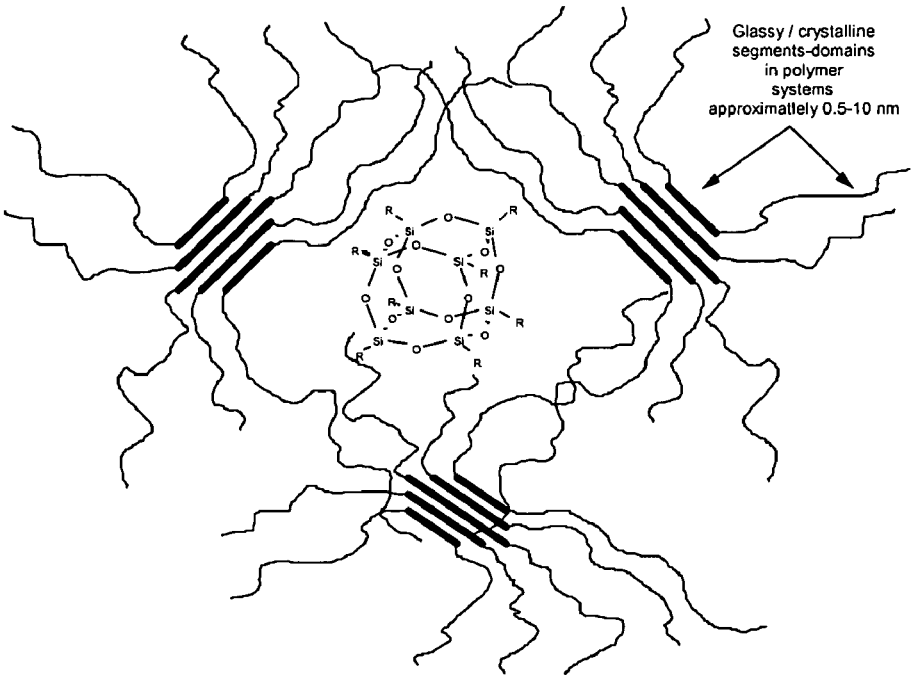
Glassy / crystalline segments-domains in polymer systems approximatlely 0.5-10 nm

FIG. 6

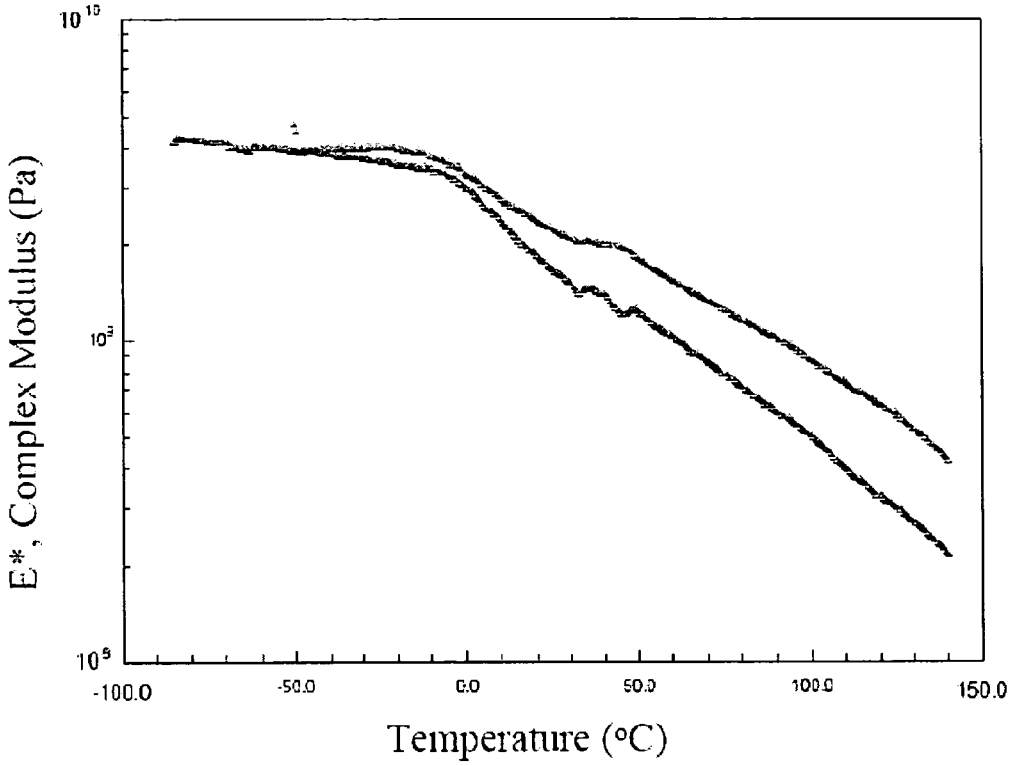

FIG. 7

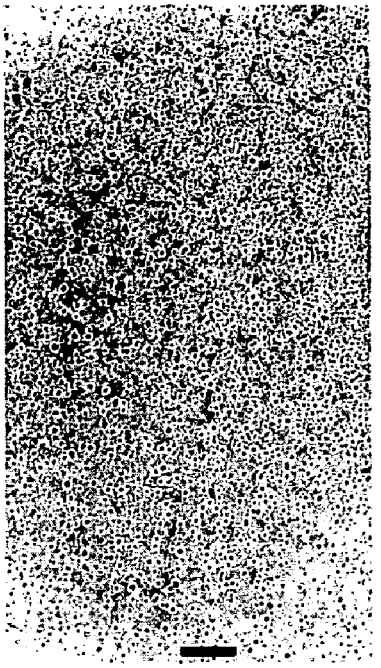
50 nm

FIG. 8

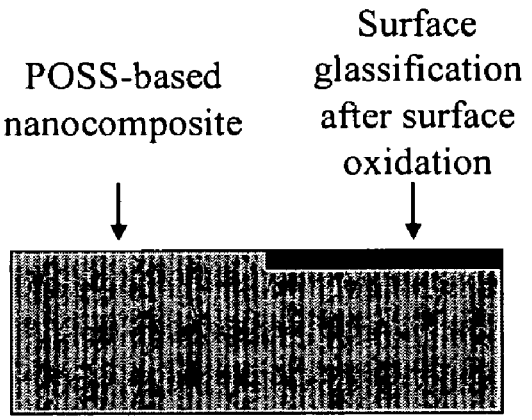
POSS-based nanocomposite
Surface glassification after surface oxidation

FIG .9

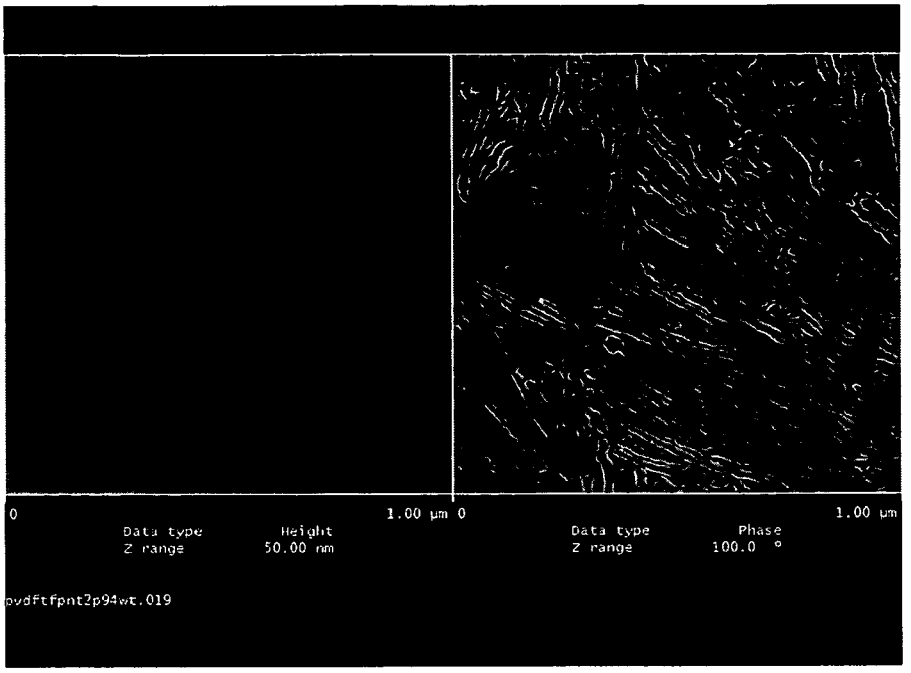
0
1.00 µm 0
1.00 µm
Data type
Height
Z range
50.00 nm
Data type
Phase
Z range
100.0 °
pvdftfpnt2p94wt.019

Fig. 10

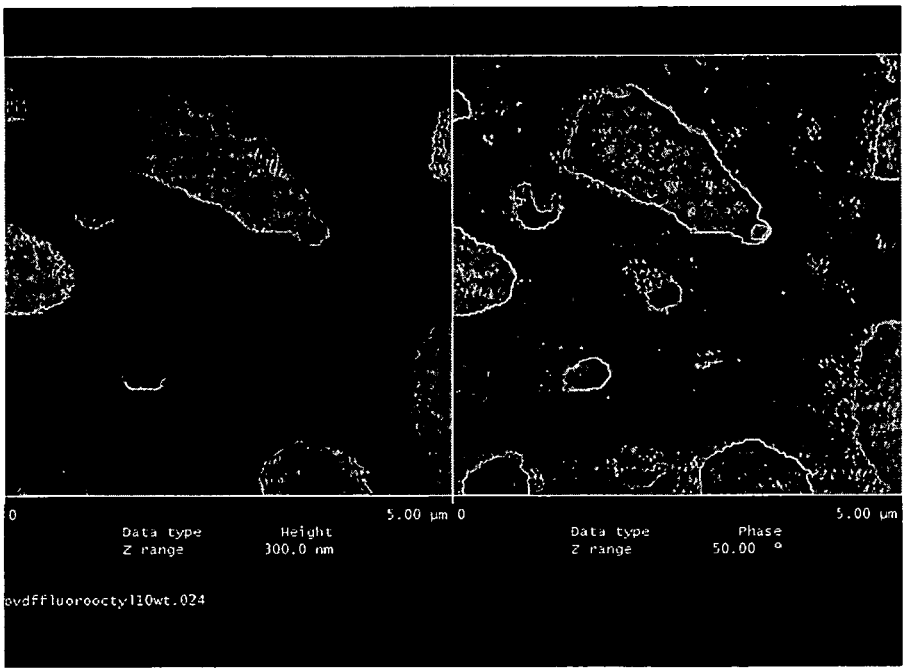
0
5.00 µm 0
5.00 µm
Data type
Height
Z range
300.0 nm
Data type
Phase
Z range
50.00 °
pvdffluorooctyl10wt.024

Fig. 11

NANOSTRUCTURED CHEMICALS AS ALLOYING AGENTS IN FLUORINATED POLYMERS

CROSS-REFERENCE TO RELATED APPLICATIONS

This application claims the benefit of U.S. Provisional Application No. 60/459,357 filed on Mar. 31, 2003, and is a continuation-in-part of U.S. patent application Ser. No. 09/818,265 filed Mar. 26, 2001, now U.S. Pat. No. 6,716,919, which claims the benefit of U.S. Provisional Application No. 60/192,083, filed Mar. 24, 2000.

FIELD OF THE INVENTION

This invention relates generally to methods for enhancing the properties of thermoplastic and thermoset fluorinated polymer and fluid compositions and, more particularly, to methods for the incorporation of nanostructured chemicals into fluorinated polymers and fluorinated fluids.

This invention also relates to several applications of the fluorinated polymers with improved properties. These applications include space-survivable materials and creep resistant seals and gaskets. Improved polymer surface properties may be useful for applications such as anti-icing or non-wetting surfaces or as low friction surfaces.

BACKGROUND OF THE INVENTION

It has long been recognized that the properties of polymers can be tailored to a high degree through variables such as polymer sequence, structure, additive and filler incorporation, composition, morphology, thermodynamic and kinetic processing control. It is similarly known that various sizes and shapes of fillers, and particulates (e.g. calcium carbonate, silica, carbon black etc.) can be incorporated into preformed polymers or prepolymers or monomer mixtures to enhance physical and material properties of the resulting formulations.

In their solid state all polymers (including amorphous, semi-crystalline, crystalline, and rubber, etc.) possess considerable amounts of internal and external free volume (see FIG. **1**). The free volume of a polymer has a tremendous impact on its physical properties, since it is within this volume that the dynamic properties (e.g. reptation, translation, rotation, crystallization) of polymer chains primarily operate and in turn influence fundamental physical properties such as density, thermal conductivity, glass transition, melt transition, modulus, relaxation, and stress transfer.

The accessibility of free volume in a polymer system depends greatly on its morphology and on the size of the agent desired to occupy the free volume. As shown in FIG. **2**, for example, denser regions and phase separation within a polymer can both increase and decrease the thermodynamic and kinetic access to such areas. Because of its influence on thermodynamic and kinetic properties, polymer morphology and free volume dimension are major factors that limit the ability of conventional fillers from accessing the free volume regions in a polymer system. Additional processing/compounding effort is normally required to force compatibilization between a filler and a polymer system because conventional fillers are physically larger than most polymer dimensions, are chemically dissimilar, and usually are high melting solids.

Prior art in fluoropolymers has focused on modifications through the formation of an inorganic interpenetrating network that is either partially or fully condensed and is in contact with or dispersed amoungst the fluoropolymer chains. See U.S. Pat. Nos. 5,876,686 and 5,726,247. Similarily modifications have been described that enhance properties through the continuous or discontinuous dispersion of macro, micro and nanoscale particulates of a dissimilar composition (e.g. inorganic) relative to that of the fluoropolymer. In either case the function of the inorganic network or filler particle is to reduce the relative slippage or motion of the fluoropolymer chains and segments relative to each other. The combination of reduced chain motion with the thermally stable inorganic component utlimately enhances physical properties such as dimensional stability, impact resistance, tensile and compressive strengths, thermal stability, electrical properties, abrasion and chemical resistance, shrinkage and expansion reduction. Unfortunately, all of the prior art either suffers from process complexity, a length scale of the reinforcement that is too large to sufficiently access polymer free volume, or reinforcement that lacks sufficient geometrical definition to provide structure regularity and reinforcement at the molecular (10^{-10} m) and nanoscopic (10^{-9} m) length scales. As illustrated in FIG. **4**, fillers are geometrically ill defined solid particulates that macroscopically or nanoscopically reinforce large associated or nearby groups of polymers rather than the individual chains and segments within these polymers. As illustrated in FIG. **5**, incompletely condensed or completely condensed interpenetrating networks also lack sufficient geometrical definition to provide structure regularity and reinforcement of fluoropolymer chains.

Furthermore, it has been calculated that as filler sizes decrease below 50 nm, they would become more resistant to sedimentation and more effective at providing reinforcement to polymer systems. The full application of this theoretical knowledge, however, has been thwarted by the lack of a practical source of particulate reinforcement or reinforcements which are geometrically well defined, and monodisperse and with diameters below the 10 nm range and especially within the 1 nm to 5 nm range. Particularly desirable are monodisperse, nanoscopically sized chemicals with precise chemical compositions, rigid and well defined geometrical shapes, and which are dimensionally large enough to provide reinforcement of polymer chains. Such nanoscopic chemicals are desirable as they are expected to form the most stable dispersions within polymer systems, would be well below the length scale necessary to scatter light and hence are visually nondetectable when incorporated into fluoropolymers, and would be chemically compatible with fluoropolymers and dissolve into and among the polymer chains, thus eliminating the need for extensive dispersion or reactive self assembly or the complex processing requirements of the prior art.

Recent developments in nanoscience have enabled the ability to cost effectively manufacture commercial quantities of materials that are best described as nanostructured chemicals due to their specific and precise chemical formula, hybrid (inorganic-organic) chemical composition, large physical size relative to the size of traditional chemical molecules (0.3–0.5 nm), and small physical size relative to larger sized traditional fillers (>50 nm).

Nanostructured chemicals are best exemplified by those based on low-cost Polyhedral Oligomeric Silsesquioxanes (POSS) and Polyhedral Oligomeric Silicates (POS). FIG. **3** illustrates some representative examples of monodisperse nanostructured chemicals, which are also known as POSS Molecular Silicas.

These systems contain hybrid (i.e., organic-inorganic) compositions in which the internal frameworks are primarily comprised of inorganic silicon-oxygen bonds. The exterior of a nanostructure is covered by both reactive and nonreactive organic functionalities (R), which ensure compatibility and tailorability of the nanostructure with organic polymers. These and other properties of nanostructured chemicals are discussed in detail in U.S. Pat. Nos. 5,412,053 and 5,484,867, both are expressly incorporated herein by reference in their entirety. These nanostructured chemicals are of low density, exhibit excellent inherent fire retardancy, and can range in diameter from 0.5 nm to 5.0 nm.

Prior art associated with fillers, plasticizers, interpenetrating networks, and polymer morphology has not been able to adequately control polymer chain, coil and segmental motion at the 1 nm–10 nm level. Furthermore, the mismatch of chemical potential (e.g., solubility, miscibility, etc.) between fluoro-based polymers and inorganic-based fillers and chemicals results in a high level of heterogeneity in compounded polymers that is akin to oil mixed with water. Therefore, there exists a need for appropriately sized chemical reinforcements for polymer systems with controlled diameters (nanodimensions), distributions and with tailorable chemical functionality. In addition, it would be desirable to have easily compoundable nanoreinforcements that have chemical potential ranges (misibilities) similar to the various fluorinated polymer and fluorinated fluid systems.

SUMMARY OF THE INVENTION

The present invention describes methods of preparing new polymer compositions by incorporating nanostructured chemicals into polymers. The resulting nano-alloyed polymers are wholly useful by themselves or in combination with other polymers or in combination with macroscopic reinforcements such as fiber, clay, glass mineral and other fillers. The nano-alloyed polymers are particularly useful for producing polymeric compositions with desirable physical properties such as adhesion to polymeric, composite and metal surfaces, water repellency, reduced melt viscosity, low dielectric constant, resistance to abrasion and fire, biological compatibility, and optical quality plastics. The preferred compositions presented herein contain two primary material combinations: (1) nanostructured chemicals, nanostructured oligomers, or nanostructured polymers from the chemical classes of polyhedral oligomeric silsesquioxanes, polysilsesquioxanes, polyhedral oligomeric silicates, polysilicates, polyoxometallates, carboranes, boranes, and polymorphs of carbon; and (2) fluorinated polymer systems such as: PFA, MFA, PVDF, semicrystalline, crystalline, glassey, elastomeric, oils, and lubricants thereof as derived from hydrocarbons, or silicones and fluoropolymers or copolymers thereof.

Preferably, the method of incorporating nanostructured chemicals into such fluoropolymers is accomplished via blending of the chemicals into the polymers. All types and techniques of blending, including melt blending, dry blending, solution blending, reactive and nonreactive blending are effective.

In addition, selective incorporation of a nanostructured chemical into a specific region of a polymer can be accomplished by compounding into the polymer a nanostructured chemical with a chemical potential (miscibility) compatible with the chemical potential of the region within the polymer to be alloyed. Because of their chemical nature, nanostructured chemicals can be tailored to show compatibility or incompatibility with selected sequences and segments within polymer chains and coils. Their physical size in combination with their tailorable compatibility enables nanostructured chemicals to be selectively incorporated into fluoroplastics and control the dynamics of coils, blocks, domains, and segments, and subsequently favorably impact a multitude of physical properties. Properties most favorably improved are time dependent mechanical and thermal properties such as heat distortion, creep, compression set, shrinkage, modulus, hardness and abrasion resistance. In addition to mechanical properties, other physical properties are favorably improved, including lower thermal conductivity, improved fire resistance, and improved oxygen permeability, improved oxidative stability, improved electrical properties and printability.

Creep Resistant Seals and Gaskets

While many fluoropolymers, such as polytetrafluoroethylene (PTFE or Teflon) and fluorinated ethylene/propylene (FEP) are resistant to organic fuels and fluids, creep is often a problem. Creep is the change in dimensions of a molded part resulting from cold flow incurred by continual loading and can cause a polymer press-fit to loosen to an unacceptable condition or even fail. Tensile strength is an important factor in controlling the amount of cold flow in plastics. The higher the tensile strength, the more resistant the plastic is to cold flow and creep. PTFE, for example, has a very low tensile strength. In addition to improving thermal and mechanical properties of fluoropolymers, blended fluorinated POSS reduces the amount of creep. The processing temperature of nearly all fluoropolymers is sufficient to allow the blending of POSS materials. A notable exception is PTFE. While the processing temperature of PTFE is too high to allow conventional blending, supercritical methods may allow fluorinated POSS to be incorporated into PTFE.

Space-survivable Fluorinated Materials

Fluorinated POSS can be blended into several fluoropolymers, including poly(vinylidinefluoride) (PVDF) and FEP, both of which are used in spacecraft coatings. These compounds significantly improve oxidation resistance due to a rapidly forming ceramic-like, passivating and self-healing silica layer when exposed to high incident fluxes of atomic oxygen (AO). AO is the predominant species in low earth orbit (LEO) responsible for material degradation. This is because the collision energy of AO (~5 eV) exceeds the bond strength of carbon—carbon bonds in fluoropolymers (~4.3 eV). The silicon-oxygen bonds present in the POSS cage have stronger bond dissociation energies (~8.3 eV). The POSS cage is not destroyed by the AO, but forms a passivating self-rigidizing/self-healing silica layer, which protects the underlying virgin polymer.

Anti-icing or Non-wetting Applications

Fluorinated POSS films show remarkable surface properties. The contact angle of water on a spin-cast surface of fluorodecyl POSS is 140° in an unoptimized process. Surprisingly, this is 30 degrees higher than PTFE. A higher the contact angle indicates lower surface energy. These fluorinated POSS compounds have the potential to form ultrahydrophobic surfaces and also reduce the surface energy of the fluoropolymers into which they are blended. This also leads to increased abrasion resistance and lubricity. Anti-icing or non-wetting applications may be possible using this technology. Lubricants and low friction surfaces can also be developed. These surfaces would be further enhanced by the creep reduction mentioned above.

BRIEF DESCRIPTION OF THE DRAWINGS

FIG. **1** shows the relative positions of an internal free volume and an external free volume of a polymer.

FIG. **2** illustrates some different regions and phase separation within a polymer.

FIG. **3** illustrates some representative examples of monodisperse nanostructured chemicals.

FIG. **4** illustrates the macroscopic reinforcement a traditional filler provides to polymers.

FIG. **5** illustrates the lack of geometrical definition of interpenetrating network polymers.

FIG. **6** illustrates a nanoreinforced polymer microstructure.

FIG. **7** is a graph of storage modulus (E*) relative to temperature (° C.) for nonreinforced fluoropolymer and POSS-reinforced fluoropolymer.

FIG. **8** is a picture of a fluoropolymer showing dispersion of cages at the 1–5 nm level.

FIG. **9** shows formation of passivating surface layer upon oxidation of a POSS fluoropolymer.

FIG. **10** is an AFM image of 3,3,3-trifluoropropyl$_n$T$_n$ blended into PVDF in 2.94 wt. %. The absence of POSS domains may indicate that the POSS is well dispersed.

FIG. **11** is an AFM image of 1H,1H,2H,2H-heptadecafluorodecyl T$_n$ blended into PVDF in 10 wt. %. The POSS appears to be forming domains within the polymer matrix, indicating that the POSS with a longer fluoroalkyl chain is less soluble in PVDF, or that a 10 wt. % blend is too high for this particular POSS compound. 10% 3,3,3-trifluoropropyl T$_n$ was blended into PVDF with no domain appearance by AFM.

DEFINITION OF FORMULA REPRESENTATIONS FOR NANOSTRUCTURES

For the purposes of understanding this invention's chemical compositions the following definitions for formula representations of Polyhedral Oligomeric Silsesquioxane (POSS) and Polyhedral Oligomeric Silicate (POS) nanostructures are made.

Polysilsesquioxanes are materials represented by the formula $[RSiO_{1.5}]_\infty$ where ∞ represents molar degree of polymerization and R=represents organic substituent (H, siloxy, cyclic or linear aliphatic or aromatic groups that may additionally contain reactive functionalities such as alcohols, esters, amines, ketones, olefins, ethers or halides or which may contain fluorinated groups). Polysilsesquioxanes may be either homoleptic or heteroleptic. Homoleptic systems contain only one type of R group while heteroleptic systems contain more than one type of R group.

POSS and POS nanostructure compositions are represented by the formula:

$[(RSiO_{1.5})_n]_{\Sigma\#}$ for homoleptic compositions

$[(RSiO_{1.5})_n(R'SiO_{1.5})_m]_{\Sigma\#}$ for heteroleptic compositions (where R≠R')

$[(RSiO_{1.5})_n(RXSiO_{1.0})_m]_{\Sigma\#}$ for functionalized heteroleptic compositions (where R groups can be equivalent or inequivalent)

In all of the above R is the same as defined above and X includes but is not limited to OH, Cl, Br, I, alkoxide (OR), acetate (OOCR), peroxide (OOR), amine (NR_2) isocyanate (NCO), and R. The symbols m and n refer to the stoichiometry of the composition. The symbol Σ indicates that the composition forms a nanostructure and the symbol # refers to the number of silicon atoms contained within the nanostructure. The value for # is usually the sum of m+n, where n ranges typically from 1 to 24 and m ranges typically from 1 to 12. It should be noted that Σ# is not to be confused as a multiplier for determining stoichiometry, as it merely describes the overall nanostructural characteristics of the system (aka cage size).

DETAILED DESCRIPTION OF THE INVENTION

The present invention teaches the use of nanostructured chemicals as alloying agents for the reinforcement of polymer coils, domains, chains, and segments at the molecular level.

The keys that enable nanostructured chemicals to function as molecular level reinforcing and alloying agents are: (1) their unique size with respect to polymer chain dimensions, and (2) their ability to be compatibilized with polymer systems to overcome repulsive forces that promote incompatibility and expulsion of the nanoreinforcing agent by the polymer chains. That is, nanostructured chemicals can be tailored to exhibit preferential affinity/compatibility with some polymer microstructures through variation of the R groups on each nanostructure. At the same time, the nanostructured chemicals can be tailored to be incompatible with other microstructures within the same polymer, thus allowing for selective reinforcement of specific polymer microstructure. Therefore, the factors to effect a selective nanoreinforcement include specific nanosizes of nanostructured chemicals, distributions of nanosizes, and compatabilities and disparities between the nanostrucutured chemical and the polymer system.

Nanostructured chemicals, such as the POSS Molecular Silicas illustrated in FIG. **3**, are available as both solids and oils. Both forms dissolve in molten or in solvents, or directly into polymers thus solving the long-standing dispersion problem associated with traditional particulate fillers or the mixing complexities associated with interpenetrating networks. Moreover, because POSS nanocages dissolve into plastics at the molecular level, the forces (i.e., free energy) from solvation/mixing are sufficient to prevent POSS from coalescing and forming agglomerated domains as occurs with traditional and other organofunctionalized fillers. Agglomeration of particulate fillers has been a problem that has traditionally plagued formulators and molders.

Table 1 below relates the size range of POSS cages relative to polymer dimensions and filler sizes. The size of POSS is roughly equivalent to that of most polymer dimensions, thus at a molecular level POSS can effectively alter the motion of polymer chains.

TABLE 1

Relative sizes of POSS, polymer dimensions, and fillers.

Particle Type	Particle Diameter
Amorphous Segments	0.5–5 nm
Octacyclohexyl POSS	1.5 nm
Random Polymer Coils	5–10 nm
Particulate Silica	9–80 nm
Crystalline Lamellae	1.0–9,000 nm
Fillers/Organoclays	2–100,000 nm

The ability of POSS to control chain motion is particularly apparent when POSS is grafted onto a polymer chain.

See U.S. Pat. Nos. 5,412,053; 5,484,867; 5,589,562; and 5,047,492, all expressly incorporated by reference herein. When POSS nanostructures are covalently linked to the polymer chain they act to retard chain motion and greatly enhance time dependent properties such as T_g, HDT, Creep and Set, which correlate to increased modulus, hardness, and abrasion resistance. The present invention now shows that similar property enhancements can be realized by the direct blending of nanostructured chemicals into plastics. This greatly simplifies the prior art processes.

Furthermore, because POSS nanostructured chemicals possess spherical shapes (per single crystal X-ray diffraction studies), like molecular spheres, and because they dissolve, they are also effective at reducing the viscosity of polymer systems. This benefit is similar to what is produced through the incorporation of plasticizers into polymers, yet with the added benefits of reinforcement of the individual polymer chains due to the nanoscopic nature of the chemicals (see FIG. **6**). Thus ease of processability and reinforcement effects are obtainable through the use of nanostructured chemicals (e.g. POSS, POS) where as prior art would have required the use of both plasticizers and fillers or the covalent linking of POSS to the polymer chains. Additional benefit may be realized by the usage of nanostructured chemicals with monodisperse cage sizes (i.e., polydispersity=1) or from polydisperse cage sizes. Such control over compatibility, dispersability, and size is unprecedented for all traditional filler, plasticizer, and interpenetrating network technologies.

EXAMPLES

General Process Variables Applicable To All Processes

As is typical with chemical processes there are a number of variables that can be used to control the purity, selectivity, rate and mechanism of any process. Variables influencing the process for the incorporation of nanostructured chemicals (e.g. POSS/POS etc.) into plastics include the size and polydispersity, and composition of the nanostructured chemical. Similarly the molecular weight, polydispersity and composition of the polymer system must also be matched with that of the nanostructured chemical. Finally, the kinetics, thermodynamics, and processing aids used during the compounding process are also tools of the trade that can impact the loading level and degree of enhancement resulting from incorporation of nanostructured chemicals into polymers. Blending processes such as melt blending, dry blending and solution mixing blending are all effective at mixing and alloying nanostructured chemical into plastics.

Example 1

Synthesis

Example 1a

(Heptadecafluoro-1,1,2,2-tetrahydrodecyl)triethoxysilane (6.10 g), deionized water (0.27 g), and potassium hydroxide (2.088 mg) were added to a 10 mL volumetric flask. The balance of the volume to 10 mL was filled with ethanol. The contents were transferred to a 25 mL round bottom flask with a Teflon covered magnetic stir bar. The contents were stirred at room temperature overnight under nitrogen. A fine white powder was formed. The product was rinsed with ethanol and dried. A 92.3% yield of pure $[(RSiO_{1.5})_8]_{\Sigma 8}$) was obtained. ^{29}Si NMR δ:—66.76 ppm.

Example 1b

(Tridecafluoro-1,1,2,2-tetrahydrooctyl)triethoxysilane (5.10 g), deionized water (0.27 g), and potassium hydroxide (2.088 mg) were added to a 10 mL volumetric flask. The balance of the volume to 10 mL was filled with ethanol. The contents were transferred to a 25 mL round bottom flask with a Teflon covered magnetic stir bar. The contents were stirred at room temperature overnight under nitrogen. A fine white powder was formed. The product was rinsed with ethanol and dried. A 92% yield of pure $[(RSiO_{1.5})_8]_{\Sigma 8}$) was obtained. ^{29}Si NMR δ:—66.69 ppm.

Example 2

Melt Compounding

Example 2a

Poly(vinylidene fluoride) (PVDF) was used. PVDF (Hylar 460) was obtained from Solvay Solexis. The melting temperature determined by differential scanning calorimetry (DSC) was in the range of 150–164° C. $[(3,3,3\text{-Trifluoropropyl}_n SiO_{1.5})_n]\Sigma_n$ was blended into PVDF using a twin screw extruder (MicroCompounder, DACA Instruments). The PVDF and POSS were mixed thoroughly for 3 minutes at 177° C. Three samples were prepared with POSS weight percents of 2.5%, 5%, and 10%, respectively.

Example 2b

PVDF was used in this study. $[(1H,1H,2H,2H\text{-heptadecafluorodecyl}_n SiO_{1.5})_n]\Sigma_n$ was blended into PVDF using a twin screw extruder. The PVDF and POSS were mixed thoroughly for 3 minutes at 177° C. Three samples were prepared with POSS weight percents of 2.5%, 5%, and 10%, respectively.

Example 2c

Perfluoroalkoxy polymer (PFA) was used in this study. PFA was obtained from duPont. The melting temperature determined by DSC was in the range of 311–319° C. $[(1H,1H,2H,2H\text{-heptadecafluorodecyl}_n SiO_{1.5})_n]\Sigma_n$ was blended into PFA using the twin screw extruder. The PFA and POSS were mixed thoroughly for 3 minutes at 375° C. Two samples were prepared with POSS weight percents of 2.5% and 10%, respectively.

Example 2d

PFA was used in this study. $[(c\text{-pentyl})SiO_{1.5})_7(c\text{-pentyl})(OH)SiO_{1.0})_3]\Sigma_7$ was blended into PFA using the twin screw extruder. The PFA and POSS were mixed thoroughly for 3 minutes at 750° C. A sample was prepared with a POSS weight percent of 2%.

Example 2e

PFA was used in this study. $[(c\text{-pentyl})SiO_{1.5})_7(H)SiO_{1.5})_3]\Sigma_8$ was blended into PFA using the twin screw extruder. The PFA and POSS were mixed thoroughly for 3 minutes at 750° C. A sample was prepared with a POSS weight percent of 5%.

A series of Nanostructured POSS Chemicals were compounded into fluoropolymer at the 1 wt %–50 wt % level using a twin screw melt extruder operating at 80–120 rpm and 190° C. Both POSS and the polymer were dried prior to compounding to ensure a maximum state of alloying. After

compounding, the POSS-reinforced samples were then molded into discs, dogbones and other test specimens and subjected to analysis and characterization. The viscoelastic response as represented by the values for storage modulus (E*) relative to temperature (° C.) of the POSS-reinforced fluoropolymer is shown in FIG. 7.

Various sizes of POSS molecular silicas were observed to have a pronounced effect on the degree to which the modulus was retained at elevated temperatures. Overall it was observed that the Octameric $[(RSiO_{1.5})_8]\Sigma_8$ and dodecametic $[(RSiO_{1.5})_{12}]\Sigma_{12}$ POSS were most effective at retaining the modulus at elevated temperatures. The fracture toughness and other mechanical properties and physical properties of the POSS-alloyed fluoropolymers were also noticeably improved. The mechanism for this enhancement was observed to be the restriction of the motion of the polymer segments and subsequent polymer chains in the fluoropolymer (see FIG. **6**). The mechanism erosion resistance in space is attributed to the in situ formation of a passivating glassy surface layer (see FIG. **9**). Similar levels of enhancement have been observed for other fluoropolymers (e.g. MFA, PFA, PVDF, TFE, etc.).

Alternate Method: Solvent Assisted Formulation. POSS can be added to a vessel containing the desired polymer, prepolymer or monomers and dissolved in a sufficient amount of an organic solvent (e.g. hexane, toluene, dichlormethane, etc.) or fluorinated solvent to effect the formation of one homogeneous phase. The mixture is then stirred under high shear at sufficient temperature to ensure adequate mixing for 30 minutes and the volatile solvent is then removed and recovered under vacuum or using a similar type of process including distillation. Note that supercritical fluids such as CO_2 can also be utilized as a replacement for the flammable hydrocarbon solvents. The resulting formulation may then be used directly or for subsequent processing.

Example 3

Incorporation into Fluorinated Fluids

Nanostructured POSS was compounded into fluoropolymer fluids in the amounts ranging from 1%, to 50%, and various physical properties of the alloyed fluids were measured and compared with the same physical properties of the base fluorpolymer fluid (Table 3). The enhanced properties of POSS-reinforced fluoropolymer fluid are apparent. Similar levels of enhancements were observed with other fluoro polymer fluids and from the incorporation of POSS fluoropolymer fluids into other polymers.

The mechanism for the physical property enhancements is attributed to the restriction of motion of the polymer chains (see FIG. **6**). The mechanism erosion resistance in space is attributed to the in situ formation of a passivating glassy surface layer (see FIG. **9**).

Example 4

A transmission electron micrograph was taken of a fractured POSS fluoropolymer monolith of that was composed of 10% $[(RSiO_{1.5})_8]_{\Sigma 8}$ (see FIG. **8**), which illustrates the molecular level dispersion that can be achieved in polymers via compounding. Specifically, the black dots in FIG. **8** represent POSS molecular silica dispersed at the 1 nm to 3 nm level.

The invention claimed is:

1. A method of alloying a nanostructured chemical selected from the group consisting of POSS and POS into a fluoropolymer, comprising the step of compounding the nanostructured chemical into the fluoropolymer.

2. A method according to claim **1**, wherein a plurality of nanostructured chemicals is compounded into the polymer.

3. A method according to claim **1**, wherein the fluoropolymer is in a physical state selected from the group consisting of oils, amorphous, semicrystalline, crystalline, elastomeric and rubber.

4. A method according to claim **1**, wherein the fluoropolymer contains a chemical sequence and related polymer microstructure.

5. A method according to claim **1**, wherein the fluoropolymer is a polymer coil, a polymer domain, a polymer chain, a polymer segment, or mixtures thereof.

6. A method according to claim **1**, wherein the nanostructured chemical reinforces the fluoropolymer at a molecular level.

7. A method according to claim **1**, wherein the compounding is nonreactive.

8. A method according to claim **1**, wherein the compounding is reactive.

9. A method according to claim **1**, wherein a physical property of the fluoropolymer is improved as a result of incorporating the nanostructured chemical into the fluoropolymer.

10. A method according to claim **9**, wherein the physical property is selected from the group consisting of adhesion to a polymeric surface, adhesion to a composite surface, adhesion to a metal surface, water repellency, density, low dielectric constant, thermal conductivity, glass transition, viscosity, melt transition, storage modulus, relaxation, stress transfer, abrasion resistance, fire resistance, biological compatibility, gas permeability, porosity, and optical quality.

11. A method according to claim **1**, wherein the compounding step is accomplished by blending the nanostructured chemical into the fluoropolymer.

12. A method according to claim **11**, wherein the compounding step is accomplished by a blending process selected from the group consisting of melt blending, dry blending, and solution blending.

13. A method according to claim **1**, wherein the nanostructured chemical functions as a plasticizer.

14. A method according to claim **1**, wherein the nanostructured chemical functions as a filler.

15. A method according to claim **1**, wherein the nanostructured chemical is selectively compounded into the fluoropolymer such that the nanostructured chemical is incorporated into a predetermined region within the fluoropolymer.

16. A method according to claim **1**, wherein the molecular motion of a fluoropolymer is controlled by comprising compounding the nanostructured chemical into the fluoropolymer.

17. A method according to claim **16**, wherein a time dependent property is enhanced as a result of compounding the nanostructured chemical into the fluoropolymer.

18. A method according to claim **17**, wherein the time dependent property is selected from the group consisting of T_g, HDT, modulus, creep, set, permeability, erosion resistance, abrasion resistance.

19. A method according to claim **15**, wherein the nanostructured chemical has chemical properties compatible with the predetermined region of the fluoropolymer, whereby the compounding reinforces the fluoropolymer.

* * * * *

APPENDIX B: U.S. PATENT 7,897,667

US007897667B2

(12) **United States Patent**
Mabry et al.

(10) **Patent No.: US 7,897,667 B2**
(45) **Date of Patent: Mar. 1, 2011**

(54) **FLUORINATED POSS AS ALLOYING AGENTS IN NONFLUORINATED POLYMERS**

(75) Inventors: **Joseph M. Mabry**, California City, CA (US); **Timothy S. Haddad**, Lancaster, CA (US); **Sarah Anne Mazzella**, Lancaster, CA (US); **Sukhendu B. Hait**, Hattiesburg, MS (US); **Joseph J. Schwab**, Huntington Beach, CA (US); **Joseph D. Lichtenhan**, Petal, MS (US)

(73) Assignee: **Hybrid Plastics, Inc.**, Hattiesburg, MS (US)

(*) Notice: Subject to any disclaimer, the term of this patent is extended or adjusted under 35 U.S.C. 154(b) by 907 days.

(21) Appl. No.: **11/725,994**

(22) Filed: **Mar. 19, 2007**

(65) **Prior Publication Data**

US 2008/0221262 A1 Sep. 11, 2008

Related U.S. Application Data

(63) Continuation-in-part of application No. 10/815,544, filed on Mar. 31, 2004, now Pat. No. 7,193,015, and a continuation-in-part of application No. 09/818,265, filed on Mar. 26, 2001, now Pat. No. 6,716,919.

(60) Provisional application No. 60/459,357, filed on Mar. 31, 2003, provisional application No. 60/192,083, filed on Mar. 24, 2000.

(51) **Int. Cl.**
C08K 5/24 (2006.01)

(52) **U.S. Cl.** **524/269**

(58) **Field of Classification Search** 524/269
See application file for complete search history.

(56) **References Cited**

U.S. PATENT DOCUMENTS

5,047,492	A	9/1991	Weidner et al.
5,412,053	A	5/1995	Lichtenhan et al.
5,484,867	A	1/1996	Lichtenhan et al.
5,589,562	A	12/1996	Lichtenhan et al.
5,726,247	A	3/1998	Michalczyk et al.
5,876,686	A	3/1999	Michalczyk et al.
5,939,576	A	8/1999	Lichtenhan et al.
5,942,638	A	8/1999	Lichtenhan et al.
6,075,068	A	6/2000	Bissinger
6,100,417	A	8/2000	Lichtenhan et al.
6,228,904	B1	5/2001	Yadav et al.
6,245,849	B1	6/2001	Morales et al.
6,329,490	B1	12/2001	Yamashita et al.
6,716,919	B2	4/2004	Lichtenhan et al.
7,193,015	B1	3/2007	Mabry et al.
2003/0018109	A1	1/2003	Hsiao et al.
2003/0050408	A1	3/2003	Puhala et al.

OTHER PUBLICATIONS

Supplemental European Search Report issued Nov. 2, 2011 for European Patent Application Serial No. 08780474.6.

Primary Examiner — Bernard Lipman
(74) *Attorney, Agent, or Firm* — David H. Jaffer; Pillsbury Winthrop Shaw Pittman LLP

(57) **ABSTRACT**

A method of using fluorinated-nanostructured POSS chemicals as alloying agents for the reinforcement of polymer microstructures, including polymer coils, domains, chains, and segments, at the molecular level. Because of their tailorable compatibility with nonfluorinated polymers, nanostructured chemicals can be readily and selectively incorporated into polymers by direct blending processes. The incorporation of a nanostructured chemical into a polymer favorably impacts a multitude of polymer physical properties. Properties most favorably improved are surface properties, such as lubricity, contact angle, water repellency, deicing, surface tension, and abrasion resistance. Improved surface properties may be useful for applications such as anti-icing surfaces, non-wetting surfaces, low friction surfaces, self cleaning. Other properties improved include time dependent mechanical and thermal properties such as heat distortion, creep, compression set, shrinkage, modulus, hardness and biological compatibility. In addition to mechanical properties, other physical properties are favorably improved, including lower thermal conductivity, dielectric properties, fire resistance, gas permeability and separation. These improved properties may be useful in a number of applications, including space-survivable materials and seals, gaskets, cosmetics, and personal care.

25 Claims, 10 Drawing Sheets

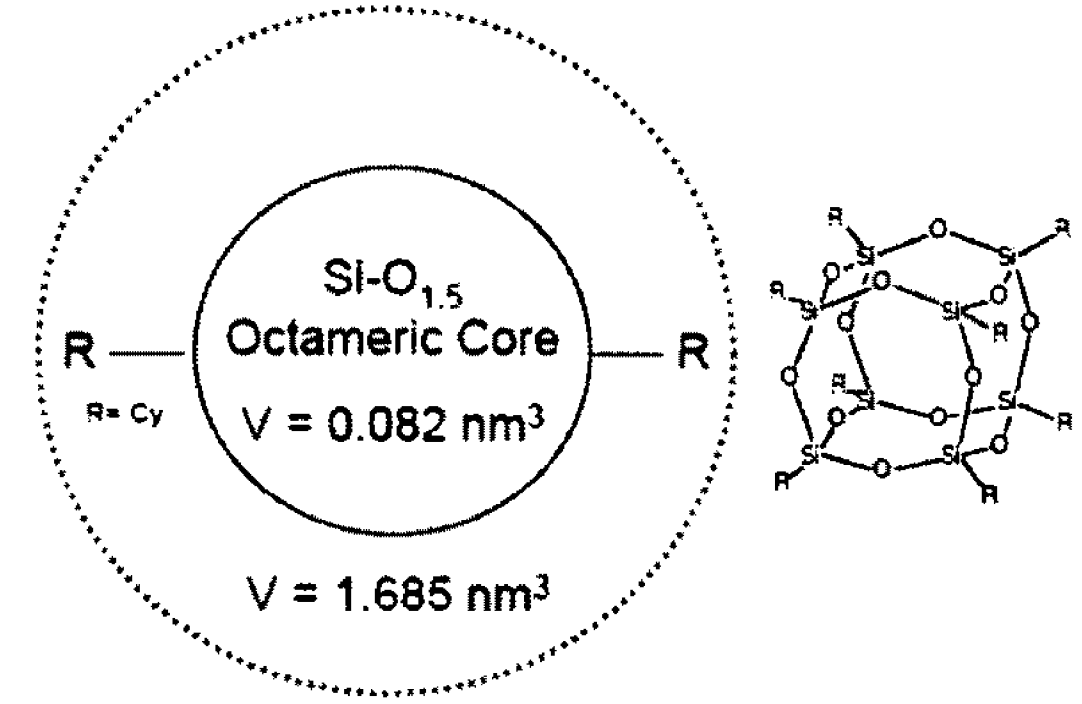
Si-O1.5
Octameric Core
V = 0.082 nm3
R
R
R= Cy
V = 1.685 nm3
Overall POSS Volume = 1.767 nm3

FIG. 1

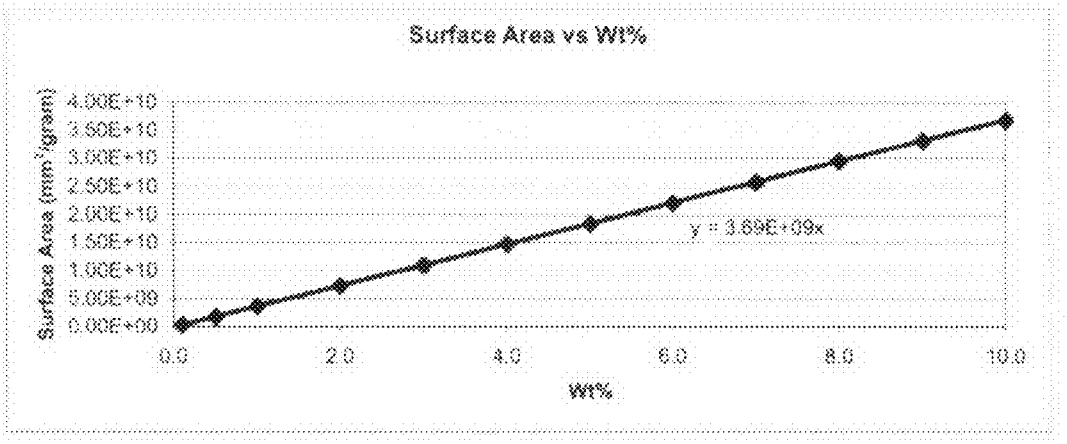
Surface Area vs Wt%
Surface Area (mm²/gram)
4.00E+10
3.50E+10
3.00E+10
2.50E+10
2.00E+10
1.50E+10
1.00E+10
5.00E+09
0.00E+00
y = 3.69E+09x
0.0
2.0
4.0
6.0
8.0
10.0
Wt%

FIG. 2

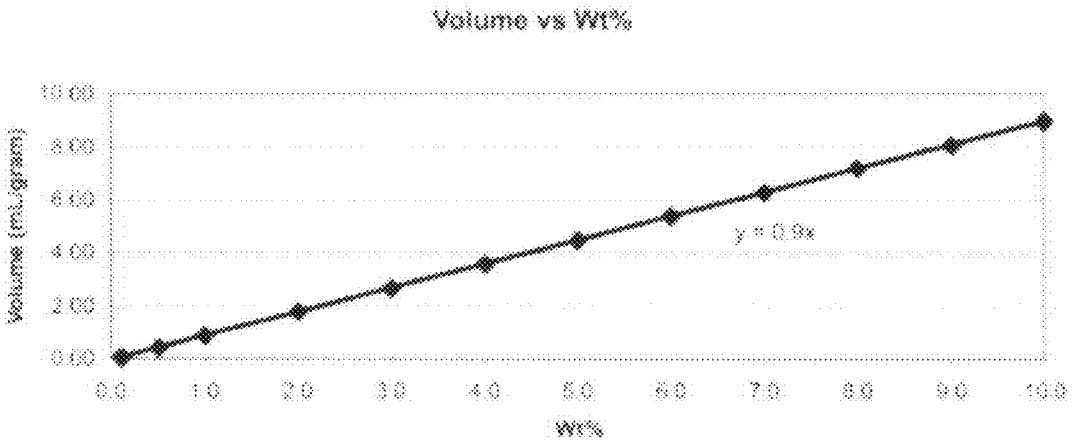
Volume vs Wt%
Volume (mL/gram)
10.00
8.00
6.00
4.00
2.00
0.00
y = 0.9x
0.0
1.0
2.0
3.0
4.0
5.0
6.0
7.0
8.0
9.0
10.0
wt%

FIG. 3

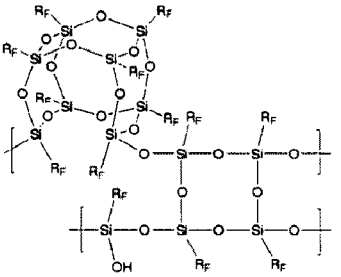

$[(R_FSiO_{1.5})n]\Sigma n$ where n = 1-1,000,000

Poly POSS Oligomers

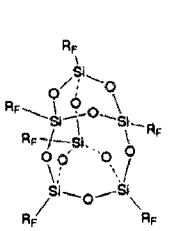

$[(R_FSiO_{1.5})_6]\Sigma_6$

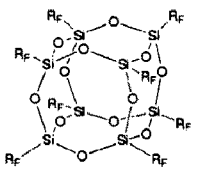

$[(R_FSiO_{1.5})_8]\Sigma_8$

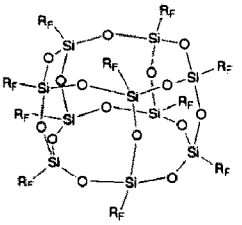

$[(R_FSiO_{1.5})_{12}]\Sigma_{12}$

POSS Oligomer Cages

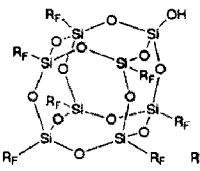

$[(R_FSiO_{1.5})_7(R_F(HO)SiO)_1]\Sigma_8$

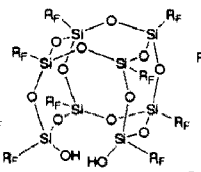

$[(R_FSiO_{1.5})_6(R_F(HO)SiO)_2]\Sigma_8$

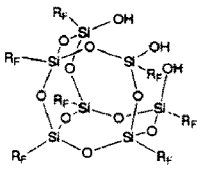

$[(R_FSiO_{1.5})_4(R_F(HO)SiO)_3]\Sigma_7$

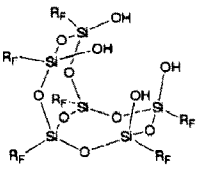

$[(R_FSiO_{1.5})_5(R_F(HO)SiO)_2]\Sigma_6$

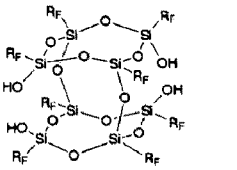

$[(R_FSiO_{1.5})_4(R_F(HO)SiO)_4]\Sigma_8$

POSS Silanol Oligomer Cages

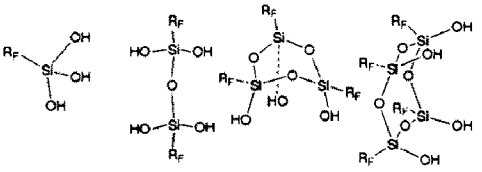

POSS Silanol Oligomer Fragments

FIG. 4

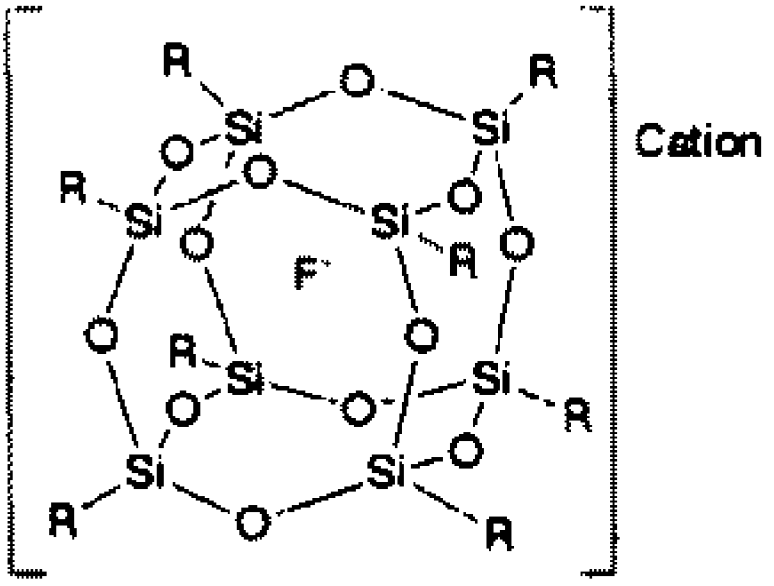

$$Cation[(RSiO_{1.5})_8@F]\Sigma_8$$

FIG. 5

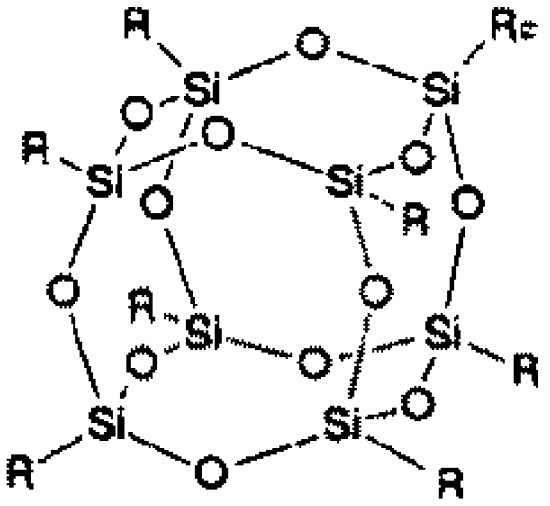

$$[(RSiO_{1.5})_7(R_FSiO_{1.5})_1]\Sigma_8$$

Fig 6

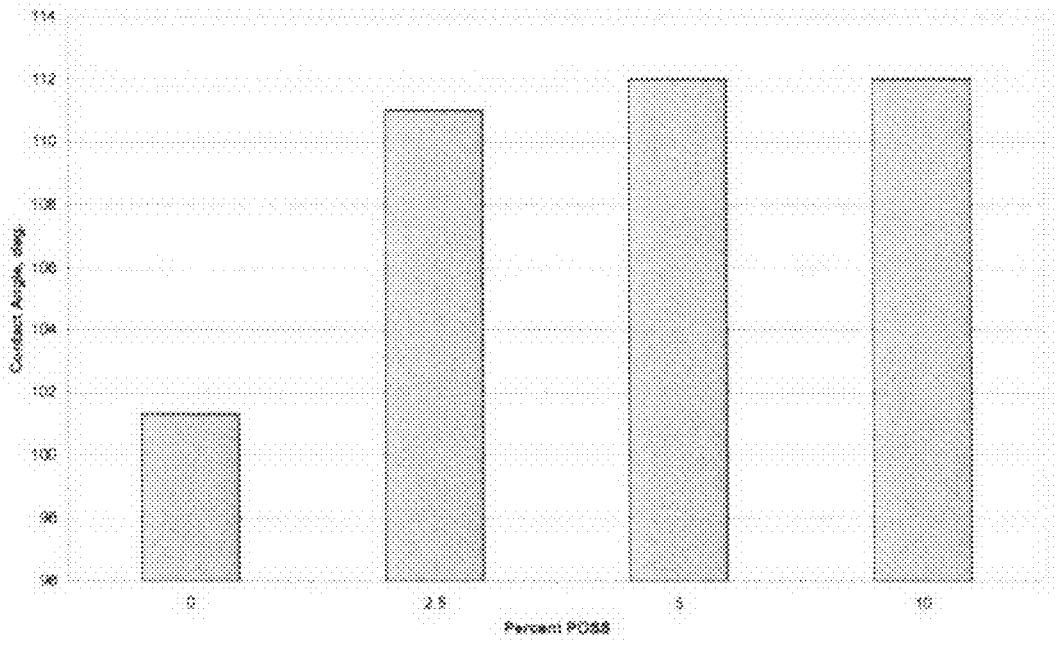
114
112
110
108
106
104
102
100
98
96
Contact Angle, deg
0
2.5
5
10
Percent POSS

FIG. 7

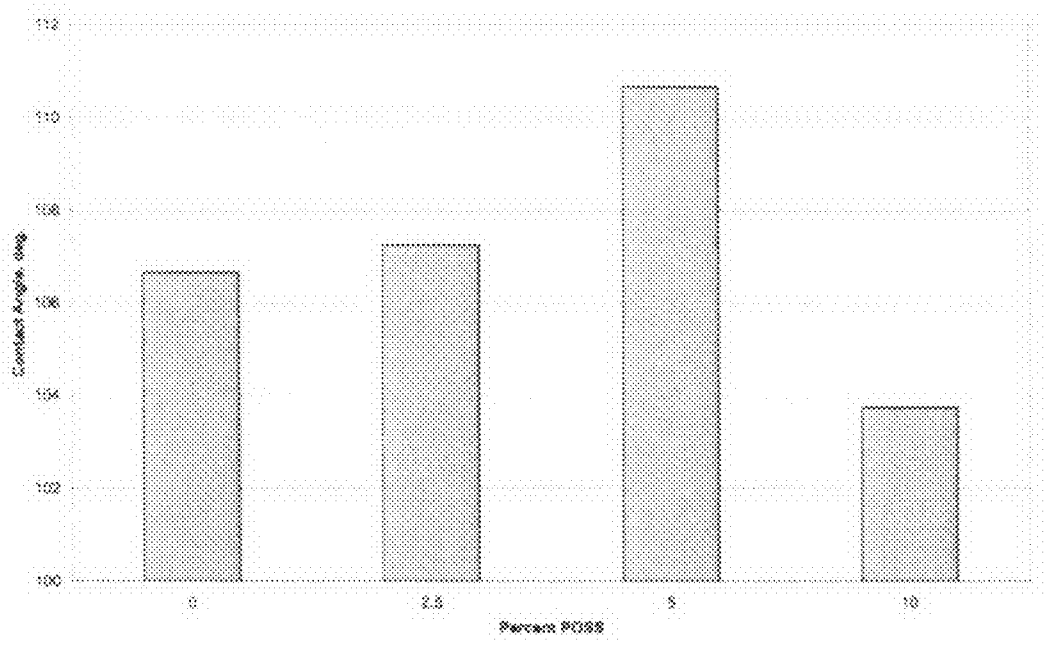

FIG 8.

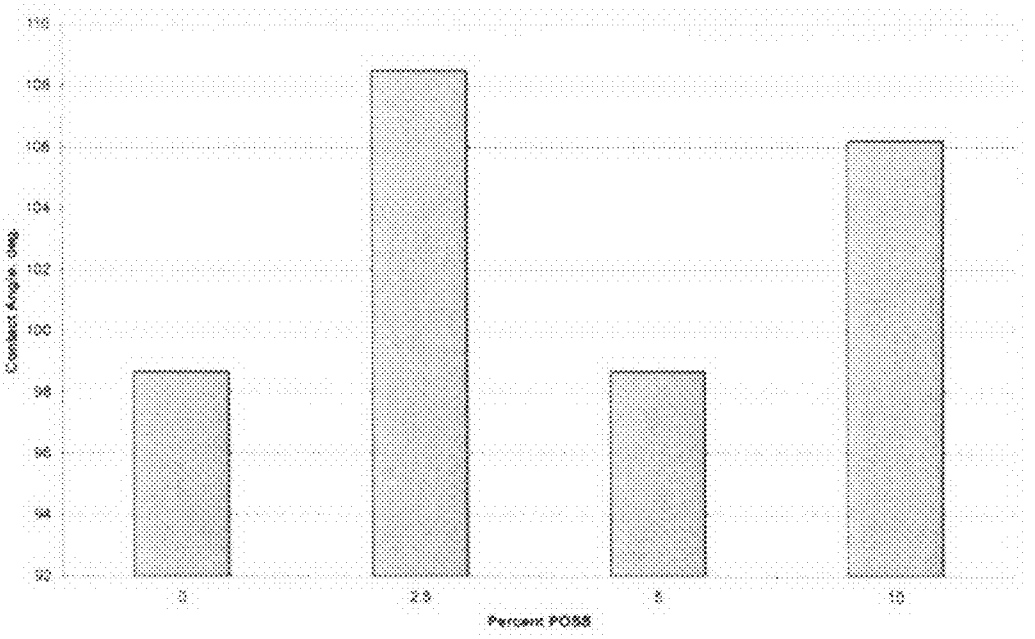

Fig 9.

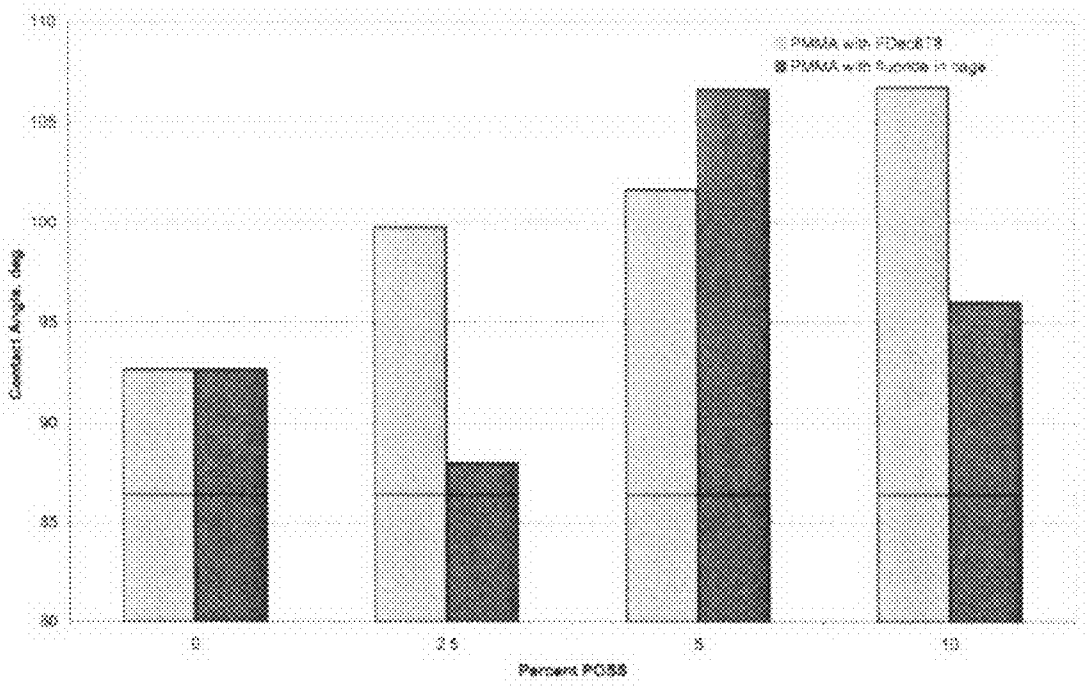

Fig. 10

FLUORINATED POSS AS ALLOYING AGENTS IN NONFLUORINATED POLYMERS

CROSS-REFERENCE TO RELATED APPLICATIONS

This application is a continuation-in-part of U.S. patent application Ser. No. 10/815,544 filed on Mar. 31, 2004, now U.S. Pat. No. 7,193,015, (which claims the benefit of U.S. Provisional Patent Application No. 60/459,357 filed on Mar. 31, 2003), which is a continuation-in-part of U.S. patent application Ser. No. 09/818,265 filed Mar. 26, 2001, now U.S. Pat. No. 6,716,919 issued Apr. 6, 2004 (which claims the benefit of U.S. Provisional Patent Application No. 60/192,083 filed Mar. 24, 2000).

This invention was made in the performance of a Cooperative Research and Development Agreement with the Department of the Air Force. The Government of the United States has certain rights to use the invention.

FIELD OF THE INVENTION

This invention relates generally to methods for enhancing the properties of nonfluorinated thermoplastic and thermoset polymers and particulate and filler surfaces through the addition of fluorine containing POSS nanostructured chemicals. The fluorinated component may be contained inside the POSS cage, external to the POSS cage or copolymerized with POSS cages. Additionally fluorinated POSS cages may contain metal atoms to improve their compatibility with polymers and surfaces and to impart catalytic activity.

This invention also relates to processes and applications of polymeric materials and composites with improved physical properties and function that resemble those of conventional fluorinated materials. These properties and applications include improved surface properties, non-wetting, anti-icing, and low friction surfaces, biological activity, permeation control, fire retardancy, improve time-dependent mechanical properties which include (heat distortion, high temperature stability, compression set, creep, color retention, biological compatibility).

BACKGROUND OF THE INVENTION

As disclosed in U.S. Pat. No. 7,193,015, the incorporation of externally fluorinated POSS into fluorinated polymers further reduces their surface energy and contact angle rendering them super hydrophobic. It is the objective of this application to convey the ability of fluorinated POSS to impart "fluoropolymer type" characteristics to nonfluorinated polymers, metal surfaces, particulates, composites and biological systems.

It has long been recognized that the properties of polymers can be tailored to a high degree through variables such as polymer sequence, structure, additive and filler incorporation, composition, morphology, thermodynamic and kinetic processing control. It is similarly known that various sizes and shapes of fillers, and particulates (e.g. Teflon®, calcium carbonate, silica, carbon black, etc.) can be incorporated into polymers, monomer mixtures, and composites to enhance physical properties.

In their solid state all polymers (including amorphous, semi-crystalline, crystalline, and rubber, etc.) possess considerable amounts of internal and external free volume and this free volume has a tremendous impact on physical properties, since it is within this volume that the dynamic properties (e.g. reptation, translation, rotation, crystallization, interaction with surfaces and fillers) of polymer chains primarily operate and in turn influence fundamental physical properties.

The accessibility of free volume in a polymer system depends greatly on morphology and on the size of the agent desired to occupy the free volume. Thermodynamic and kinetic properties, polymer morphology and free volume dimension are major factors, which limit the ability of conventional fillers from accessing the free volume in a polymer system. Significant processing/compounding effort is normally required to force compatibilization between fillers and polymers since conventional fillers are physically larger than most polymer dimensions, chemically dissimilar, and viscometricaly different than most polymers.

Prior art in nonfluoropolymers has utilize fluorinated additives and fluorinated filler particulates to impart characteristics of the fluorinated entity to the nonfluorinated polymer. Unfortunately, the prior art suffers from process complexity, inappropriate length scale of the reinforcement to access polymer free volume, or the reinforcement lacks sufficient geometrical definition to provide structural regularity and reinforcement at the molecular (10^{-10} m) and nanoscopic (10^{-9} m) length scales. Consequently many desirable properties of the nonfluorinated polymer are lost upon incorporation of conventional fluorinated components.

Furthermore, it has been calculated that as filler sizes decrease below 50 nm, they become more resistant to sedimentation and more effective at providing reinforcement to polymer systems. The full application of this knowledge, however, has been thwarted by the lack of a practical source of fluorinate particulates or fluorinated additives less than 50 nm and preferably with a rigid 1 nm to 5 nm size range. Particularly desirable are monodisperse, nanoscopic chemicals with precise chemical compositions, rigid and well defined geometrical shapes, and which are dimensionally large enough to provide reinforcement of polymer chains. Such nanoscopic chemicals are desirable as they form stable dispersions within polymer systems, well below the length scale necessary to scatter light and hence are visually nondetectable when incorporated. Further fluorinated nanoscopic chemicals would be chemically compatible with nonfluoropolymers and dissolve into and among the polymer chains, thus eliminating the need for the complex processing requirements of the prior art.

The fundamental premise behind this invention is underpinned mathematically through computation of the surface area and volume contribution provided at various loadings of 1 nm diameter fluorine containing nanostructured chemical entities into or onto a nonfluorinated polymeric material. Computation reveals that a fluorinated nanostructured chemical contributes more surface area and more volume as a wt % of its incorporation into a material than is possible for larger particles (see FIG. **1**, FIG. **2**, and FIG. **3**). The net effect is that even small loadings of nanostructured chemicals can dominate the surface characteristics of a material. This is an important economic consideration since fluorinated materials are traditionally expensive and desired to be used in minimal quantities.

Further, the incorporation of fluorinated nanostructured chemicals onto the surface of a secondary material (such as TiO_2, $CaCO_3$, glass or mineral fillers, and fibers) can be utilized to creating more surface area on such particle and improve their compatibility with fluorinated and nonfluorinated polymers.

Recent developments in nanoscience have enabled the cost effective manufacture of commercial quantities of materials that are best described as nanostructured chemicals due to their specific chemical formula, hybrid (inorganic-organic)

chemical composition, geometrically precise and rigid shape, large physical size relative to traditional chemicals (0.3-0.5 nm), and small physical size relative to larger sized traditional fillers (>50 nm).

Nanostructured chemicals are best exemplified by those based on low-cost Polyhedral Oligomeric Silsesquioxanes (POSS) and Polyhedral Oligomeric Silicates. FIGS. **4**, **5**, **6** illustrate some representative examples of fluorinated nanostructured chemicals, which are also referred to as fluorinated POSS in this application. It is recognized that oligomeric, polymeric, and metal containing versions of fluorinated POSS may also be utilized. Nanostructured chemicals based on polyhedral oligomeric silsesquioxanes and polyhedral metallosesquioxanes are discussed in detail in U.S. Pat. Nos. 5,412,053; 5,484,867; 6,329,490; and 6,716,919, which are expressly incorporated herein by reference in their entirety.

SUMMARY OF THE INVENTION

As disclosed in U.S. Pat. No. 7,193,015, the incorporation of externally fluorinated POSS into fluorinated polymers further reduces surface energy and contact angles rendering them super hydrophobic. It is the objective of this application to attain control over the contact angle, coefficient of friction, and hydrophobicity of nonfluorinated polymers and filler additives and metal surfaces through the use of fluorinated POSS.

The present invention describes methods of preparing new compositions by incorporating fluorinated-nanostructured chemicals into nonfluorinated polymers. The resulting nano-alloyed polymers are wholly useful by themselves or in combination with other polymers or in combination with macroscopic reinforcements such as fiber, clay, glass, mineral and other fillers and fibers. The nano-alloyed polymers are particularly useful for producing polymeric compositions with desirable physical properties such processing aids, surface lubricity, adhesion to polymeric surfaces, composite and metal surfaces, water repellency, reduced melt viscosity, reduced surface energy, low dielectric constant, resistance to abrasion and fire, biological compatibility, optical quality plastics, cosmetic applications.

The preferred compositions presented herein contain three primary material combinations: (1) fluorinated nanostructured chemicals, fluorinated-nanostructured oligomers, or fluorinated-nanostructured polymers from the chemical classes of fluorine containing polyhedral oligomeric silsesquioxanes, polysilsesquioxanes, polyhedral oligomeric silicates, polysilicates, polyoxometallates, carboranes, boranes, and fluorinated polymorphs of carbon; (2) nonfluorinated polymer systems such as aromatic and aliphatics, semicrystalline, crystalline, glassy, elastomeric, oils, and lubricants thereof as derived from hydrocarbons, or silicones and copolymers thereof; and (3) inorganics metals, and particulate minerals and silicatious powders, and all forms of carbon including diamond powder, graphite, carbon black, tubes, spheres, mesophase, pitch, and fiber.

Preferably, the method of incorporating nanostructured chemicals into nonfluoropolymers is accomplished via blending of the fluorinated nanostructured chemicals with the nonfluorinated materials. All types and techniques of coating, blending, including melt blending, dry blending, solution blending, reactive and nonreactive blending are effective.

In addition, selective incorporation of a nanostructured chemical into a specific region of a polymer can be accomplished by compounding into the polymer a nanostructured chemical with a chemical potential (miscibility) compatible with the chemical potential of the region desired within the material. This is most preferably accomplished using POSS chemicals with partially externally fluorinated cage such as $[(RSiO_{1.5})_{8-x}(R_FSiO_{1.5})_x]\Sigma_8$ or cages containing fluorine inside of the cage cavity such as $Cation[(RSiO_{1.5})_8@F]\Sigma_8$. The internally fluorinate cages $Cation[(RSiO_{1.5})_8@F]\Sigma_8$ are particularly useful for incorporation into polar polymers (such as hydrogels because they are also polar and hence exhibit compatibility.

The physical size of POSS cages in combination with tailorable compatibility enables fluorinated POSS to be selectively incorporated into polymers, composites, metals, ceramics and biological materials to control the surface topology, surface properties, and chain dynamics and subsequently favorably impact a multitude of physical properties. Properties most favorably improved are surface properties, including contact angle, coefficient of friction, anti-icing, surface tension, hydrophobicity, and lubricity. Other properties improved include time dependent mechanical and thermal properties such as heat distortion, heat stability, creep, compression set, shrinkage, modulus, hardness, and abrasion resistance. In addition to mechanical properties, other physical properties are favorably improved, including thermal conductivity, refractive index, fire resistance, oxygen permeability, oxidative stability, electrical properties, printability and biological compatibility and activity.

BRIEF DESCRIPTION OF THE DRAWINGS

FIG. **1** illustrates diameter and volume contributions for $[(c\text{-}C_6H_{11}SiO_{1.5})_8]\Sigma_8$ POSS cage.

FIG. **2** illustrates the surface area contribution for $[(c\text{-}C_6H_{11}SiO_{1.5})_8]\Sigma_8$ POSS cage relative to wt % loading.

FIG. **3** illustrates the volume contribution for $[(c\text{-}C_6H_{11}SiO_{1.5})_8]\Sigma_8$ POSS cage relative to wt % loading.

FIG. **4** illustrates representative examples of externally fluorinated POSS nanostructured chemicals.

FIG. **5** illustrates representative examples of internally fluorinated POSS nanostructured chemical which also contain a counter cation to balance charge and assert additional compatibility.

FIG. **6** illustrates a representative example of partially externally fluorinated POSS nanostructured chemical.

FIG. **7** illustrates the contact angles for polystyrene showing increasing contact angle with $[(CF_3(CF_2)_7(CH_2)_2SiO_{1.5})_8]\Sigma_8$ POSS incorporation.

FIG. **8** illustrates the contact angles for LDPE showing increasing contact angle with $[(CF_3(CF_2)_7(CH_2)_2SiO_{1.5})_8]\Sigma_8$ POSS incorporation.

FIG. **9** illustrates the contact angles for styrene acrylonitrile showing increasing contact angle with $[(CF_3(CF_2)_7(CH_2)_2SiO_{1.5})_8]\Sigma_8$ POSS incorporation.

FIG. **10** illustrates the contact angles for polymethylmethacrylate showing increasing contact angle with $[(CF_3(CF_2)_7(CH_2)_2SiO_{1.5})_8]\Sigma_8$ and $(CH_3)_4N[(CF_3(CF_2)_7(CH_2)_2SiO_{1.5})_8@F]\Sigma_8$ POSS incorporation.

DEFINITION OF FORMULA REPRESENTATIONS FOR NANOSTRUCTURES

For the purposes of understanding this invention's chemical compositions the following definitions for formula representations of Polyhedral Oligomeric Silsesquioxane (POSS) and Polyhedral Oligomeric Silicate (POS) nanostructures are made.

Polysilsesquioxanes are materials represented by the formula $[RSiO_{1.5}]_x$ where x represents molar degree of polymerization and R=represents organic substituent (H, siloxy,

cyclic or linear aliphatic or aromatic groups that may additionally contain reactive functionalities such as alcohols, esters, amines, ketones, olefins, ethers and R_F=represents halogenated organic groups which includes fluorinated groups). Polysilsesquioxanes may be either homoleptic or heteroleptic. Homoleptic systems contain only one type of R group while heteroleptic systems contain more than one type of R group.

POSS and POS nanostructure compositions are represented by the formula:

$[(RSiO_{1.5})_n]_{\Sigma\#}$ for homoleptic compositions

$[(RSiO_{1.5})_n(R'SiO_{1.5})_m]_{\Sigma\#}$ for heteroleptic compositions (where R≠R')

$[(RSiO_{1.5})_n(RXSiO_{1.0})_m]_{\Sigma E\#}$ for functionalized heteroleptic compositions (where R groups can be equivalent or inequivalent)

In all of the above R is the same as defined above and X includes but is not limited to OH, Cl, Br, I, F, alkoxide (OR), acetate (OOCR), peroxide (OOR), amine (NR_2) isocyanate (NCO), and R. The symbols m and n refer to the stoichiometry of the composition. The symbol Σ indicates that the composition forms a nanostructure and the symbol # refers to the number of silicon atoms contained within the nanostructure. The value for # is usually the sum of m+n, where n ranges typically from 1 to 24 and m ranges typically from 1 to 12. It should be noted that Σ# is not to be confused as a multiplier for determining stoichiometry, as it merely describes the overall nanostructural characteristics of the system (aka cage size). The symbol @ is also used in association with the POSS formula representations and indicates the presence of an F anion inside of the cage cavity.

DETAILED DESCRIPTION OF THE INVENTION

The present invention teaches the use of fluorinated POSS nanostructured chemicals as agents for imparting the characteristics of a fluorinated material (such as polymers) to non-fluorinated polymers, composites, additives, metals, and all types of particles.

The keys that enable POSS nanostructured chemicals to impart fluorinated characteristics to such a diverse number of materials are: (1) their unique size with respect to polymer chain dimensions, and (2) their ability to be compatibilized with polymer systems to overcome forces that promote incompatibility and expulsion of the nanoreinforcing agent by polymer chains and surfaces and (3) their ability to bind to dissimilar surfaces.

Additionally advantageous are the fundamental aspects of high surface area, low density, and controlled volume contributions imparted by the nanoscopic size of the POSS cage. The nanoscopic cage size imparts these properties to materials at very small loading amounts and affords POSS to dominate the surface and volume characteristics of materials.

The chemical nature of POSS cages renders their dispersion characteristics to be governed by the Gibbs free energy of mixing equation ($\Delta G=\Delta H-T\Delta S$) rather than kinetic dispersive mixing as for insoluble particulates. Thus the ability of POSS to interact with a surface or with polymers through Van der Waals interactions, covalent, ionic, or hydrogen bonding that can be utilized to chemically, thermodynamically, and kinetically drive their dispersion and surface modification. Furthermore since POSS cages are monoscopic in size, entropic dispersion (ΔS) is favored.

While fluoropolymers are known for their hydrophobicity, low surface energy, and low coefficients of friction, the incorporation of fluorinated POSS has been shown in U.S. Pat. No. 7,193,015 to further improve these properties in fluorinated polymers. Therefore extension of fluorinated POSS into non-fluorinated systems is a logical means for cost-effectively attaining such properties in nonfluorinated polymers.

EXAMPLES

General Process Variables Applicable to all Processes

As is typical with chemical processes there are a number of variables that can be used to control the purity, selectivity, rate and mechanism of any process. Variables influencing the process for the incorporation of nanostructured chemicals (e.g. POSS/POS etc.) into plastics include the size and polydispersity, and composition of the nanostructured chemical. Similarly the molecular weight, polydispersity and composition of the polymer system must also be matched with that of the nanostructured chemical. Finally, the kinetics, thermodynamics, and processing aids used during the compounding process are also tools of the trade that can impact the loading level and degree of enhancement resulting from incorporation of nanostructured chemicals into polymers. Blending processes such as melt blending, dry blending and solution mixing blending are all effective at mixing and alloying nanostructured chemical into plastics.

Water contact angles are a measure of surface hydrophobicity and provide insight into the free energy of the surface. Critical surface tension of the POSS, POSS polymers, and POSS blends were determined. The surface tension of the fluid is graphed in relation to its contact angle on the surface. It should be noted that a surface with a contact angle of 90° or higher is considered a "non-wetting" surface, while a surface with a contact angle below 900 is considered "wetting."

Synthesis of Internally Fluorinated CationPOSS@F Cages

$(BU_4N[(PhSiO_{1.5})_8@F]_{\Sigma 8}$ (via literature Bassindale, et al Angew. Chem. Int. Ed. (2003), vol 42, 3488) Tetrabutylammonium octaphenyl octasilsesquioxane fluoride $(Bu_4N)[(PhSiO_{1.5})_8@F]_{\Sigma 8}$: Tetrabutylammonium fluoride (1 m solution in THF, 2.5 ml, with 5% water) was added to phenyl triethoxysilane (1.02 g, 4.2 mmol) dissolved in dry THF (20 ml). The mixture was stirred at room temperature for 24 h and a yellow viscous liquid obtained after removal of the solvent. Dry chloroform (10 ml) was added, and a white powder was obtained after filtration. Recrystallization from acetone afforded colorless crystals (1.25 g, 46%). ^{29}Si NMR (79.30 MHz, $CDCl_3$, TMS): d=80.6 ppm.

$(Me)_4N[(PhSiO_{1.5})_8@F]_{\Sigma 8}$ To a 1 gram anhydrous THF (50 mL) suspension of $[(PhSiO_{1.5})_8]_{\Sigma 8}$ (0.968 mmole) was added a slight excess of anhydrous tetramethylammonium fluoride (91 mg, 0.98 mmole). After stirring under a nitrogen atmosphere for several hours the solution clarified as the product dissolves in THF. The solution was filtered through diatomaceous earth and the solvent removed under vacuum to give a quantitative yield of the salt with fluoride inside the silsesquioxane cage. ^{19}F NMR (in THF) −26.5 (s) ppm. ^{29}Si NMR (in THF) −80.7 (s) ppm.

$(Me)_4N[(ViSiO_{1.5})_8@F]_{\Sigma 8}$ To a 0.5 gram anhydrous THF (50 mL) suspension of $[(ViSiO_{1.5})_8]_{\Sigma 8}$ (0.790 mmole) was added a slight excess of anhydrous tetramethylammonium fluoride (75 mg, 0.80 mmole). After stirring under a nitrogen atmosphere for several hours the solution clarified as the product dissolves in THF. The solution was filtered through diatomaceous earth and the solvent removed under vacuum to give a quantitative yield of the salt with fluoride inside the silsesquioxane cage. ^{19}F NMR (in THF) −25.5 (s) ppm. ^{29}Si NMR (in THF) −83.0 (s) ppm.

$(Me)_4N[(CF_3(CH_2)_3SiO_{1.5})_8@F]_{\Sigma 8}$ To a 1 gram anhydrous THF (50 mL) suspension of $[(CF_3(CH_2)_3SiO_{1.5})_8]_{\Sigma 8}$ (0.816 mmole) was added a slight excess of anhydrous tetramethylammonium fluoride (76 mg, 0.82 mmole). After stirring under a nitrogen atmosphere for several hours the solution clarified as the product dissolves in THF. The solution was filtered through diatomaceous earth and the solvent removed under vacuum to give a quantitative yield of the salt with fluoride inside the silsesquioxane cage. ^{19}F NMR (in THF) −28.8 (s, 1F), −69.9 (s, 24F) ppm. ^{29}Si NMR (in THF) −70.4 (s) ppm.

$(Me)_4N[(CF_3CF_2CF_2CF_2CH_2CH_2SiO_{1.5})_8@F]_{\Sigma 8}$ To a 1 gram anhydrous THF (50 mL) suspension of $[(CF_3CF_2CF_2CF_2CH_2CH_2SiO_{1.5})_8]_{\Sigma 8}$ (0.396 mmole) was added a slight excess of anhydrous tetramethylammonium fluoride (37 mg, 0.40 mmole). After stirring under a nitrogen atmosphere for several hours the solution clarified as the product dissolves in THF. The solution was filtered through diatomaceous earth and the solvent removed under vacuum to give a quantitative yield of the salt with fluoride inside the silsesquioxane cage. ^{19}F NMR (in THF) −28.8 (s, 1F), −82.4 (t, 24F), −117.2 (m, 16F), −125.4 (m, 16F), −127.1 (m, 16F) ppm. ^{29}Si NMR (in THF) −70.1 (s) ppm.

$(Me)_4N[(CF_3CF_2CF_2CF_2CF_2CH_2CH_2SiO_{1.5})_8@F]_{\Sigma 8}$ To a 1 gram anhydrous THF (50 mL) suspension of $[(CF_3CF_2CF_2CF_2CF_2CH_2CH_2SiO_{1.5})_8]_{\Sigma 8}$ (0.295 mmole) was added a slight excess of anhydrous tetramethylammonium fluoride (28 mg, 0.30 mmole). After stirring under a nitrogen atmosphere for several hours the solution clarified as the product dissolves in THF. The solution was filtered through diatomaceous earth and the solvent removed under vacuum to give a quantitative yield of the salt with fluoride inside the silsesquioxane cage. ^{19}F NMR (in THF) −30.6 (s, 1F), −84.1 (t, 24F), −119.0 (m, 16F), −124.7 (m, 16F), −125.7 (m, 16F), −126.3 (m, 16F) ppm. ^{29}Si NMR (in THF) −70.6 (s) ppm.

$(Me)_4N[(CF_3CF_2CF_2CF_2CF_2CF_2CF_2CH_2CH_2SiO_{1.5})_8@F]_{\Sigma 8}$ To a 1 gram anhydrous THF (10 mL) suspension of $[(CF_3CF_2CF_2CF_2CF_2CF_2CF_2CH_2CH_2SiO_{1.5})_8]_{\Sigma 8}$ (0.279 mmole) was added a slight excess of anhydrous tetramethylammonium fluoride (27 mg, 0.29 mmole). After stirring under a nitrogen atmosphere for several hours the solution clarified as the product dissolves in THF. The solution was filtered through diatomaceous earth and the solvent removed under vacuum to give a quantitative yield of the salt with fluoride inside the silsesquioxane cage. ^{19}F NMR (in THF) −28.7 (s, 1F), −82.2 (t, 24F), −117.2 (m, 16F), −122.6 (m, 16F), −122.8 (m, 32F), −123.7 (m, 16F), −124.5 (m, 16F), −127.2 (m, 16F) ppm. ^{29}Si NMR (in THF) −70.7 (s) ppm.

Cation Exchange for CationPOSS@F Cages

The utility of F@POSS cages can be controlled through variation of the R group on the cage and through variation of the counter cation associated with the cage. Numerous advantages can be realized by exchanging nonreactive onium cations such as tetramethyl ammonium, and tetrabutyl ammonium with onium cations containing reactive groups capable of polymerization, catalytic activity, wettability, color and pigmentation properties, radiation absorbance, biological activity, or therapeutic properties. Such functional activity is highly desired for the practical utility of F@POSS.

Onium exchange can be carried out by dissolving tetramethylammonium octaphenyl octasilsesquioxane fluoride $(Me)_4N[(PhSiO_{1.5})_8@F]_{\Sigma 8}$ into THF followed by addition of a stoichiometrically equivalent amount of cetyltrimethyl ammonium chloride and stirring for 10 minutes at 25° C. Then 50 ml of hexane was added to the mixture to form a second layer into which the resulting $Cetyl(Me)_3N[(PhSiO_{1.5})_8@F]_{\Sigma 8}$ was extracted. Upon removal of volatiles and drying a quantitative amount of product was obtained. The $Cetyl(Me)_3N[(PhSiO_{1.5})_8@F]_{\Sigma 8}$ was observed to be significantly more effective as a biocidal agent that the tetramethylammonium cation.

$K[(PhSiO_{1.5})_8@F]_{\Sigma 8}$ Similarly, cation exchange of the onium groups on F@POSS with an inorganic cation such as K+, Na+, Li+, Ag+ is desirable as they afford higher temperature stability and do not produce a noticeable smell when heated. Onium exchange for inorganic cations was successfully accomplished for example, by addition of KPF6 to a THF solution of tetramethylammonium octaphenyl octasilsesquioxane fluoride $(Me)_4N[(PhSiO_{1.5})_8@F]_{\Sigma 8}$. This mixture was allowed to stir for about 15 minutes, at which time the solution was filtered and the POSS product was isolated by filtration and the $[(Me)_4N]^+PF_6^-$ salt was retained in solution. The POSS product was collected in near quantitative yield upon removal of volatiles and evaluated with TGA and FTIR relative to the starting materials. Similar cation exchange can be carried out using other inorganic salts (e.g. AgNO3, CuSO4) in which one of the products is water soluble.

Polymerization of Fluorinated POSS Cages to $[CF_3(CH_2)_3SiO_{1.5})_7(propylmethacrylate)_1SiO_{1.5})_7]\Sigma_8$/methylmethacrylate Copolymers

Copolymers of hepta(trifluoropropyl)propylmethylmethacrylate octamer POSS ($[(CF_3(CH_2)_3SiO_{1.5})_7(propylmethacrylate)SiO_{1.5})_1]_{\Sigma 8}$) and methylmethacrylate were prepared using the following general procedure. Under a nitrogen atmosphere, a dry, oxygen free solution of toluene (2.72 mL, 2.35 g), $[(CF_3(CH_2)_3SiO_{1.5})_7(propylmethacrylate)SiO_{1.5})_1]_{\Sigma 8}$ (300 mg, 0.245 mmol), methylmethacrylate (2702 mg, 26.99 mmol) and AIBN (11.0 mg, 0.068 mmol) was prepared and heated to 63° C. for 16 hours. This solution was then diluted with 15 mL of $CHCl_3$ and precipitated into 75 mL of methanol. After stirring overnight a white solid formed, and was collected by vacuum filtration in 85% yield and ^1H NMR spectroscopy showed no unreacted monomers. In general it was observed that glass transition of the copolymers decreases with increasing $[(CF_3(CH_2)_3SiO_{1.5})_7(propylmethacrylate)SiO_{1.5})_1]_{\Sigma 8}$ content relative to that of methylmethacrylate and ranges from 120° C. to 130° C., while the heat capacity and thermal gravimetric performance increases with higher POSS loadings. The contact angle for a series of these copolymers is listed in Table 1.

TABLE 1

Contact angles of $[CF_3(CH_2)_3SiO_{1.5})_7(propylmethacrylate)_1SiO_{1.5})_7]\Sigma_8$/methylmethacrylate copolymers.

Composition	Average Contact Angle	Standard Deviation
PMMA	78.5	8.5
3/97 $[CF_3(CH_2)_3SiO_{1.5})_{12}]\Sigma_{12}$/PMMA	89.7	5.8
5/95 $[CF_3(CH_2)_3SiO_{1.5})_{12}]\Sigma_{12}$/PMMA	80.5	11.2
10/90 $[CF_3(CH_2)_3SiO_{1.5})_{12}]\Sigma_{12}$/PMMA	84.3	10.9
20/80 $[CF_3(CH_2)_3SiO_{1.5})_{12}]\Sigma_{12}$/PMMA	88.4	7.0

Synthesis of Externally Fluorinated POSS

In a 1 L volumetric flask, combine one mole of $[(CF_3CF_2CF_2CF_2CF_2CF_2CF_2CH_2CH_2Si(OEt)_3$ or $[(CF_3CF_2CF_2CF_2CF_2CF_2CH_2CH_2Si(OEt)_3$, 27.20 g was made from 100 mL of DI water and 0.774 g of 85% KOH and absolute ethanol. Transfer to a 2 L flask and stir under nitrogen for 5 days. A white precipitate forms, which is removed

by vacuum filtration. The precipitate is dissolved in dichloromethane and washed three times with DI water. The solvent is removed in vacuo just until precipitate starts to form. This cloudy solution is dripped into rapidly stirring methanol yielding a fluffy white precipitate. The solid is removed by vacuum filtration. ^{29}Si NMR (CD_2Cl_2) δ: $[(CF_3CF_2CF_2CF_2CF_2CF_2CH_2CH_2SiO_{1.5})_8@F]_{\Sigma 8}$/ $[(CF_3CF_2CF_2\ CF_2\ CF_2CF_2CF_2CF_2CH_2CH_2SiO_{1.5})_8@F]_{\Sigma 8}$, −66.7 ppm. Melting point $[(CF_3CF_2CF_2CF_2CF_2CF_2CH_2CH_2SiO_{1.5})_8@F]_{\Sigma 8}$ 124° C., $[(CF_3CF_2CF_2CF_2\ CF_2CF_2CF_2CF_2CH_2CH_2SiO_{1.5})_8@F]_{\Sigma 8}$ 138° C. Typical yields of product range from 98-99% can be obtained at reaction concentrations of 0.1M. More concentrated preparations can also be carried out with mechanical stirring of the reaction.

Additionally fluorinated POSS cages also bearing reactive groups are desirable for surface modification of metals, fillers, and composites can be prepared. Preferred reactive groups include but are not limited to silanols, siloxides, methacrylates, thiols, amines, acids, esters, alcohols, isocyanates, epoxides, and Lewis acidic metals.

Incorporation of Fluorinated POSS Cages into Nonfluorinated Polymers.

A wide variety of fluorinated POSS cages can be prepared and potentially incorporated into polymers and the proper selection of POSS cage is dependent upon its compatibility with the desired polymer. Also of importance is the surface properties of the cage. For example fluorinated POSS cages exhibiting low surface energy, high water contact angle, with low powder density and crystal density are desired. Table 2 contains as summary of preferred systems for incorporation into polymers.

TABLE 2

Selected physical properties for externally fluorinated POSS cages.

POSS	$[(CF_3CF_2CF_2CF_2CF_2CF_2CF_2CF_2CH_2CH_2SiO_{1.5})_8]_{\Sigma 8}$	$[(CF_3CF_2CF_2CF_2CF_2CF_2CH_2CH_2SiO_{1.5})_8]_{\Sigma 8}$	$[(CF_3CF_2CF_2CF_2CH_2CH_2SiO_{1.5})_8]_{\Sigma 8}$
Critical Surface Tension	8.68 mN/m	—	14.98 mN/m
Water Contact Angle	154°	115°	117°
Powder Density	1.95 g/mL	1.88 g/mL	1.86 g/mL
Crystal Density	2.06 g/mL	2.05 g/mL	1.98 g/mL

The incorporation of $[CF_3(CH_2)_3SiO_{1.5})_{12}]\Sigma_{12}$ into commercial grade PMMA (polymethylmethacrylate) was accomplished by solution blending and melt blending with POSS weight percents of 3%, 5%, and 10% and 20% respectively. The resulting formulations were subsequently heated to 140° C. to anneal the systems and secondarily heated at 175° C. until optically clear. The water contact angle was measured after each heat treatment to determine the impact on contact angle. Incorporation of the $[CF_3(CH_2)_3SiO_{1.5})_{12}]\Sigma_{12}$ resulted in an increase of contact angle and corresponding increase in hydrophobicity and surface energy reduction of the formulation. Increasing the hydrophobicity of PMMA is highly desirable as water absorption by PMMA is well known to reduce its durability and aesthetics for signage, utensils and optical applications. PMMA is widely utilized in dental and prosthetic application, paints, adhesives, and coatings in which the uptake of moisture causes degradation of mechanical properties. The contact angles for a series of these blends were measured after annealing for 2 hours at 140° C. (Table 3) and after annealing for 2 hours at 175° C. (Table 4).

TABLE 3

Contact angles of $[CF_3(CH_2)_3SiO_{1.5})_{12}]\Sigma_{12}$ and PMMA blends annealed at 140° C.

Composition	Average Contact Angle	Standard Deviation
PMMA	74.6	14.3
3% $[CF_3(CH_2)_3SiO_{1.5})_{12}]\Sigma_{12}$ blend	78.2	4.6
5% $[CF_3(CH_2)_3SiO_{1.5})_{12}]\Sigma_{12}$ blend	87.6	2.1
10% $[CF_3(CH_2)_3SiO_{1.5})_{12}]\Sigma_{12}$ blend	97.4	3.5
20% $[CF_3(CH_2)_3SiO_{1.5})_{12}]\Sigma_{12}$ blend	100.5	2.6

TABLE 4

Contact angles of $[CF_3(CH_2)_3SiO_{1.5})_{12}]\Sigma_{12}$ and PMMA blends annealed at 175° C.

Composition	Average Contact Angle	Standard Deviation
PMMA	82.1	12.1
3% $[CF_3(CH_2)_3SiO_{1.5})_{12}]\Sigma_{12}$ blend	82.6	5.25
5% $[CF_3(CH_2)_3SiO_{1.5})_{12}]\Sigma_{12}$ blend	83.3	2.0
10% $[CF_3(CH_2)_3SiO_{1.5})_{12}]\Sigma_{12}$ blend	90.0	1.3
20% $[CF_3(CH_2)_3SiO_{1.5})_{12}]\Sigma_{12}$ blend	96.5	3.9

Properties of Nonfluorinated Polymers Containing Externally Fluorinated POSS and Internally Fluorinated POSS

Nonfluorinated thermoplastics were obtained from a variety of commercial suppliers. The melting and processing temperature for each polymer was determined by differential scanning calorimetry (DSC). Externally and internally fluorinated POSS were prepared as described. A general method for incorporation of the POSS into the thermoplastic polymer utilized a twin screw extruder (MicroCompounder, DACA Instruments) and compounding of the polymer and POSS thoroughly until a steady-state of mixer torque was observed.

Thermosetting polymers can similarly be utilized in which the POSS is incorporated via both high and low shear mixing and copolymerization. The preferred method is dependent upon the visual homogenization of the system and the viscosity of the initial resin mixture.

In general the incorporation of externally fluorinated and internally fluorinated POSS was effective at increasing the hydrophobicity of the polymers into which it was incorporated.

Examples provided in FIGS. **7-10** illustrate trends for the enhancement and are not intended to represent limitations on

the scope, range or utility, or effectiveness of the method. It is realized that differing degrees of hydrophobicity are required for specific applications along with other desirable properties such as mechanical, thermal, biological, optical, processing, and finish properties.

While certain representative embodiments and details have been shown for purposes of illustrating the invention, it will be apparent to those skilled in the art that various changes in the methods and apparatus disclosed herein may be made without departing from the scope of the invention which is defined in the appended claims.

What is claimed is:

1. A method of alloying an internally fluorinated nanostructured chemical selected from the group consisting of POSS cages containing a fluorine ion inside the cage and POS cages containing a fluorine ion inside the cage into a nonfluoropolymer, comprising the step of compounding the internally fluorinated nanostructured chemical into the polymer.

2. A method according to claim **1**, wherein a mix of different nanostructured chemicals is blended into the polymer.

3. A method according to claim **1**, wherein the nonfluorinated polymer is in a physical state selected from the group consisting of oils, amorphous, semicrystalline, crystalline, elastomeric, rubber, and crosslinked materials.

4. A method according to claim **1**, wherein the nonfluorinated polymer contains a chemical sequence and related polymer microstructure.

5. A method according to claim **1**, wherein the polymer is a polymer coil, a polymer domain, a polymer chain, a polymer segment, or mixtures thereof.

6. A method according to claim **1**, wherein the nanostructured chemical reinforces the nonfluorinated polymer at a molecular level.

7. A method according to claim **1**, wherein the nanostructured chemical contributes to volume of the polymer.

8. A method according to claim **1**, wherein the nanostructured chemical contributes to surface area of the polymer.

9. A method according to claim **1**, wherein the compounding is nonreactive.

10. A method according to claim **1**, wherein the compounding is reactive.

11. A method according to claim **1**, wherein a physical property of the nonfluorinated polymer is improved as a result of incorporating the nanostructured chemical into the polymer.

12. A method according to claim **11**, wherein the physical property comprises a member selected from the group consisting of lubricity, contact angle, water repellency, adhesion to a polymeric surface, adhesion to a composite surface, adhesion to a metal surface, water repellency, density, low dielectric constant, thermal conductivity, glass transition, viscosity, melt transition, storage modulus, relaxation, stress transfer, abrasion resistance, tire resistance, biological compatibility, gas permeability, and porosity.

13. A method according to claim **1**, wherein the compounding step is accomplished by blending the nanostructured chemical into the polymer.

14. A method according to claim **1**, wherein the compounding step is accomplished by a blending process selected from the group consisting of melt blending, dry blending, and solution blending.

15. A method according to claim **1**, wherein the nanostructured chemical functions as a plasticizer.

16. A method according to claim **1**, wherein the nanostructured chemical functions as a filler.

17. A method according to claim **1**, wherein the nanostructured chemical functions as both a plasticizer and a filler.

18. A method according to claim **1**, wherein the nanostructured chemical is selectively compounded into the polymer such that the nanostructured chemical is incorporated into a predetermined region within the polymer.

19. A polymer composition produced by a method according to claim **1**.

20. The method of claim **1**, wherein the compounding allows control of the molecular motion of the polymer.

21. A method according to claim **20**, wherein a time dependent property is enhanced as a result of compounding the nanostructured chemical into the polymer.

22. A method according to claim **21**, wherein the time dependent property is selected from the group consisting of T_g, HDT, modulus, creep, set, permeability, erosion resistance, abrasion resistance.

23. The method of claim **1**, wherein the nanostructured chemical is selected to have chemical properties compatible with a selected region of the polymer, and thereby reinforces a selected region of the polymer.

24. The method of claim **1**, further comprising the step of blending the nanostructured chemical with a particulate material.

25. The method of claim **24**, wherein the particulate material is selected from the group consisting of metals, minerals, silicatious powders, and carbon.

* * * * *

APPENDIX C: ANGEWANDTE CHEMIE, INTERNATIONAL EDITION ARTICLE

Hydrophobic Compounds

DOI: 10.1002/anie.200705355

Fluorinated Polyhedral Oligomeric Silsesquioxanes (F-POSS)**

Joseph M. Mabry, Ashwani Vij,* Scott T. Iacono, and Brent D. Viers*

Water-repellent materials, possessing a high degree of hydrophobicity are currently under a spotlight. Preparative approaches are often inspired by naturally evolved biological systems.[1] Specifically, a leaf of the lotus plant exhibits an inherent self-cleaning mechanism resulting from micron-sized waxy nodes protruding from its surface such that water is naturally repelled, removing any foreign debris.[2,3] This cleansing mechanism, commonly referred to as the "lotus effect", has been artificially reproduced in order to prepare materials with pronounced hydrophobicity. Utilized techniques include surface patterning,[4] molecular self-assembly,[5] deposition,[6] and etching.[7] However, these examples often require aggressive chemical surface treatments, high temperature post-surface modification, or elaborate patterning. For such reasons, there exists a demand to engineer hydrophobic materials that are easy to prepare on a large scale.

Fluorinated compounds are an obvious choice for hydrophobic applications due to their low surface energy. Polyhedral molecules may also improve hydrophobic character by increasing the roughness of the material surface. There have been many reported attempts to synthesize and characterize partially or fully fluorinated polyhedra. These reports include the fluorination or fluoroalkylation of C_{60}.[8] Unfortunately, $C_{60}F_{48}$ cannot be used as a hydrophobic material, as it is metastable and is hydrolyzed in aqueous solutions.[9] The perfluorocarborane species, perfluoro-deca-β-methyl-*para*-carborane, characterized by single crystal X-ray studies, shows remarkable hydrolytic and oxidative stability.[10] Fluorinated carbon nanotubes and nanofibers have also been produced.[11] These fluorinated polyhedral compounds may be useful in hydrophobic applications, but are generally hazardous to prepare, require air and moisture sensitive manipulations, and have limited economies of scale. For these reasons, alternative fluorinated polyhedra are highly desired.

Polyhedral oligomeric silsesquioxanes (POSS) are thermally robust cages consisting of a silicon–oxygen core framework possessing alkyl functionality on the periphery. They are used for the development of high performance materials in medical, aerospace, and commercial applications.[12] POSS molecules can be functionally tuned, are easily synthesized with inherent functionality, are discreetly nano-sized, and are often commercially available. Furthermore, POSS compounds may possess a high degree of compatibility in blended polymers and can easily be covalently linked into a polymer backbone.[13] The incorporation of POSS into polymers produces nanocomposites with improved properties, such as, but not limited to, glass transition temperature, mechanical strength, thermal and chemical resistance, and ease of processing.

Attempts to produce fluorinated POSS compounds have met with little success. The hydrolysis of (3,3,3-trifluoropropyl)trichlorosilanes resulted in a mixture of products.[14] After purification, the octamer, $(3,3,3\text{-trifluoropropyl})_8Si_8O_{12}$ (**FP**) POSS was isolated in 10–32% yield. More recently, **FP** was produced by a "corner-capping" methodology that requires multiple steps, as well as the use of the moisture sensitive trisodium salt, $Na_3(3,3,3\text{-trifluoropropyl})_7Si_7O_{12}$.[15] To date, attempts to produce long-chain fluoroalkyl POSS compounds have proved unsuccessful.

Herein, we demonstrate the facile preparation of a novel class of octameric fluorinated POSS compounds (F-POSS) by the facile, single-step, base-catalyzed condensation of trialkoxysilanes in alcoholic media to produce nearly quantitative yields of octameric F-POSS compounds (Scheme 1).

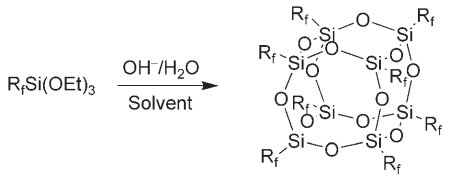

FH R_f = $CH_2CH_2CF_2CF_2CF_2CF_3$
FO $CH_2CH_2CF_2CF_2CF_2CF_2CF_2CF_3$
FD $CH_2CH_2CF_2CF_2CF_2CF_2CF_2CF_2CF_2CF_3$

Scheme 1. Synthesis of F-POSS compounds **FH**, **FO**, and **FD**.

$(1H,1H,2H,2H\text{-NonaFluorohexyl})_8Si_8O_{12}$ (**FH**), $(1H,1H,2H,2H\text{-tridecafluorooctyl})_8Si_8O_{12}$ (**FO**), and $(1H,1H,2H,2H\text{-heptadecafluorodecyl})_8Si_8O_{12}$ (**FD**) POSS have been produced by this operationally simple, one-pot synthesis. For hydrophobicity comparative studies, **FP** (where $R_f = CH_2CH_2CF_3$) was produced using an alternate methodology.[15]

These F-POSS compounds are soluble in fluorinated solvents and their melting points lie between 122 and 140 °C. Unlike most non-fluorinated POSS compounds, thermogravimetric analysis (TGA) indicates F-POSS volatilize rather than decompose, as no residue remains after heating under either nitrogen or dry air. **FD** is the most stable compound,

[*] Dr. J. M. Mabry, Dr. A. Vij, Dr. S. T. Iacono, Dr. B. D. Viers
Space and Missile Propulsion Division
Air Force Research Laboratory
10 E. Saturn Blvd., Edwards AFB, CA 93524 (USA)
Fax: (+1) 661-275-5857
E-mail: joseph.mabry@edwards.af.mil
ashwani.vij@edwards.af.mil

[**] The authors thank the Air Force Office of Scientific Research and the Air Force Research Laboratory, Propulsion Directorate for their support . We also thank Dr. Charles Campana, Sherly Largo, Dr. Timothy Haddad, Brian Moore, and Dr. Erik Weber for their technical support.

Supporting information for this article is available on the WWW under http://www.angewandte.org or from the author.

subliming at over 300 °C. F-POSS are also very dense, high molecular weight materials. For example, **FD** has a molecular weight of 3993.54 g mol^{-1} and a density of 2.067 g cm^{-3}.

The ability to crystallize F-POSS compounds from fluorinated solvents, using solvent evaporation/vapor diffusion techniques, enabled the growth of single crystals for high resolution (0.75 Å) X-ray diffraction studies (Figure 1). Both

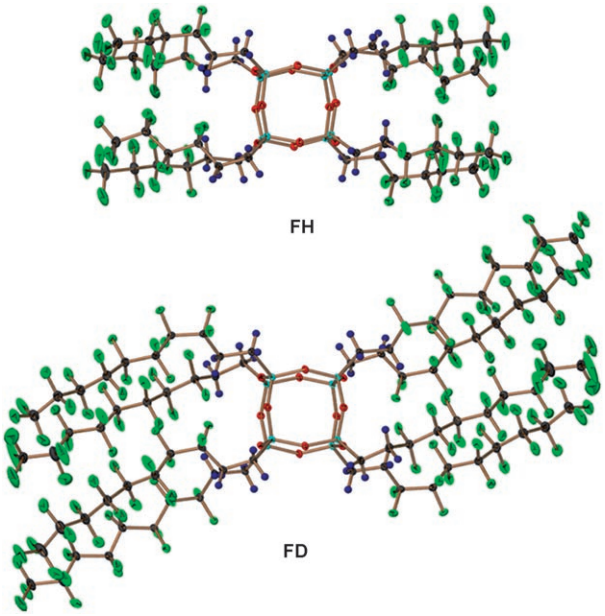

Figure 1. ORTEP representation of **FH** and **FD** POSS at 103 K, with thermal ellipsoids set at 50% probability. Green F, black C, dark blue H, red O, light blue Si.

FH and **FD** are triclinic ($P\bar{1}$) showing the presence of one and two crystallographically independent "half" molecules in the asymmetric unit, respectively. In both cases, there is an inversion center in the middle of the POSS core, which results in four pairs of fluoroalkyl chains with similar conformations. The molecular structure of F-POSS contains rigid, rod-like fluoroalkyl chains, which are attached to the silicon atoms of the POSS cage by flexible methylene groups. The relative arrangement of these components and resulting molecular interactions determine their thermal properties and may also contribute to surface properties, including hydrophobicity. The crystal structures of **FH** and **FD** showed a near-parallel arrangement of the fluoroalkyl chains. These result from the formation of strong intramolecular interactions between electropositive silicon and electron-rich fluorine atoms. These intramolecular contacts of approximately 3.0 Å are significantly shorter than the sum of van der Waals radii for silicon and fluorine at 2.10 and 1.47 Å, respectively.[16] The packing of **FD** results in the POSS cores resting at an angle, with respect to the linear fluoroalkyl groups (mean least square angle ca. 104°). This results in a rougher packing surface than **FH**, as seen in the electrostatic potential surfaces (Figure 2). This may also contribute to differences in hydrophobicity.

The hydrophobicity of spin-cast F-POSS surfaces was tested using water drop shape analysis and measured for the

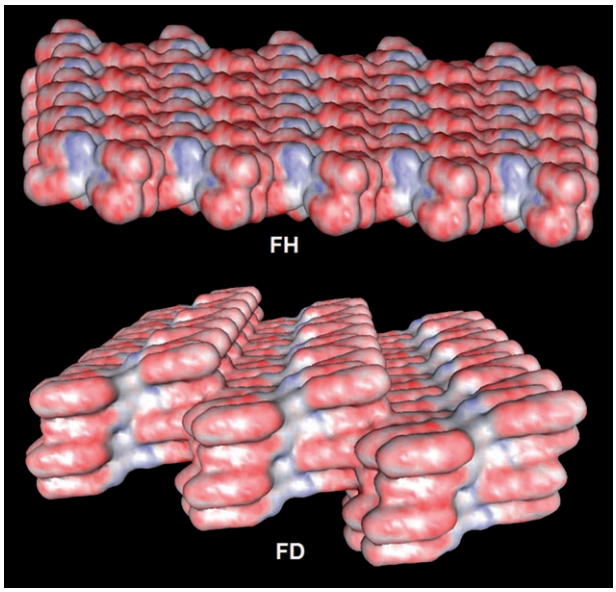

Figure 2. Electrostatic potential surfaces of **FH** and **FD** POSS.

corresponding water contact angle (Figure 3). The relationship of contact angle and surface energy is governed by Young's equation, which relates the interfacial tension of the

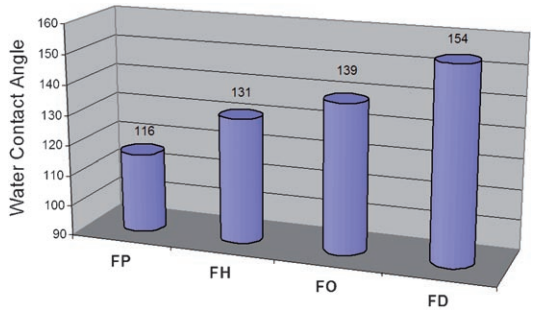

Figure 3. Graph showing water contact angles of **FP**, **FH**, **FO**, and **FD**. Hydrophobicity increases with fluoroalkyl chain length.

surface to the liquid and gas phases of water.[17] A trend was observed where the F-POSS static water contact angles increased with longer fluorocarbon chain length. Similar observations have been made in many fluorinated systems, including polymers,[18] copolymers,[19] and monolayers,[20] as well as corresponding to total fluorine content.[21] **FD** was surprisingly found to have a static water contact angle over 150°. In fact, **FO** and **FD** are so hydrophobic that, even with a density over 2 g cm^{-3}, crystals (ca. 15 mm × 15 mm × 3 mm) of these F-POSS compounds float on the surface of water!

It is well known that hydrophobicity is a function of both surface tension and surface roughness, as demonstrated by Cassie and Baxter[22] and Wenzel.[23] Figure 4a is a height image taken with an atomic force microscope (AFM) of a spin-cast **FD** surface. This surface has a root-mean-squared (rms) roughness of approximately 4 μm. Surfaces of all F-POSS compounds were prepared in the same manner, with

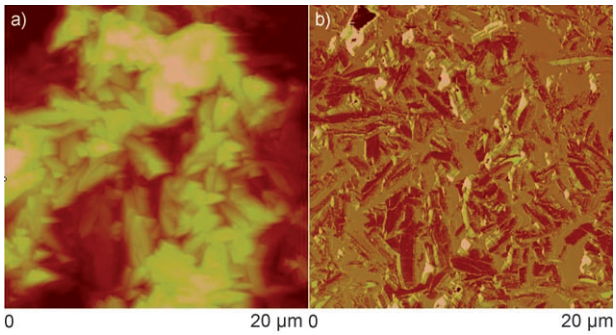

Figure 4. AFM analysis of the height (a) and phase image (b) of a spin-cast film surface of **FD**. Micron-sized crystallites can be observed in the height image. The rms roughness values for all spin-cast films were between 3 and 4 μm.

similar 3–4 μm rms surface roughness. Figure 4b is the phase image of the same surface.

In conclusion, new octameric fluorinated polyhedral oligomeric silsesquioxanes (F-POSS) have been produced by a facile "one-pot" synthetic method. The polyhedral compounds can be prepared in nearly quantitative yields and hundred gram quantities, eliminating the need for complex processes and patterning techniques to produce hydrophobic fluorinated surfaces. The compounds were shown to be thermally and hydrolytically stable and are less-hazardous to prepare than many other fluorinated compounds. These compounds are also soluble and have low melting temperatures, indicating that they may be solvent/melt-processed into polymers for desired property enhancements. The incorporation of F-POSS into polymers may produce nanocomposites with improved surface properties, including hydrophobicity. To our knowledge, **FD** is the most hydrophobic crystalline solid material known.

Experimental Section

All reagents were purchased from commercial sources and purified according to established procedures.[24]

Synthesis of **FH**: To a solution of 1*H*,1*H*,2*H*-nonafluorohexyltriethoxysilane (4.1 g) in ethanol (10 mL) was added KOH (2 mg) dissolved in deionized water (270 mg) at room temperature. After continuous stirring for 24 h, a white precipitate was filtered and washed repeatedly with ethanol. The solid was collected and redissolved in Asahiklin AK-225G (1,3-dichloro-1,1,2,2,3-pentafluoropropane), and residual KOH was extracted by washing repeatedly with deionized water. The organic layer was dried with $MgSO_4$, filtered, concentrated, and dried under vacuum to afford $(1H,1H,2H,2H\text{-nonafluorohexyl})_8Si_8O_{12}$ (**FH**) as a white solid in nearly quantitative yield. **FO** and **FD** were prepared in a similar manner using 1*H*,1*H*,2*H*,2*H*-tridecafluorooctyltriethyoxysilane and 1*H*,1*H*,2*H*,2*H*-heptadecafluorodecyltriethoxysilane, respectively.

Attempts to obtain **FP** using the same process resulted in a mixture of eight-, ten-, and twelve-membered polyhedra. Therefore, **FP** was prepared by the recently reported "corner-capping" of $(3,3,3\text{-trifluoropropyl})_7Si_7O_{12}$ trisodium salt with 3,3,3-trifluoropropyltrichlorosilane.[15]

Detailed X-ray crystallography data,[25] surface preparation data, and analytical characterization data of F-POSS compounds are included in the Supporting Information.

Received: November 21, 2007
Published online: April 24, 2008

Keywords: fluorinated polyhedra · hydrophobicity · lotus effect · silsesquioxanes · surface roughness

[1] T. Sun, L. Feng, X. Gao, L. Jian, *Acc. Chem. Res.* **2005**, *38*, 644.
[2] C. Neinhuis, W. Barthlott, *Ann. Bot.* **1997**, *79*, 667.
[3] W. Barthlott, C. Neinhuis, *Planta* **1997**, *202*, 1.
[4] a) N. Takeshita, L. A. Paradis, D. Oner, T. J. McCarthy, W. Chen, *Langmuir* **2004**, *20*, 8131; b) J.-Y. Shiu, C.-W. Kuo, P. Chen, C.-Y. Mou, *Chem. Mater.* **2004**, *16*, 561.
[5] a) G. Crevoisier, P. Fabre, J.-M. Corpart, L. Leibler, *Science* **1999**, *285*, 1246; b) G. Zhang, D. Wang, Z.-Z. Gu, H. Möhwald, *Langmuir* **2005**, *21*, 9143.
[6] a) K. K. S. Lau, J. Bico, K. B. K. Teo, M. Chhowalla, G. A. J. Amaratunga, W. I. Milne, G. H. McKinley, K. K. Gleason, *Nano Lett.* **2003**, *3*, 1701; b) E. Hosono, S. Fujihara, I. Honma, H. Zhou, *J. Am. Chem. Soc.* **2005**, *127*, 13458.
[7] a) Y. H. Erbil, L. A. Demirel, Y. Avci, O. Mert, *Science* **2003**, *299*, 1377; b) M. Morra, E. Occhiello, F. Garbassi, *Langmuir* **1989**, *5*, 872.
[8] a) A. A. Gakh, A. A. Tuinman, J. L. Adcock, R. A. Sachleben, R. N. Compton, *J. Am. Chem. Soc.* **1994**, *116*, 819; b) P. J. Fagan, P. J. Krusic, C. N. McEwen, J. Lazar, D. Holmes-Parker, N. Herron, E. Wasserman, *Science* **1993**, *262*, 404.
[9] R. Taylor, A. G. Avent, T. J. Dennis, J. P. Hare, H. W. Kroto, D. R. M. Walton, *Nature* **1992**, *355*, 275.
[10] A. Herzog, R. P. Callahan, C. L. B. Macdonald, V. M. Lynch, M. F. Hawthorne, R. J. Lagow, *Angew. Chem.* **2001**, *113*, 2179; *Angew. Chem. Int. Ed.* **2001**, *40*, 2121.
[11] T. Hayashi, M. Terrones, C. Scheu, Y. A. Kim, M. Rühle, T. Nakajima, M. Endo, *Nano Lett.* **2002**, *2*, 491.
[12] a) K. Pielichowski, J. Njuguna, B. Janowski, J. Pielichowski, *Adv. Polym. Sci.* **2006**, *201*, 225; b) S. H. Phillips, T. S. Haddad, S. J. Tomczak, *Curr. Opin. Solid State Mater. Sci.* **2004**, *8*, 21.
[13] G. Li, L. Wang, N. Hanli, C. U. Pittman, Jr., *J. Inorg. Organomet. Polym.* **2001**, *11*, 123.
[14] a) V. I. Lavrent'ev, *Russ. J. Gen. Chem.* **2004**, *74*, 1188; b) V. I. Lavrent'ev, V. B. Durasov, *Zh. Obshch. Khim.* **1992**, *62*, 2722.
[15] a) K. Koh, S. Sugiyama, T. Morinaga, K. Ohno, Y. Tsujii, T. Fukuda, M. Yamahiro, T. Iijima, H. Oikawa, K. Watanabe, T. Miyashita, *Macromolecules* **2005**, *38*, 1264; b) S. T. Iacono, A. Vij, W. W. Grabow, D. W. Smith, Jr., J. M. Mabry, *Chem. Commun.* **2007**, 4992.
[16] A. Bondi, *J. Phys. Chem.* **1966**, *70*, 3006.
[17] T. Young, *Philos. Trans. R. Soc. London* **1805**, *95*, 65.
[18] H. Kobayashi, *Makromol. Chem.* **1993**, *194*, 259.
[19] B. Baradie, M. S. Shoichet, *Macromolecules* **2003**, *36*, 2343; K. Li, P. Wu, Z Han, *Polymer* **2002**, *43*, 4079; D. R. Iyengar, S. M. Perutz, C.-A. Dai, C. K. Ober, E. J. Kramer, *Macromolecules* **1996**, *29*, 1229.
[20] M. J. Owen, H. Kobayashi, *Macromol. Symp.* **1994**, *82*, 115; D. K. Owens, R. C. Wendt, *J. Appl. Polym. Sci.* **1969**, *13*, 1741.
[21] F. J. du Toit, R. D. Sanderson, W. J. Engelbrecht, J. B. Wagener, *J. Fluorine Chem.* **1995**, *74*, 43; L. G. Jacobsohn, M. E. H. Maia da Costa, V. J. Trava-Airoldi, F. L. Freire, Jr., *Diam. Relat. Mater.* **2003**, *12*, 2037.
[22] A. B. D. Cassie, S. Baxter, *Trans. Faraday Soc.* **1944**, *40*, 546.
[23] R. N. Wenzel, *Ind. Eng. Chem.* **1936**, *28*, 988.
[24] W. L. F. Armarego, D. D. Perrin, *Purification of Laboratory Chemicals*, Butterworth Heinemann, Boston, **1996**.

[25] Crystal data for **FH** and **FD** was collected at $T = 103.0(2)$ K using Bruker 3-circle, SMART APEX CCD with χ-axis fixed at 54.74°, running on SMART V 5.625 program (Bruker AXS: Madison, 2001). Graphite monochromated $Mo_{K\alpha}$ ($\lambda = 0.71073$ Å) radiation was employed for data collection and corrected for Lorentz and polarization effects using SAINT V 6.22 program (Bruker AXS: Madison, **2001**), and reflection scaling (SADABS program, Bruker AXS: Madison, WI, **2001**). Both the structures were solved by direct methods (SHELXTL 5.10, Bruker AXS: Madison, **2000**) and all non-hydrogen atoms refined anisotropically using full-matrix least-squares refinement on F^2. Hydrogen atoms were added at calculated positions. For **FH**, $M_r = 2393.46$, triclinic, space group $P\bar{1}$, $a = 11.806(5)$, $b = 12.393(5)$, $c = 15.729(6)$ Å, $\alpha = 75.073(6)$, $\beta = 76.024(6)$, $\gamma = 66.151(5)°$, $V = 2009.0(14)$ Å^3, $F(000) = 1176$, $\rho_{calcd}(Z=1) = 1.987$ g cm^{-3}, $\mu = 0.356$ mm^{-1}, approximate crystal dimensions $0.37 \times 0.24 \times 0.20$ mm^3, θ range = 1.36 to 25.35°, 19582 measured data of which 7288 ($R_{int} = 0.0194$) unique with 718 refined parameters, final R indices [$I > 2\sigma(I)$]: $R1 = 0.0368$, $wR2 = 0.0981$, $R1 = 0.0389$, $wR2 = 0.1002$ (all data), GOF on $F^2 = 1.038$. For **FD**, $M_r = 3993.78$, triclinic, space group $P\bar{1}$, $a = 10.352(1)$, $b = 21.984(2)$, $c = 28.653(3)$ Å, $\alpha = 102.082(1)$, $\beta = 95.702(1)$, $\gamma = 90.907(1)°$, $V = 6340.2(1)$ Å^3, $F(000) = 3888$, $\rho_{calcd}(Z=2) = 2.092$ g cm^{-3}, $\mu = 0.341$ mm^{-1}, approximate crystal dimensions $0.43 \times 0.30 \times 0.15$ mm^3, θ range = 1.31 to 25.37°, 49607 measured data of which 23049 ($R_{int} = 0.0203$) unique with 2125 refined parameters, final R indices [$I > 2\sigma(I)$]: $R1 = 0.0564$, $wR2 = 0.1599$, $R1 = 0.0676$, $wR2 = 0.1728$ (all data), GOF on $F^2 = 1.005$. CCDC 608207 (**FH**) and 608209 (**FD**) contain the supplementary crystallographic data for this paper. These data can be obtained free of charge from The Cambridge Crystallographic Data Centre via www.ccdc.cam.ac.uk/data_request/cif.

APPENDIX D: SCIENCE ARTICLE

Designing Superoleophobic Surfaces
Anish Tuteja, *et al.*
Science **318**, 1618 (2007);
DOI: 10.1126/science.1148326

Designing Superoleophobic Surfaces

Anish Tuteja,[1] Wonjae Choi,[2] Minglin Ma,[1] Joseph M. Mabry,[3] Sarah A. Mazzella,[3] Gregory C. Rutledge,[1] Gareth H. McKinley,[2]* Robert E. Cohen[1]*

Understanding the complementary roles of surface energy and roughness on natural nonwetting surfaces has led to the development of a number of biomimetic superhydrophobic surfaces, which exhibit apparent contact angles with water greater than 150 degrees and low contact angle hysteresis. However, superoleophobic surfaces—those that display contact angles greater than 150 degrees with organic liquids having appreciably lower surface tensions than that of water—are extremely rare. Calculations suggest that creating such a surface would require a surface energy lower than that of any known material. We show how a third factor, re-entrant surface curvature, in conjunction with chemical composition and roughened texture, can be used to design surfaces that display extreme resistance to wetting from a number of liquids with low surface tension, including alkanes such as decane and octane.

Many surfaces in nature, including various plant leaves (*1*, *2*), legs of the water strider (*3*), troughs on the elytra of desert beetles (*4*), and geckos' feet (*5*, *6*), are superhydrophobic, displaying apparent contact angles with water (surface tension γ_{lv} = 72.1 mN/m) greater than 150° and low contact angle hysteresis. Understanding the complementary roles of the two key surface parameters, surface energy and roughness (*7*–*11*), for these materials has led to the development of a number of artificial superhydrophobic surfaces (*6*, *12*, *13*). However, superoleophobic surfaces—structured surfaces that resist wetting of liquids with much lower surface tension, such as decane (γ_{lv} = 23.8 mN/m) or octane (γ_{lv} = 21.6 mN/m)—are extremely rare (*14*). We have developed several different textured surfaces displaying contact angles greater than 160°, even with octane. This observed superoleophobicity can be explained by considering local surface curvature as the third parameter that affects both the apparent contact angle and hysteresis on any surface. This understanding also allows us to rationalize numerous earlier observations of unexpectedly high liquid repellency on rough surfaces (*14*–*18*).

The best-known example of a natural superhydrophobic surface is the surface of the lotus leaf, *Nelumbo nucifera* (*1*). Numerous studies have suggested that the superhydrophobic character of the lotus leaf surface is attributable to a combination of surface chemistry and roughness on multiple scales. However, a liquid with a markedly lower surface tension, such as hexadecane (γ_{lv} = 27.5 mN/m), spreads rapidly across the lotus leaf, leading to a contact angle of ~0° (fig. S8) (*19*). Such surface oleophilicity can have an impact on a wide range of phenomena, including biofouling by marine organisms, loss of self-cleaning ability of plant leaves in polluted waters, and swelling of elastomeric seals and O-rings.

Two distinct models, developed independently by Wenzel (*7*) and Cassie and Baxter [(*8*), henceforth the Cassie model], are commonly used to explain the effect of roughness on the apparent contact angle of liquid drops (*20*, *21*). The Wenzel model recognizes that surface roughness increases the available surface area of the solid, which modifies the surface contact angle according to the expression

$$\cos\theta^* = r\cos\theta \qquad (1)$$

where θ^* is the apparent contact angle on the textured surface, r is the surface roughness, and θ is the equilibrium contact angle on a smooth surface of the same material, given by Young's equation (*22*) as $\cos\theta = (\gamma_{sv} - \gamma_{sl})/\gamma_{lv}$, where γ refers to the interfacial tension and the subscripts s, l, and v refer to the solid, liquid, and vapor phases, respectively.

The Cassie model, on the other hand, postulates that the superhydrophobic nature of a rough surface is caused by microscopic pockets of air remaining trapped below the liquid droplet, leading to a composite interface. If ϕ_s is the fraction of the solid in contact with the liquid, the Cassie equation yields

$$\cos\theta^* = -1 + \phi_s(1 + \cos\theta) \qquad (2)$$

In contrast to the Wenzel relation, the Cassie relation allows for the possibility of $\theta^* > 90°$, even with $\theta < 90°$. Thermodynamic considerations can be used to determine whether a particular textured surface will exist in the Wenzel or the Cassie state [see recent work by Marmur (*10*) and Nosonovsky (*11*)]. The situation is somewhat complicated by the presence of multiple local free energy minima leading to so-called "metastable" configurations (*2*, *10*, *23*, *24*). Indeed, Krupenkin *et al*. (*25*) have highlighted the possibility of transitioning reversibly between the Wenzel and Cassie states (*19*). However, careful experimentation with model microstructured surfaces and corresponding free energy calculations show that a series of rough substrates with progressively increasing equilibrium contact angles exhibits a transition from the Wenzel to the Cassie state (*24*, *26*, *27*). The threshold value of the equilibrium contact angle (θ_c) for this transition is obtained by equating Eqs. 1 and 2:

$$\cos\theta_c = (\phi_s - 1)/(r - \phi_s) \qquad (3)$$

Because $r > 1 > \phi_s$, the critical value of the equilibrium contact angle θ_c for this transition is necessarily greater than 90°. Thus, it may be anticipated that for $\theta < 90°$, a surface cannot exist in the Cassie state or that the creation of highly nonwetting surfaces ($\theta^* >> 90°$) requires $\theta > \theta_c > 90°$. These arguments highlight the difficulty of developing surfaces for which $\theta^* > 150°$ when in contact with alkanes such as decane or octane, as there are no reports of a natural or artificial surface with a low enough surface energy (*19*) to enable $\theta > 90°$ with these liquids (*14*–*17*, *28*).

However, studies on leaves of plants such as *Cotinus coggygria* and *Ginkgo biloba* suggest the possibility of designing textured surfaces with unexpectedly high nonwetting properties. Herminghaus (*2*) first pointed out that these leaves display superhydrophobic properties, even with $\theta < 90°$. Indeed, recent experiments show that even the wax on the lotus leaf surface is weakly hydrophilic with $\theta \approx 74°$ (*29*). The superhydrophobic state of these textured surfaces is not the true equilibrium state, and submerging the leaf in water to a certain depth can cause a transition from this metastable Cassie state to the Wenzel state. Correspondingly, it may be possible to design metastable superoleophobic surfaces even though we are limited to materials with $\theta < 90°$.

We have synthesized a class of hydrophobic polyhedral oligomeric silsesquioxane (POSS) molecules in which the rigid silsesquioxane cage is surrounded by perfluoro-alkyl groups (inset, Fig. 1A). A number of molecules with different organic groups including 1*H*,1*H*,2*H*,2*H*-heptadecafluorodecyl (referred to as fluorodecyl POSS) and 1*H*,1*H*,2*H*,2*H*-tridecafluorooctyl (fluorooctyl POSS) were synthesized. We refer to this class of materials generically as fluoroPOSS (*19*). The high surface concentration and surface mobility of $-CF_2$ and $-CF_3$ groups, together with the relatively high ratio of $-CF_3$ groups with respect to $-CF_2$ groups, results in a very hydrophobic material with low surface energy. A film of fluorodecyl POSS, spin-coated on a Si wafer, has an advancing (θ_{adv}) and receding (θ_{rec}) contact angle of 124.5° ± 1.2°, with a root mean square (RMS) roughness r_q = 3.5 nm.

By varying the mass fraction of specific fluoroPOSS molecules blended with a polymer, we can systematically change γ_{sv} for the polymer-fluoroPOSS blend. We studied blends of a moderately hydrophilic polymer, poly(methyl methacrylate) (PMMA), and fluorodecyl POSS (which had the lowest surface energy of the POSS molecules synthesized). Varying the mass fraction of fluo-

[1]Department of Chemical Engineering, Massachusetts Institute of Technology, Cambridge, MA 02139, USA. [2]Department of Mechanical Engineering, Massachusetts Institute of Technology, Cambridge, MA 02139, USA. [3]Air Force Research Laboratory, Edwards Air Force Base, CA 93524, USA.

*To whom correspondence should be addressed. E-mail: gareth@mit.edu (G.H.M.); recohen@mit.edu (R.E.C.)

rodecyl POSS systematically changed both θ_{adv} and θ_{rec} for water on spin-coated films of PMMA and fluorodecyl POSS (Fig. 1A). The atomic force microscope (AFM) phase images of the spin-coated surfaces, as well as the shapes of water droplets (volume ≈ 2 μl) on those surfaces, are shown in Fig. 1B. Comparing the phase images of the pure PMMA and 1.9 weight % fluorodecyl POSS indicates substantial surface migration of POSS during solvent evaporation, as would be expected because of its low surface energy (*30*, *31*).

The corresponding rough fluorodecyl POSS–PMMA surfaces are created by electrospinning (*32*–*34*). In Fig. 1C we show the advancing (θ^*_{adv}) and receding θ^*_{rec} contact angles with water for the various electrospun surfaces. The inset shows the "beads on a string" (*35*) morphology of a representative fiber mat, as well as the multiple scales of roughness and high porosity generated by the electrospinning process. There is no observable change in the micrometer-scale structure with increasing mass fraction of POSS as viewed with a scanning electron microscope (SEM). X-ray photoelectron spectroscopy (XPS) analysis indicates substantial surface migration of the fluoroPOSS molecules during electrospinning (fig. S9). The surfaces become superhydrophobic (movie S1) for all POSS concentrations above ~10 weight % ($\theta^*_{adv} = \theta^*_{rec} = 161° \pm 2°$).

An important observation from Fig. 1C is that $\theta^*_{adv} > 90°$ for pure PMMA and 1.9 weight % POSS–PMMA electrospun surfaces, even though in each case $\theta_{adv} < 90°$ (Fig. 1A). This is surprising, because for $\theta < 90°$ the rough surfaces are expected to be in the Wenzel state, and from Eq. 1 we expect $\theta^*_{adv} < \theta_{adv}$. This unusual effect is further explored in the form of the general wetting diagram (*13*) in Fig. 1D, which shows a plot of cos θ^*_{adv} and cos θ^*_{rec} on the rough electrospun surfaces as a function of cos θ_{adv} and cos θ_{rec} for the corresponding smooth (spin-coated) surfaces. Even at low POSS concentrations (<2 weight %), the surfaces display high apparent advancing contact angles indicative of being in the Cassie state. However, these textured surfaces also exhibit high contact angle hysteresis. Separate experiments show that this Cassie state is metastable, as water droplets released from a height can penetrate and wet the fiber mat.

The electrospun fibers similarly display extremely oleophobic properties ($\theta^* >> 90°$), even though all of the corresponding spin-coated surfaces are oleophilic ($\theta < 90°$). Plots of θ^*_{adv} and θ^*_{rec} for hexadecane and decane (Fig. 2, A and B) show that in many cases both θ^*_{adv} and θ^*_{rec} for the electrospun surfaces are much greater than 90°, and a transition from the Wenzel to the metastable Cassie state can also be observed for each alkane. This metastable state is related to a local minimum in free energy (*19*) that systematically shifts to higher POSS concentrations (lower surface energy) with decreasing liquid surface tension. The electrospinning process also enables fibers to be deposited on fragile or natural surfaces (such as a lotus leaf) to confer oleophobicity in addition to superhydrophobicity (fig. S8).

The advancing contact angles for various liquid alkanes on the electrospun and spin-coated surfaces can be combined to form a master curve of θ^*_{adv} versus θ_{adv} (Fig. 2C). A sharp transition from the Wenzel state to the nonwetting Cassie state is observed at an equilibrium contact angle of $\theta_c \approx 69°$ (see also fig. S10). This value of θ_c depends on the free

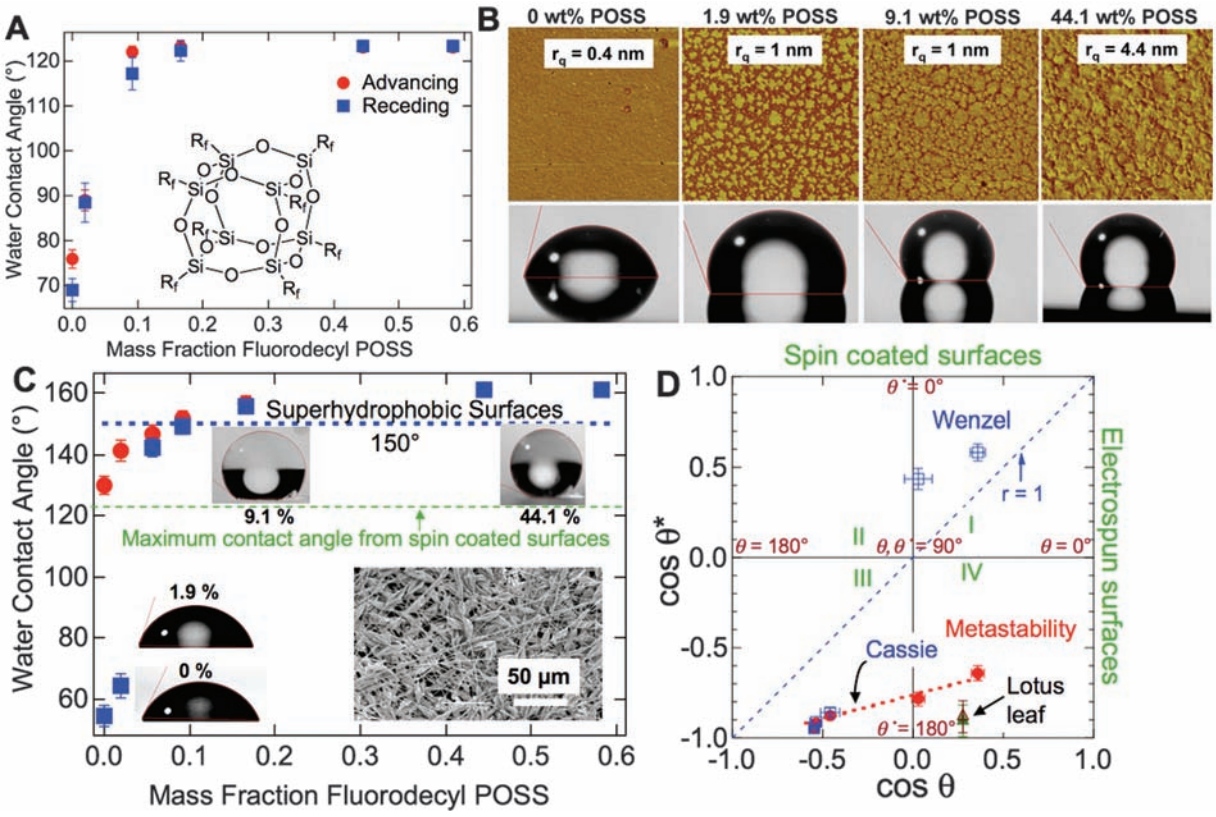

Fig. 1. Tunable hydrophobicity of fluoroPOSS-PMMA blends. (**A**) θ_{adv} and θ_{rec} for water as a function of the mass fraction of fluorodecyl POSS. The inset shows the general molecular structure of fluoroPOSS molecules. The alkyl chains (R_f) have the general molecular formula $-CH_2CH_2(CF_2)_nCF_3$, where n = 0, 3, 5, or 7. (**B**) The phase angle scale on the AFM images is 0° to 10° for the 0, 9.1, and 44.1 weight % POSS images and 0° to 90° for the 1.9 weight % POSS image. The RMS roughness (r_q) for each film is also given. By comparison, r_q for a Si wafer is ~0.2 nm. (**C**) θ^*_{adv} (red dots) and θ^*_{rec} (blue squares) for water on the electrospun surfaces. The inset shows a SEM micrograph for an electrospun surface containing 9.1 weight % POSS. The maximum contact angle for water on the spin-coated surfaces is also shown. (**D**) Plot of cos θ^*_{adv}(solid red dots) and cos θ^*_{rec} (open blue squares) for water as a function of θ_{adv} and θ_{rec}. The surfaces in the lower right quadrant (IV) of this diagram correspond to hydrophilic substrates that are rendered hydrophobic purely by topography. The advancing and receding contact angles for the lotus leaf (solid and open triangles, respectively) are also provided for comparison.

energy landscape separating the Cassie and Wenzel states (*19*) and will be dependent on the topography of the surfaces under consideration; however, it is clear from Fig. 2C and fig. S10 that θ_c can be considerably less than 90°.

The robustness of the metastable Cassie state for the electrospun fiber surfaces is determined by measuring the height of liquid (or static pressure) required for forcing the liquid through the fibers (denoted h^*). The surfaces do not transition to the Wenzel state even when submerged under 150 mm of hexadecane. To scale such observations, we use the characteristic capillary rise height

$$h_{cap} = 2\gamma_{lv} \cos\theta/\rho g D \qquad (4)$$

for the porous substrate, where the relevant capillary pore size $2D$ is the average edge-to-edge spacing of the nanofibers (Fig. 3A) (*8*), ρ is the fluid density, and g is the acceleration due to gravity. In Fig. 2D we plot the normalized breakthrough pressure

$$h^*/h_{cap} = \rho g D h^*/(2\gamma_{lv} \cos\theta) \qquad (5)$$

required to wet a fiber mat containing 44 weight % POSS. Calculations shown in (*19*) yield the pressure required to increase the curvature of a liquid droplet until it impinges on the next level of fibers. These pressures (normalized with the capillary pressure) are also shown in Fig. 2D.

An extremely useful application for these porous electrospun materials can be deduced by noticing that many of the electrospun surfaces with low POSS concentrations are both superhydrophobic and superoleophilic ($\theta^*_{alkane} \approx 0°$). Thus, these surfaces are ideal for separating mixtures or dispersions of alkanes (oils) and water (*36*), as shown in Fig. 2E.

It is the local surface curvature that plays a key role in driving the oleophobicity of electro-

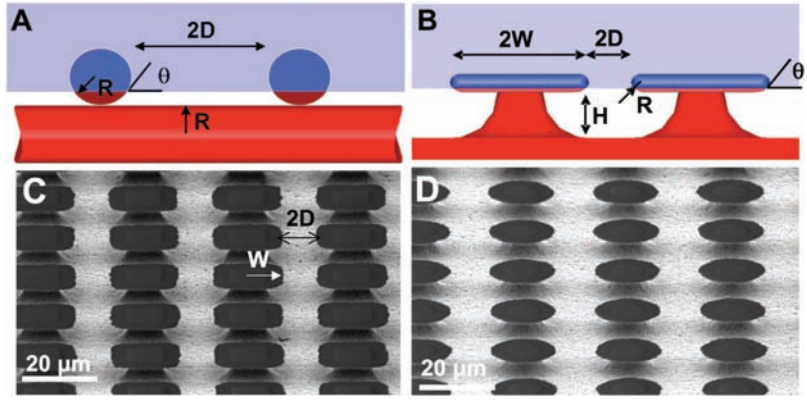

Fig. 3. Critical role of re-entrant curvature. (**A** and **B**) Cartoons highlighting the formation of a composite interface on surfaces with re-entrant topography (for both fibers and micro-hoodoos). The geometric parameters R, D, H, and W characterizing these surfaces are also shown. The blue surface is wetted while the red surface remains nonwetted when in contact with a liquid whose equilibrium contact angle is θ (< 90°). (**C** and **D**) SEM micrographs for two micro-hoodoo surfaces having square and circular flat caps, respectively. The samples are viewed from an oblique angle of 30°.

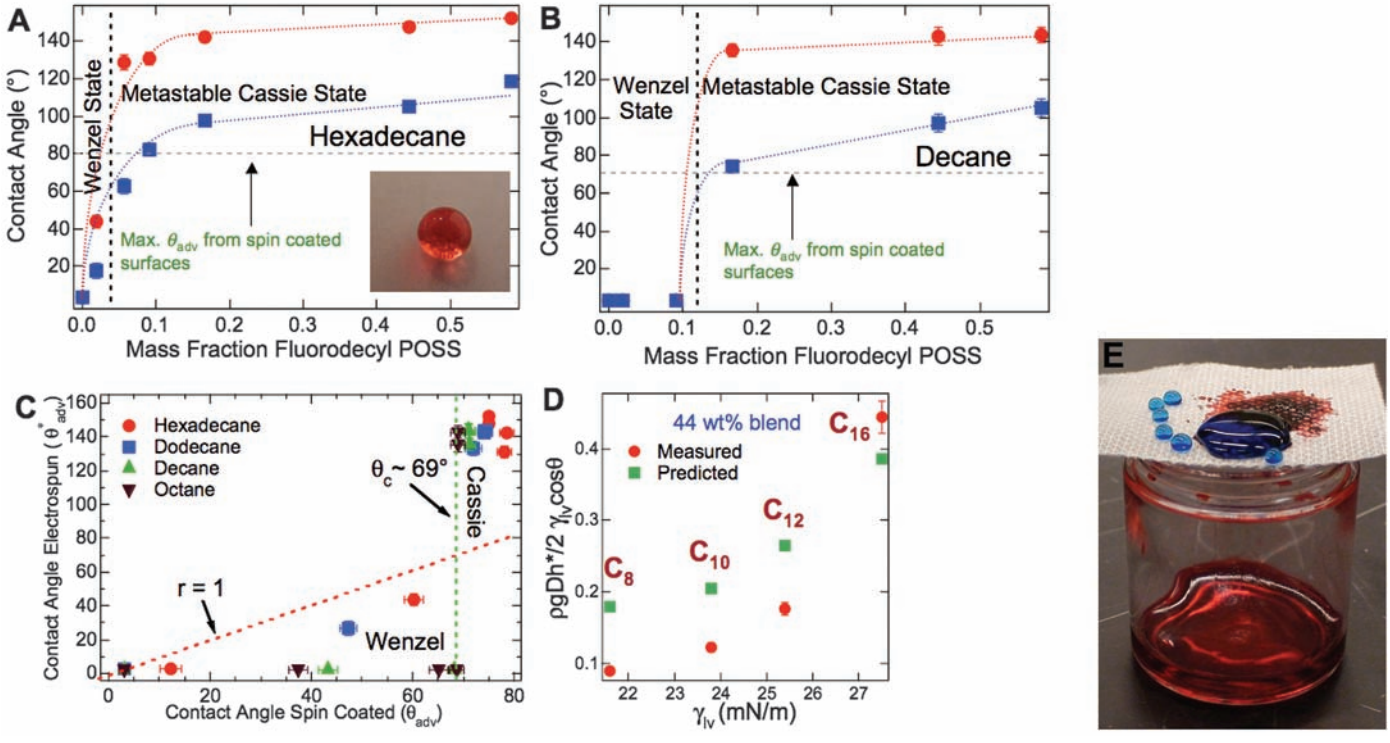

Fig. 2. (**A** and **B**) θ^*_{adv} (red dots) and θ^*_{rec} (blue squares) for hexadecane and decane, respectively, on the electrospun surfaces. The maximum contact angles on corresponding spin-coated surfaces (θ_{adv}) are also shown. The inset of (A) shows a drop of hexadecane (dyed with Oil Red O) on a 44 weight % fluorodecyl POSS electrospun surface. (**C**) θ^*_{adv} for hexadecane, dodecane, decane, and octane as a function of θ_{adv}. (**D**) Normalized breakthrough pressure required to transition irreversibly from the metastable Cassie to the Wenzel state on the surface of fibers containing 44 weight % fluorodecyl POSS. Our predictions for the breakthrough pressure (*19*) using R = 500 nm and D = 4 μm are also shown. (**E**) A steel grid (square pores with 1-mm spacing) coated with electrospun fibers containing 9.1 weight % fluorodecyl POSS used for oil-water separation. Octane droplets (colored with Oil Red O) easily pass through the membrane, whereas water droplets (dyed with methylene blue) bead up on the surface (see movie S2).

spun fibers. To support this thesis, we fabricated model re-entrant structures (i.e., surfaces having concave topographic features) of the form shown in Fig. 3, B to D. These structures were fabricated on flat Si wafers by means of SiO_2 deposition followed by a two-step etching process comprising reactive ion etching of SiO_2 and subsequent isotropic etching of Si with the use of vapor-phase XeF_2 (*19*). This results in undercut silicon pillars (covered with a 300-nm layer of SiO_2) and troughs. Because of their similarity to geomorphological features, we refer to these structures as micro-hoodoos (*37*). A key design feature of both of the electrospun fiber and hoodoo surfaces is that they possess re-entrant curvature, in addition to exhibiting both the desired characteristics of "roughness" (i.e., $r > 1$) and low wetted surface fraction (i.e., $\phi_s < 1$) embodied in Eqs. 1 and 2.

The flat liquid-air interface shown schematically in Fig. 3, A and B (*38*) is in contact with the electrospun fibers and the micro-hoodoos. As a direct result of re-entrant curvature, for any value of $0° < \theta < 180°$, each surface in Fig. 3, A and B, provides a point somewhere along the fiber or cap length at which Young's equation is satisfied locally at the air-liquid-solid interface (*10*, *11*, *34*). This is in contrast to other common patterned supports [e.g., arrays of vertical posts (*25*)], which can form a composite interface and satisfy the Young equation only if $\theta > 90°$. It is therefore possible to form a composite interface on re-entrant curved surfaces, with the drop sitting partially on air, and thus have $\theta^* >> 90°$ even with $\theta < 90°$. However, this Cassie state is only locally stable, because the total energy of the system decreases appreciably (*19*) if the liquid advances and completely covers the fibers/hoodoos, leading to a fully wetted interface (*11*, *39*).

Analysis of these re-entrant geometries yields two important design parameters (*19*). For the electrospun fibers, the first is the spacing ratio $D^* = (R + D)/R$ (where R is the radius of the fibers), which directly affects ϕ_s (*8*) and thus the apparent contact angle. The second is the robustness parameter $H^* = 2(1 - \cos\theta)Rl_{cap}/D^2$ [where $l_{cap} = (\gamma_{lv}/\rho g)^{1/2}$], which measures the robustness of the metastable Cassie state with respect to the fluid properties, equilibrium contact angle, and surface geometry. Varying the R and D values of these structures has competing effects on the apparent contact angles and the stability of the composite interface. Thus, the metastable Cassie state may not be accessible in practice on every surface that possesses re-entrant curvature, depending on the applied pressure required to transition irreversibly from the metastable Cassie to the Wenzel state. However, it is clear that to maximize both θ^* and the stability of the Cassie state, we seek sparsely spaced, highly re-entrant surfaces with both $H^* >> 1$ and $D^* >> 1$. This is why our electrospun mats of nanofibers ($D^* = 9$; $H^* = 46$ for octane on fibers containing 44.1 weight % POSS) provide a more robust Cassie state than do prototypical wire gratings (*8*) ($D^* = 1.9$ to 5.8; $H^* = 0.76$ to 7.6 for octane), even at higher porosities.

Evaluating the magnitudes of these dimensionless design parameters also helps explain the oleophobicity observed for aggregates of anodized alumina (*15*, *16*), plasma-treated cotton fibers (*14*), and spherical arrays of poly(tetrafluoroethylene) (PTFE) particles (*17*), as well as superhydrophobicity obtained on a hydrophilic substrate with a "popcorn-like" morphology (*18*). Re-entrant structures on the lotus leaf surface, in the form of "overhangs" (*2*, *40*) on the hemispherical nubs (inset, fig. S8A), are also the reason for its unexpectedly high hydrophobicity.

For the micro-hoodoo geometry, the design parameters take the form $D^* = [(W + D)/W]^2$ and $H^* = 2[(1 - \cos\theta)R + H]l_{cap}/D^2$. Because the hoodoo spacing (W) and height (H) can be varied independently for these surfaces (Fig. 3B), we can easily decouple variations in D^* and H^* and thus engineer surfaces with both higher apparent contact angles and much greater robustness than even the electrospun fibers can provide.

During the patterning and etching process for fabricating the micro-hoodoos, we also left untextured areas, thus enabling the measurement of both θ and θ^* on the same wafer. For water on the textured surfaces (Fig. 4A), re-entrant curvature in the absence of any chemical surface treatment leads to $\theta^*_{adv} \approx 143°$ ($\theta^*_{rec} \approx 104°$; $D^* = 2.3$). By comparison, for water on the smooth portion of the same wafer, $\theta_{adv} \approx 10°$. The robustness of the metastable Cassie state on the SiO_2 micro-hoodoo surface (with $H^* = 1560$ for water) is illustrated in Fig. 4B. The re-entrant surface resists both the advancing (*41*) and receding of the water droplet. The images of the receding droplet also highlight the high hysteresis ($\Delta\theta^* \approx 39°$) on the textured surface; however, it is clear that the water droplet has not reached the SiO_2 surface at the base of the hoodoos, in which case it would have been impossible to withdraw the water droplet completely.

The SiO_2 hoodoos were then treated with vapor-phase 1*H*,1*H*,2*H*,2*H*-perfluorodecyltrichlorosilane to lower γ_{sv} chemically and hence combine low surface energy with re-entrant surface curvature. The advancing and receding contact angles for octane on the silanized hoodoo surfaces ($D^* = 2.3$ to 9; $H^* = 64$ to 1040 for octane) are shown in Fig. 4C as a function of ϕ_s or $1/D^*$. The inset of Fig. 4C shows a drop of octane on a silanized micro-hoodoo surface ($\phi_s = 0.11$, $D^* = 9$, $H^* = 64$; $\theta^*_{adv} \approx 163°$, $\theta^*_{rec} \approx 145°$). A 10-μl drop of octane can easily be rolled off this surface by tilting to 15°. Corresponding measurements for octane on a smooth SiO_2 surface ($r_q \approx 0.5$ nm) covered with the same silane coating yielded only $\theta_{adv} \approx 55°$, $\theta_{rec} \approx 50°$. The contact angles monotonically increased with decreasing wetted area fraction ϕ_s. This is in broad agreement with Eq. 2 (*42*) and results from the variable resistance offered to the receding meniscus, which is expected to be proportional to the total number of re-entrant structural elements at the air-liquid-solid three-phase contact line. Silanized micro-hoodoos with $\phi_s = 0.03$ ($D^* = 36$, $H^* = 10$) are fully wetted by octane.

We have demonstrated two different approaches for fabricating surfaces possessing re-entrant curvature. In each case, the re-entrant textures allow for the possibility of constructing extremely nonwetting surfaces that can support

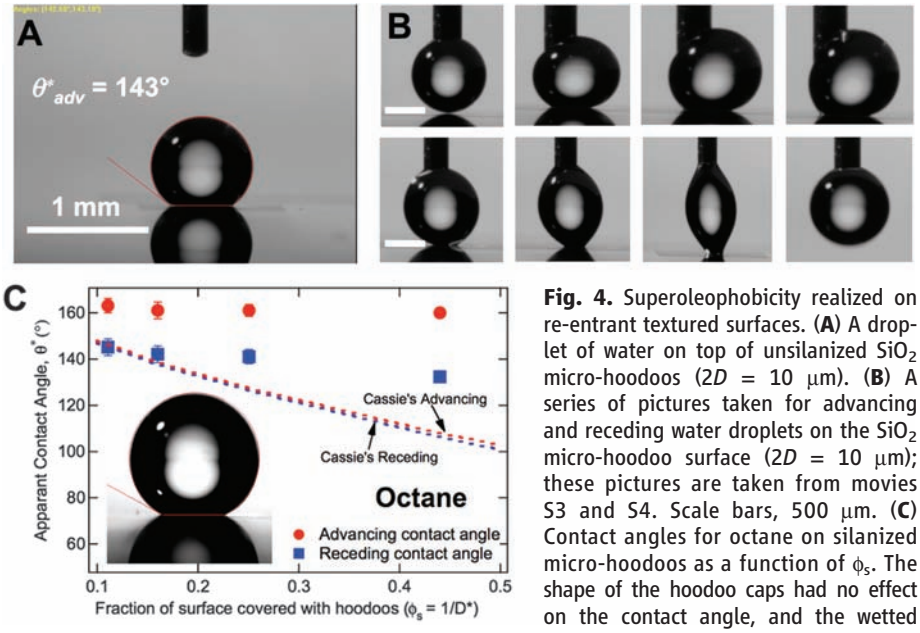

Fig. 4. Superoleophobicity realized on re-entrant textured surfaces. (**A**) A droplet of water on top of unsilanized SiO_2 micro-hoodoos ($2D = 10$ μm). (**B**) A series of pictures taken for advancing and receding water droplets on the SiO_2 micro-hoodoo surface ($2D = 10$ μm); these pictures are taken from movies S3 and S4. Scale bars, 500 μm. (**C**) Contact angles for octane on silanized micro-hoodoos as a function of ϕ_s. The shape of the hoodoo caps had no effect on the contact angle, and the wetted area fraction ϕ_s was found to be the only important parameter. Predictions from the Cassie equation (*8*) are also included for comparison (dashed lines).

the Cassie state with water and various organic liquids. The presence of re-entrant curvature, though, is not a sufficient condition for developing highly nonwetting surfaces; the Cassie state may be inaccessible in practice if the applied pressure (or energy barrier) required to transition from the Cassie to the Wenzel state is small. However, by independently controlling both the chemical and topographic nature of surfaces (as embodied in two dimensionless design parameters, D^* and H^*), we have shown that it is possible to design extremely robust nonwetting surfaces.

References and Notes

1. W. Barthlott, C. Neinhuis, *Planta* **202**, 1 (1997).
2. S. Herminghaus, *Europhys. Lett.* **52**, 165 (2000).
3. X. Gao, L. Jiang, *Nature* **432**, 36 (2004).
4. A. R. Parker, C. R. Lawrence, *Nature* **414**, 33 (2001).
5. K. Autumn *et al.*, *Nature* **405**, 681 (2000).
6. J. Genzer, K. Efimenko, *Biofouling* **22**, 339 (2006).
7. R. N. Wenzel, *Ind. Eng. Chem.* **28**, 988 (1936).
8. A. B. D. Cassie, S. Baxter, *Trans. Faraday Soc.* **40**, 546 (1944).
9. M. Callies, D. Quere, *Soft Mat.* **1**, 55 (2005).
10. A. Marmur, *Langmuir* **19**, 8343 (2003).
11. M. Nosonovsky, *Langmuir* **23**, 3157 (2007).
12. A. Nakajima, K. Hashimoto, T. Watanabe, *Monatsh. Chem.* **132**, 31 (2001).
13. D. Quere, *Rep. Prog. Phys.* **68**, 2495 (2005).
14. S. R. Coulson, I. S. Woodward, J. P. S. Badyal, S. A. Brewer, C. Willis, *Chem. Mater.* **12**, 2031 (2000).
15. K. Tsujii, T. Yamamoto, T. Onda, S. Shibuichi, *Angew. Chem. Int. Ed. Engl.* **36**, 1011 (1997).
16. S. Shibuichi, T. Yamamoto, T. Onda, K. Tsujii, *J. Colloid Interface Sci.* **208**, 287 (1998).
17. W. Chen *et al.*, *Langmuir* **15**, 3395 (1999).
18. M. Zhu, W. Zuo, H. Yu, W. Yang, Y. Chen, *J. Mater. Sci.* **41**, 3793 (2006).
19. See supporting material on *Science* Online.
20. L. Gao, T. J. McCarthy, *Langmuir* **23**, 3762 (2007).
21. Recent work by McCarthy and colleagues (*20*) points out that these models are applicable only at the solid-liquid-vapor three-phase contact line (drop perimeter) and that the interfacial area within the drop perimeter does not affect either the apparent contact angle or the hysteresis; thus, these models can be easily applied only to surfaces with a homogeneous texture, as considered here.
22. T. Young, *Philos. Trans. R. Soc. London* **95**, 65 (1805).
23. N. A. Patankar, *Langmuir* **19**, 1249 (2003).
24. B. He, N. A. Patankar, J. Lee, *Langmuir* **19**, 4999 (2003).
25. T. N. Krupenkin *et al.*, *Langmuir* **23**, 9128 (2007).
26. L. Barbieri, E. Wagner, P. Hoffmann, *Langmuir* **23**, 1723 (2007).
27. A. Lafuma, D. Quere, *Nat. Mater.* **2**, 457 (2003).
28. W. A. Zisman, in *Contact Angle, Wettability and Adhesion*, F. M. Fowkes, Ed. (American Chemical Society, Washington, DC, 1964), pp. 1–51.
29. Y.-T. Cheng, D. E. Rodak, *Appl. Phys. Lett.* **86**, 144101 (2005).
30. D. E. Suk *et al.*, *Macromolecules* **35**, 3017 (2002).
31. D. H. K. Pan, W. M. Prest Jr., *J. Appl. Phys.* **58**, 2861 (1985).
32. D. H. Reneker, A. L. Yarin, H. Fong, S. Koombhongse, *J. Appl. Phys.* **87**, 4531 (2000).
33. M. Ma, Y. Mao, M. Gupta, K. K. Gleason, G. C. Rutledge, *Macromolecules* **38**, 9742 (2005).
34. M. Ma *et al.*, *Adv. Mater.* **19**, 255 (2007).
35. H. Fong, I. Chun, D. H. Reneker, *Polym.* **40**, 4585 (1999).
36. L. Feng *et al.*, *Angew. Chem.* **116**, 2046 (2004).
37. These surfaces are referred to as micro-hoodoos because their geometry and process of creation are reminiscent of geological features called hoodoos, which are created by soil erosion. Hoodoos are composed of a soft sedimentary rock topped by a piece of harder, less easily eroded stone.
38. Because $2D << (\gamma_{lv}/\rho g)^{0.5}$ (capillary length; ρ is the density of liquid), the effect of gravity is negligible and we approximate the liquid-air interface to be a horizontal plane.
39. Nosonovsky (*11*) recently derived another important criterion for the creation of a local minimum in free energy, and thus for the creation of a stable heterogeneous interface: $dA_{sl}d\theta < 0$, where dA_{sl} is the change in solid-liquid contact area with the advancing or receding of the liquid, and $d\theta$ is the change in local contact angle. This criterion also emphasizes the importance of re-entrant surfaces.
40. L. Cao, H. H. Hu, D. Gao, *Langmuir* **23**, 4310 (2007).
41. As the surface is pushed toward the water droplet, the droplet moves, and hence the normal force is not transferred perfectly.
42. The difference in contact angle values from the Cassie prediction is related to contact line pinning.

43. Supported by Air Force Research Laboratory contract FA9300-06M-T015 and Air Force Office of Scientific Research contracts FA9550-07-1-0272 and LRIR-92PL0COR, with additional student support provided by the NSF Nanoscale Interdisciplinary Research Team on Nanoscale Wetting (DMR-0303916). We thank the Institute for Soldier Nanotechnologies at MIT for the use of facilities.

Supporting Online Material

www.sciencemag.org/cgi/content/full/318/5856/1618/DC1
Materials and Methods
SOM Text
Figs. S1 to S10
Tables S1 to S3
References
Movies S1 to S4

25 July 2007; accepted 22 October 2007
10.1126/science.1148326

The Equatorial Ridges of Pan and Atlas: Terminal Accretionary Ornaments?

Sébastien Charnoz,[1]* André Brahic,[1] Peter C. Thomas,[2] Carolyn C. Porco[3]

In the outer regions of Saturn's main rings, strong tidal forces balance gravitational accretion processes. Thus, unusual phenomena may be expected there. The Cassini spacecraft has recently revealed the strange "flying saucer" shape of two small satellites, Pan and Atlas, located in this region, showing prominent equatorial ridges. The accretion of ring particles onto the equatorial surfaces of already-formed bodies embedded in the rings may explain the formation of the ridges. This ridge formation process is in good agreement with detailed Cassini images showing differences between rough polar and smooth equatorial terrains. We propose that Pan and Atlas ridges are kilometers-thick "ring-particle piles" formed after the satellites themselves and after the flattening of the rings but before the complete depletion of ring material from their surroundings.

In images sent by the Voyager spacecraft in the early 1980s, two small satellites were discovered orbiting inside Saturn's rings (*1*, *2*), where Roche (*3*) had shown that strong tidal forces prevent the formation of any big satellite. Pan is located in the A ring's Encke Gap at 133,600 km from Saturn's center, and Atlas orbits at 137,700 km from Saturn's center, just outside the A ring. The Cassini spacecraft has recently resolved them both. Their shapes (Fig. 1) are close to oblate ellipsoids, with equatorial radii of 16.5 and ~19.5 km, and polar radii of ~10.5 km and 9 km for Pan and Atlas, respectively. These dimensions (*4*) are close to the moons' Hill radii (corresponding to the satellites' gravitational cross sections). More unexpectedly, both have a prominent equatorial ridge. These ridges are roughly symmetric about the bodies' equators and give them the appearance of a "flying saucer." Assuming that Pan and Atlas are rotating synchronously around Saturn (like the Moon around the Earth), consistent with Cassini images taken at several different times (*5*), Pan's ridge extends from –15° to +15° latitude (±~5°) and apparently entirely encircles the satellite. Atlas' ridge extends from –30° to +30° latitude (±10°) on the trailing side, whereas on the leading side the ridge is much less prominent, with a modest depression on the leading side near the equator (*4*) (Fig. 1C).

Recent work (*6*) has shown that a fast rotation may explain the diamond shape of the near-earth asteroid 1999 KW4 because of the balance of the centrifugal and gravity forces at the asteroid's equator. This mechanism seems, however, inadequate to explain the shapes of Pan and Atlas: Their rotation periods T (~14 hours) are much too long for centrifugal forces to balance surface gravity (which requires $T \sim 5$ hours). In addition, Saturn's tidal stress would elongate the moons in the radial direction (*3*, *7*) rather than create an equatorial ridge. Therefore, neither centrifugal nor tidal forces seem adequate to explain these ridges.

A number of circumstances led us to investigate a different scenario for the creation of the ridges: (i) Contrary to other resolved satellites, Pan and Atlas are embedded in Saturn's rings. (ii) The ridges are equatorial and precisely in the same plane as Saturn's rings. (iii) The vertical motion of Atlas (and perhaps Pan) through the rings is approximately equal to the

[1]Laboratoire AIM, Commissariat à l'Énergie Atomique (CEA)/Université Paris 7/CNRS, 91191 Gif-sur-Yvette Cedex, France. [2]Center for Radiophysics and Space Research, Cornell University, Ithaca, NY 14853, USA. [3]Cassini Imaging Central Laboratory for Operations, Space Science Institute, Boulder, CO 80301, USA.

*To whom correspondence should be addressed: charnoz@cea.fr

AFRL-RZ-ED-TR-2012-0034
Primary Distribution of this Report:

AFRL/RQRP (1 CD)
Dr. Joseph M. Mabry
10 E. Saturn Blvd
Edwards AFB CA 93524-7680

AFRL/RQRP (Electronic)
Record Custodian
10 E. Saturn Blvd
Edwards AFB CA 93524-7680

AFRL/RQ Technical Library (2 CD + 1 HC)
6 Draco Drive
Edwards AFB CA 93524-7130

Chemical Propulsion Information Analysis Center
Attn: Tech Lib (Mary Gannaway) (1 CD)
10630 Little Patuxent Parkway, Suite 202
Columbia MD 21044-3200

Defense Technical Information Center
(1 Electronic Submission via STINT)
Attn: DTIC-ACQS
8725 John J. Kingman Road, Suite 94
Ft. Belvoir VA 22060-6218